ROMA TRE
UNIVERSITÀ DEGLI STUDI

Dipartimento di Matematica e Fisica

Ph.D. Thesis in Physics

Autocatalytic networks and the origin of life

Candidate:
Alessandro Ravoni

Supervisor:
Prof. Marco Pedicini

Academic Year: 2020/2021

Abstract

The exact sequence of events that led to the formation of the first living organisms from non-living matter is still a debated question. Nevertheless, the acquired ability of the early life forms to emerge and maintain themselves using simple molecules as resources, appears as a fundamental step. In this scenario, the *Autocatalytic sets* (ASs) are of great interest. Introduced by Kauffman (1971), an AS is a set of chemical species capable of spontaneously emerging and self-reproducing through catalytic reactions, starting from a finite set of species assumed to be available from the environment. Several definitions of ASs have been proposed over the years. Recently, Hordijk and Steel (2004) introduced the notion of *Reflexively Autocatalytic and Food-generated* (RAF) set, a formal definition of ASs in the field of graph theory. The RAF sets have been widely studied in a series of recent works, which have provided important theoretical results (see Hordijk and Steel (2018) for a brief resume), as well as the evidence of the presence of RAF structures in real biological systems (Sousa et al., 2015; Xavier et al., 2020), suggesting that ASs actually played an important role in the origin of life. However, several aspects of the ASs are still under investigation. In particular, ASs have been criticised for not being able to experience biological evolution (Vasas et al., 2010), mainly because their dynamics do not seem to have many different attractors. Efforts to clarify this point have been made, and recent numerical results suggest that compartmentalisation of several interacting RAF sets would allow an adaptive evolution (Hordijk et al., 2018a).

In Part I of this doctoral thesis work, we briefly introduce the problem of the origin of life and the RAF theory.

In Part II, we focus on the dynamical emergence of RAF sets and the associated evolutionary properties. In particular, we first address the problem of adaptive evolution by studying how different interactions among RAF sets affect their dynamics. To this aim, we develop a model in which interactions are presented through composition operations among networks, and the dynamics of the networks is reproduced via stochastic simulations. We find that the dynamical emergence of the RAF sets depends on the adopted composition operations. In particular, operations involving chemical species that are sources for ASs can promote the formation of different autocatalytic subsets, opening the door to various dynamical behaviours necessary for biological evolution.

Moreover, this approach allows us to observe that large RAF sets obtained by composition of smaller networks can reach different asymptotic states. This result suggests that compartmentalisation is not a necessary requirement for the appearance of various dynamical behaviours of these systems. More generally, actually, the connection between the topology of a RAF set and its dynamics is not yet fully understood (Filisetti et al., 2011; Serra and Villani, 2019; Hordijk et al., 2018b). In order to deeper study this aspect, we represent RAF sets in terms of *Chemical Reaction Networks*, and we use the Chemical Reaction Network theory (Feinberg, 2019) to connect the structure of RAF sets with their dynamical properties. We find that the conditions a set of interacting chemical species must satisfy in order to be a RAF set are not sufficient for the dynamical emergence of the set itself. In particular, we identify additional topological conditions compared to the one introduced by the RAF theory, which more strictly constrain the dynamics of the system and allow the detection of networks with biologically interesting dynamical properties.

Finally, in Part III we study the thermodynamics of RAF sets. To our knowledge, this aspect has not yet been addressed by the RAF theory. However, general results on the thermodynamics of open Chemical Reaction Networks have been recently obtained, and the connections between the thermodynamic quantities and the network topology have been highlighted (Schmiedl and Seifert, 2007; Polettini and Esposito, 2014; Polettini et al., 2015; Rao and Esposito, 2016, 2018). We use these results to study the RAF sets as nonequilibrium thermodynamic systems. In particular, we investigate the role of catalysis in the thermodynamic efficiency of these particular networks. Our preliminary results suggest that the effects of catalyses on the thermodynamic fluxes can result in an advantage for RAF sets, compared to non autocatalytic networks, in energy storage.

To summarise, the thesis is structured as follows:

- In Part I, after a brief description of the historical background of the problem of the origin of life, we introduce living systems and some of the scenarios proposed for their appearance, Chapter 1. We conclude the introduction by defining the RAF sets and presenting some of the major results of the RAF theory, Chapter 2.

- In Part II, we study the dynamics of RAF sets, focusing on its biological aspects. In particular, in Chapter 3 we investigate the impact of composition on the dynamics of RAF sets. The Chapter is based on the manuscript Ravoni (2020a). In Chapter 4 we present the connection between the dynamics of RAF sets and their topology, as discussed in Ravoni (2020b).

- The thermodynamic aspects of RAF sets are exposed in Part III: after introducing in Chapter 5 the thermodynamic properties of chemical networks, we present the preliminary results obtained in the study of thermodynamic efficiency of RAF sets in Chapter 6.

– Finally, in Part IV we discuss the conclusions.

Contents

Part I

Introduction

Chapter 1

Abiogenesis: the problem of the origin of life

In 1864, the chemist and microbiologist Louis Pasteur won the prize offered by the "Acadèmie des sciences de l'Institut de France" to anyone who had clarified which, between *spontaneous generation* and *biogenesis*, was the correct theory to explain the origin of life. At that time, indeed, there was a heated debate on which of the two theories was the correct one: either the spontaneous generation, which hypothesised a spontaneous emergence of organisms starting from inanimate matter, or the biogenesis, which considered that complex living systems come only from other life forms. In order to resolve the issue, Pasteur devised a simple experiment: he put chicken broth in a container with a long S-shaped neck, letting the broth come into contact with the air but not with dust or other substances in which microorganisms could be present, and boiled the broth for a time sufficient to kill the microorganisms present in it (and those contained in the experimental apparatus). Pasteur observed that, under these conditions, no microorganisms were born from the broth[1]. Conversely, some life forms appeared in the broth if the neck was broken and the container was completely exposed to air and dust. He deduced that organisms can be born only from other organisms, and that spontaneous generation is therefore not possible, commenting his results with the following words (Vallery-Radot, 1926):

> *"Never will the doctrine of spontaneous generation recover from the mortal blow of this simple experiment."*

This is certainly true. However, at present, the most accredited theories to explain the life's origin share, with the spontaneous generation, the fundamental idea that life has arisen from

[1]It is interesting to note that the success of Pasteur's experiment is due, in part, to a dose of luck: for example, today we know the existence of spores that would have survived Pasteur's sterilization process, and which would therefore have led to conclusions different from those of the original experiment. For more details on the acceptance of Pasteur's results and for a general discussion of the role of experiments and socio-cultural factors in the formulation and validation of scientific theories, see Latour (1993).

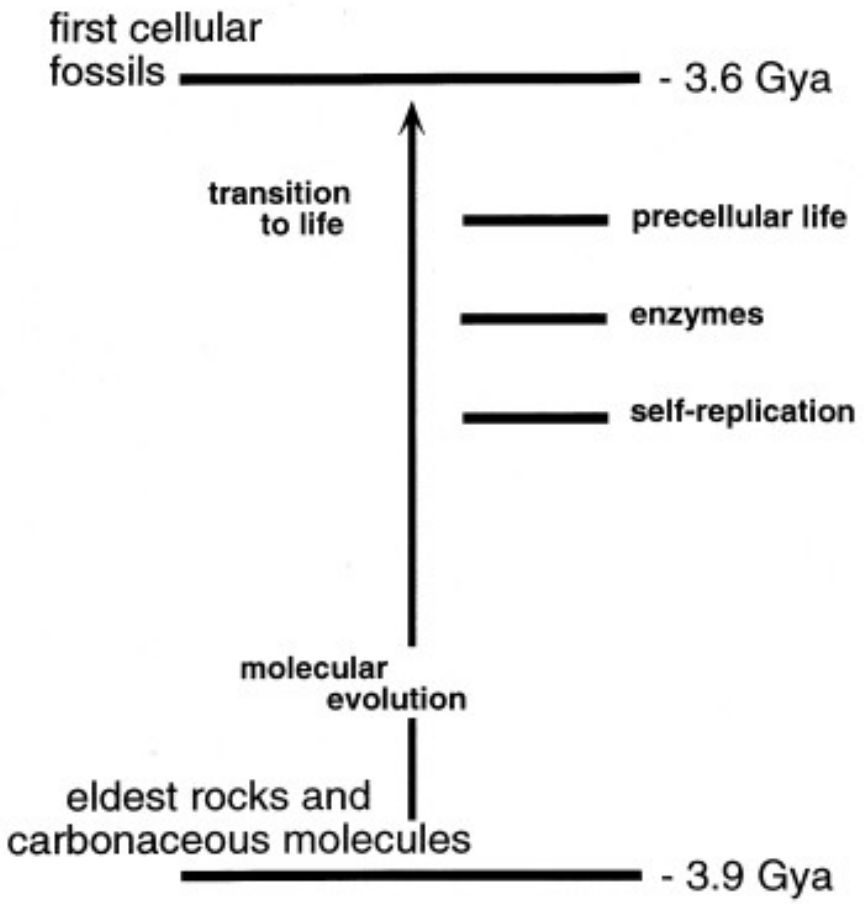

Figure 1.1. Oparin' scenario of transition to life. From Luisi (1998).

non-living matter. In fact, even if the appearance of organisms "out of the blue" is excluded, the modern explanations of the origin of life assumes that, under suitable conditions, the appearance of (bio)chemical elements and a progressive increase in molecular complexity occurred, and eventually, at some point, the first living systems emerged (Luisi, 2006; Szostak, 2017; Rasmussen et al., 2004; Benner et al., 2012b; Bernhardt, 2012). Hereafter, we will refer to the emergence of life from non-living matter with the term *abiogenesis*.

The modern idea of abiogenesis rises from the works of the biologists Aleksandr Ivanovic Oparin and John Burdon Sanderson Haldane (Oparin, 1924; Haldane, 1929). The two scientists hypothesised, independently of each other, the existence of a primitive soup of organic molecules from which, under the particular conditions of the primordial Earth, the first forms of life would self-organise (Figure 1.1). The famous Miller-Urey experiment (Miller, 1953), and various subsequent works (see Kitadai and Maruyama (2018) for a review), have shown that, starting from a "simple" prebiotic environment, the organic molecules at the base of living cells (amino acids, nucleotides, sugars, lipids) can be formed

Table 1.1. Definitions of life

M. Perret (1952) and J. D. Bernal (1965) (Perret, 1952; Waterman et al., 1965):	*Life is a potentially self-perpetuating system of linked organic reactions, catalyzed stepwise and almost isothermally by complex and specific organic catalysts which are themselves produced by the system.*
J. Joyce (Deamer and Fleischaker, 1994):	*Life is a self-sustained chemical system capable of undergoing Darwinian evolution.*
P. L. Luisi (Luisi, 1998):	*Life is a system which is self-sustaining by utilizing external energy/nutrients owing to its internal process of component production and coupled to the medium via adaptive changes which persist during the time history of the system.*
S. A. Kauffman (Kauffman, 2000):	*Life is a self-reproducing system that does at least one thermodynamic work cycle.*
E. N. Trifonov (Trifonov, 2011):	*Life is self-reproduction with variations.*

(Figure 1.2). Moreover, another source of organic compounds has been identified in space dust falling on Earth (see, for instance, Oro et al. (2006)). Therefore, it would be reasonable to assume that the building blocks of life can be obtained starting from non-living matter. Notably, catalytic activity of some of these molecules has been observed, suggesting that catalytic processes would be present at the early stages of life (Plankensteiner et al., 2002; Li et al., 2000; Luisi, 2006). However, it is not clear how, starting from these blocks, it is possible to obtain the complex molecules present today in living organisms, nor it is known how these molecules are organised in a system that we can consider as living.

The origin of life is, in fact, a very broad subject, ranging from biosynthesis experiments to theoretical studies on, for example, *homochirality*, i.e., the geometric uniformity exhibited by the molecules present in living organisms (see Luisi (2006) for a discussion on these topics). In this work we focus on one of the aspects that characterise the problem of abiogenesis. In particular, assuming that the conditions for the formation and the development of the organic compounds underlying life are met, we try to better understand how, starting from these compounds, a first form of life self-organises and spontaneously emerges. Before addressing this question, however, we must introduce some definitions of living system, useful for our study.

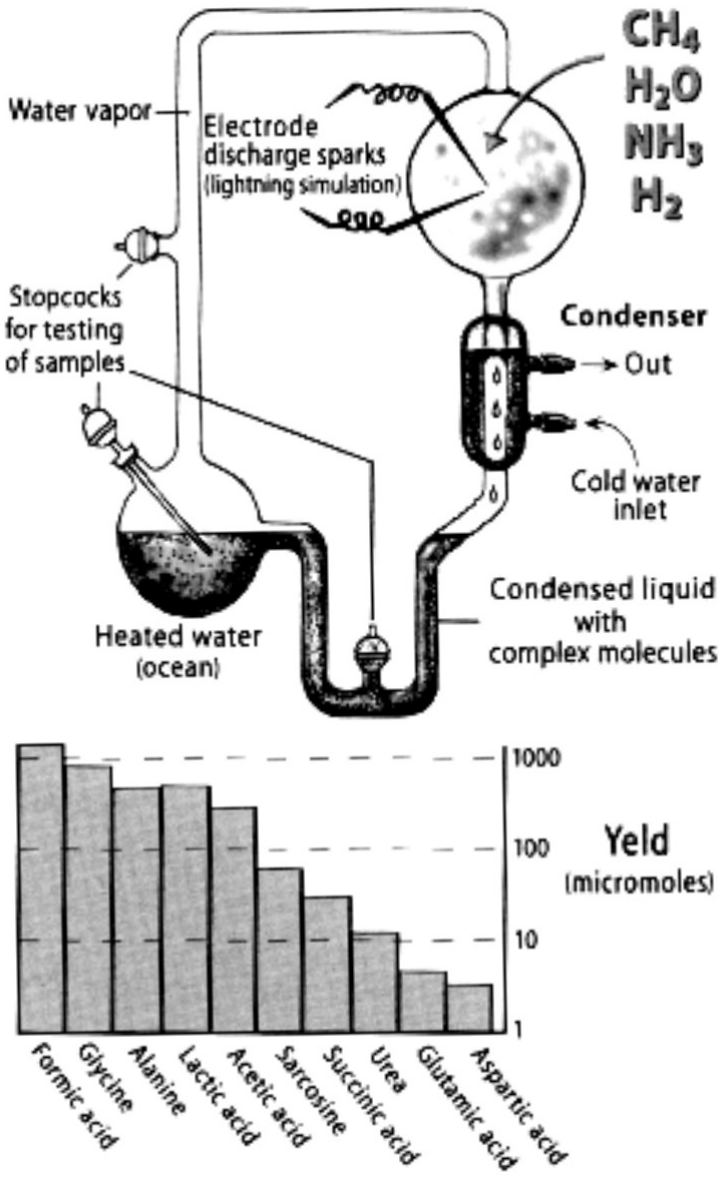

Figure 1.2. The Miller-Urey experiment: a strongly reducing atmosphere consisting of the four gases, and electric discharges as energy source. From Luisi (2006).

1.1 Defining life

Providing a definition of (minimal) life is a hard problem, and in fact a unique definition does not exist[2]. Without any claim to completeness, we recall some definitions in Table 1.1. Our intent is to highlight the properties commonly accepted as peculiar of living systems. These properties are the baseline of the scenarios that try to describe the origin of life.

In particular, on the basis of definitions of Table 1.1 and according to Dyson (1985); Luisi (2006); Penrose and Penrose (1957); Deamer and Fleischaker (1994) (just to name a few works on this field), we can state that a fundamental property of life is the capability of *self-reproduction*. With this term we refer to the ability of a living system to autonomously produce all its components, starting from adequate resources. In this sense, the term self-reproduction is closely related to the notion of *self-maintenance*. It is in fact evident that, despite the thousands of transformations that take place inside an organism, the latter is able to draw matter and energy from the environment in order to maintain its "structure", by regenerating all the components involved in the transformations.

Implicitly, we are assuming another evident property of living systems, that is, they are thermodynamic systems open to the exchange of both matter and energy. As highlighted in the seminal work of Schrödinger (Schrödinger, 1944), the request for an open system is necessary to avoid the "paradox" of a local increase in order. In particular, after the work of Prigogine and Nicolis (Prigogine and Nicolis, 1971), it was suggested that living organisms could be related to *dissipative structures*, i.e., nonequilibrium structures able to maintain themselves thanks to the continuous exchange of energy and matter with the environment (we will discuss thermodynamics aspects of biological systems in Part III). For instance, Kauffman (2020) proposed the idea of a living organism as a thermodynamic system in which, consequently to a flow of energy and matter and depending on the boundary conditions, a "macroscopic pattern" emerges. The further prerequisite introduced by Kauffman is that life itself builds up its own constraints. This characteristic would be at the basis of both the increase in complexity and the enormous diversification observed in living systems. Note that Kauffman's idea is connected with the concept of *autopoiesis* introduced by Maturana and Varela (Varela et al., 1974; Maturana and Varela, 1980), see Luisi (2003) for a brief review.

Another crucial feature of living systems is the way in which they interact with the surrounding world. It is evident, indeed, that a peculiarity of organisms is that of performing an *adaptive interaction* with the environment (Luisi, 2003). In this regard, consider, for instance, the control on the flow of matter implemented by the cell membrane, and the mechanisms of regulation of gene expression in living cells. It is reasonable to assume, as a necessary condition for life, the ability to coordinate internal processes, reacting to

[2] An interesting approach for finding a definition of living systems is given in Trifonov (2011), where the author performs a linguistic analysis of several published life's definitions, to seek an unanimous one.

external perturbations and selecting certain chemicals from the environment in order to ensure self-maintenance. Note that this feature is indicated in the autopoietic theory with the suggestive term *cognition* (Maturana and Varela, 1980). Importantly, the autopoietic theory identifies the metabolism as the mechanism used by cells to perform a dynamic interaction with the environment (Luisi, 2003; Bitbol and Luisi, 2004).

Finally, there is *self-replication*, that is, the generation by a living system of a copy similar to itself. This is, probably, the most debated feature in the definition of life. In fact, approaches to life focused on the presence of genetic material consider replication as a fundamental property (Adami and LaBar, 2015; Luisi, 2003), while theories such as autopoiesis relegate self-replication to a consequence of self-reproduction (Varela, 1979; Luisi, 2006). Here we embrace the autopoietic hypothesis, considering self-replication as a not necessary condition for minimal life. However, it is a fundamental feature for the diversification and biological evolution of living systems. For this reason, we believe that self-replication should be included in a scenario that attempts to explain the origin and the evolution of life. In conclusion, we can summarise the above considerations assuming that a living system is:

i. an **open thermodynamic system** that exchanges energy and matter with the environment;

ii. able to perform **self-reproduction**, i.e., it produces all its components, starting from suitable resources;

iii. able to perform **adaptive interaction** with the environment, i.e., it reacts to external stimuli and selects suitable resources, in order to ensure self-maintenance;

iv. (still debated) able to perform **self-replication**, i.e., it constructs copies of itself, in a dynamical process that allows the biological evolution of a population of organisms.

Now that we have (ideally) clarified the fundamental aspects of living systems, we can move on to the possible scenarios that explain their emergence.

1.2 From non-living to living matter

Living systems are a typical example of complex systems, and modern theories agree that a certain "mechanism", in addition to the abiotic synthesis of organic molecular components, is necessary for the emergence of life (Luisi, 2006; Sharov, 2009). Different scenarios have been proposed in order to explain the transition from non-living to living matter. Generally, they are categorised into two different "schools": the *replication-first* and the *metabolism-first* hypotheses (Pross, 2004; Mulkidjanian and Galperin, 2007). Roughly speaking, the replication-first hypothesis suggests that life started from the advent of an

information-carrying polymer, usually identified with RNA, capable of replication (Szathmáry and Smith, 1995; Dawkins, 1976; Chen et al., 2007; Mulkidjanian and Galperin, 2007). The metabolism-first approach, instead, derives life from autocatalytic chemical cycles able to increase their complexity, and that would have preceded replicators (Kauffman, 1993; Russell and Hall, 1997; Mulkidjanian and Galperin, 2007). Notice that, even if these two paradigms are usually considered as alternative, they are not actually mutually exclusive (Mulkidjanian and Galperin, 2007; Hordijk et al., 2010; Vasas et al., 2012; Hordijk et al., 2018b; Xavier et al., 2020). In the next section we introduce examples of the scenarios proposed for the origin of life, trying to highlight the strengths and weaknesses of each of them.

1.2.1 Replication-first: the RNA word

The RNA world (see Figure 1.3 for a simple sketch) is a popular hypothesis for the origin of life (Orgel, 2004; Robertson and Joyce, 2010). In this scenario, first living systems are identified with genetic systems based solely on RNA (Gilbert, 1986). Regardless the considerations of various authors on the definition of a living system (see Section 1.1), the model of the RNA world implicitly assumes that life can be represented by genetic information that can be inherited through replication, according to Darwinian evolution (Walker, 2017). In a sense, therefore, the RNA world hypothesis is a process of extrapolating backward from biology, that instead of investigating fundamental properties, assumes that primordial replication systems were identical to the present-day nucleic acids (Sharov, 2009; Walker, 2017). The key point of this scenario is the evidence of the ability of replicators both to store a huge amount of information, and to transmit this information through a mechanism that shows to undergo natural selection. The appeal of this scenario is mainly due to its simplicity, and to the fact that it introduces a mechanism of heredity directly connected with that of current living cells (Sharov, 2009; Walker, 2017). Moreover, RNA systems are relatively easy to study as empirical models for exploring molecular evolution (Higgs and Lehman, 2015; Mojzsis et al., 1999).

However, the RNA world has been challenged by the observation that RNA molecules are too complex to have arisen abiotically, as well as they are unstable in water (Bernhardt, 2012). Furthermore, even if nucleotides can be synthesised starting from non-living systems (Benner et al., 2012a; Powner et al., 2009, 2010), they are unlikely to emerge under prebiotically plausible conditions, and in quantities sufficient for RNA replication (Lazcano and Miller, 1996; Shapiro, 1988; Sharov, 2016). Finally, a still debated question is the increase in complexity of genetic replicators as a consequence of the Darwinian evolution only (Walker, 2017). For instance, the authors in Spiegelman et al. (1965) have shown that a 4500 nucleotides RNA virus can evolve, under competitive selection, in a shorter virus of 218 bases. This experiment is an example of how the complexity of a replicator can

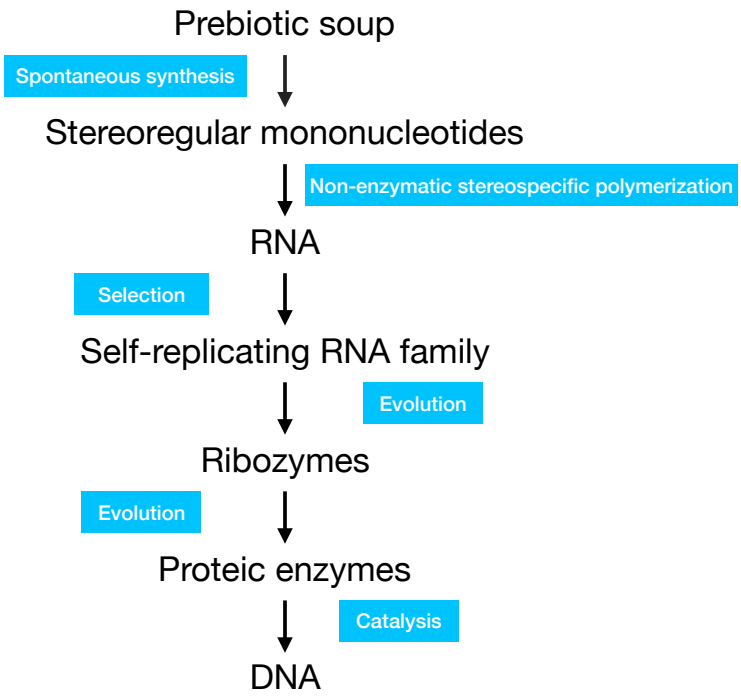

Figure 1.3. Origin of life, in the prebiotic RNA world scenario. Adapted from Luisi (2006).

decrease if, for instance, the environment becomes simpler (Ofria et al., 2003). Therefore, a central question for the plausibility of the RNA world is the identification of complex and information-rich environments that allow both the spontaneous emergence of replicators and their evolvability (Walker, 2017). By contrast, alternative scenarios propose that replicating polymers such as RNA could arise only after primordial living systems based on metabolism (Kauffman, 1986; Sharov, 2009; Walker, 2017; Vasas et al., 2012; Hordijk et al., 2010, 2018b; Xavier et al., 2020). In the next section we introduce these other hypotheses for the origin of life.

1.2.2 Metabolism-first: (auto)catalytic networks

The metabolism-first hypothesis proposes that the advent of a genetic apparatus has been preceded by the emergence of a prebiotic metabolism, based either on organic or inorganic molecules (Anet, 2004). Many of this scenarios usually assume that "life began with a mutually sustaining set of catalytic reactions involving small molecules" (Shapiro, 2000). Therefore, life is considered to emerge as a collective self-reproducing system of organic reactions, in which inorganic molecules or ions (instead of the current efficient enzymes) act as catalysts, and polypeptides and proteins are not necessarily determined by a genetic apparatus (Kauffman, 1993; Anet, 2004). Hereafter, we refer to a set of chemical species capable of mutually catalyse each other's production through chemical reactions (generally

assuming a basic set of resources provided by the external environment), with the term AS (Kauffman, 1971, 1986, 1993). The notion of AS captures the idea of a system capable of spontaneously emerging and self-reproducing, using the resources at its disposal. Here, the role of the catalysts is to accelerate biochemical reactions by several orders of magnitude, making dynamically feasible reactions whose proceeding would otherwise be impossible in a biological context (Wolfenden and Snider, 2001). Therefore, ASs potentially meet the requirements for minimal life introduced in Section 1.1 (for results and discussion regarding self-replication and biological evolution of ASs, see Part II). Several authors have proposed the emergence of ASs as an alternative scenario to the replication-first approach to the origin of life (Kauffman, 1971, 1986, 1993; Dyson, 1985; De Duve, 2003; Eigen and Schuster, 1977; Gánti, 1997; Letelier et al., 2006; Rosen, 1991). However, notice that, as mentioned in Section 1.2, an approach to metabolism based on catalytic networks is, in principle, not in contrast with the presence of information-storage molecules (such as RNA) in the first life forms (Mulkidjanian and Galperin, 2007; Hordijk et al., 2010; Vasas et al., 2012; Hordijk et al., 2018b; Xavier et al., 2020). For instance, the concept of *minority control* introduced in Kaneko and Yomo (2002); Kamimura and Kaneko (2010) attempts to unify catalytic networks with the presence of a pseudo-genetic core, represented by few molecules that control the reproduction rate of the entire system, actually storing the information about its reproduction.

The lipid world

An example of metabolism-first model is represented by the *Graded Autocatalysis Replication Domain* (GARD) model (Segrè et al., 2000, 2001b,a). The GARD model numerically simulates, via stochastic algorithms (Gillespie, 1976, 1977), the behaviours of noncovalent molecular assemblies, attempting to provide an inheritance mechanism not based on information-carrying polymers. In particular, let N_G denote the size of a molecular repertoire, $n_1, n_2, \cdots, n_{N_G}$ the (internal to the assembly) molecular counts and ρ_i the external concentration of molecular species i. The GARD model assumes that each molecule joins and leaves the assembly via uncatalysed forward and backward reactions of rate κ_f and κ_b, respectively. The rates κ_f and κ_b are assumed to be equal for all the molecules. The dynamics of the systems is governed by the the differential equations:

$$\frac{dn_i}{dt} = (\rho_i \kappa_f N - \kappa_b n_i)(1 + \frac{1}{N} \sum_{j=1}^{j=N_G} \beta_{ij} n_j), i = 1, 2, \cdots, N_G \tag{1.1}$$

where $N = \sum_{i=1}^{N_G} n_i$ is the assembly size and β_{ij} is the catalytic rate enhancement that species j exerts on species i. The values β_{ij} are drawn from a lognormal distribution, that is an approximation of the receptor affinity distribution (Lancet et al., 1993; Rosenwald

et al., 2002) The model simulates a growth-splitting process, in which a growing vesicle splits into two daughter assemblies. In particular, when the size of the assembly N reaches a threshold value, each molecule of the progenitor is assigned to each of the daughter with a probability of 0.5. Under these conditions, it has been shown that the compositional information of an assembly is transferred to its daughter (Segrè et al., 2000); notice that the choice of a lognormal distribution from which to extract the values of $\beta_{i,j}$ plays a crucial role to achieve this result (Segrè et al., 2001b).

However, the GARD model has been criticised for showing little capability to evolve in a Darwinian sense (Szathmáry, 2000; Vasas et al., 2010). Moreover, it has been pointed out that its mathematical apparatus has a poor connection with real chemical systems (Dyson, 1985; Anet, 2004). These are general critics moved to the concept of AS (Dyson, 1985; Lifson, 1997; Szathmáry, 2000; Vasas et al., 2010). Nevertheless, recent experimental results (Ashkenasy et al., 2004; Hayden et al., 2008; Sievers and Von Kiedrowski, 1994; Taran et al., 2010) and theoretical advances (Hordijk and Steel, 2004; Hordijk et al., 2011) make ASs convincing candidates as systems at the origin of life (Hordijk and Steel, 2017; Vasas et al., 2012; Walker, 2017; Xavier et al., 2020).

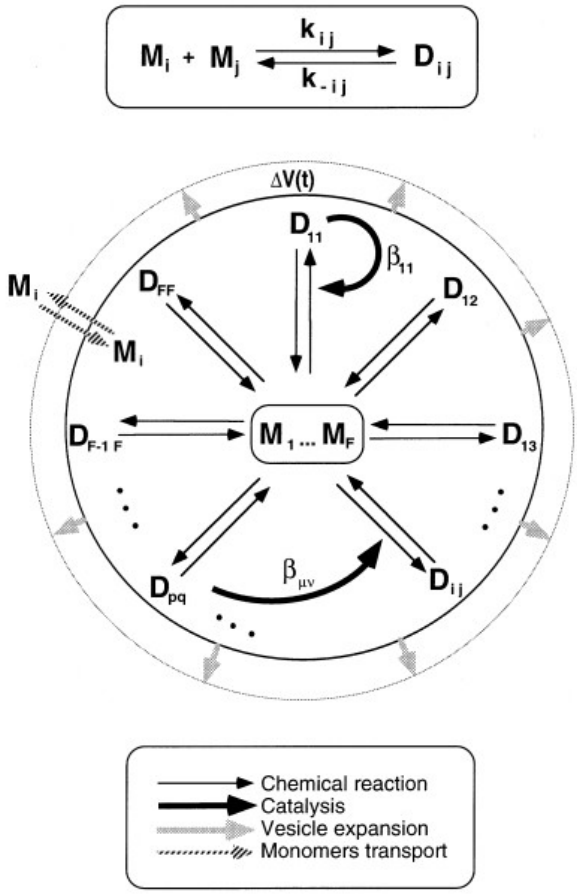

Figure 1.4. An example of a metabolism-first model: the GARD model. A vesicle contains monomers and dimers connected by reactions $M_i + M_j \rightleftharpoons D_{ij}$. The wall of the vesicle is impermeable to the dimers, while monomers are supplied from outside the system. The vesicle expansion arrows indicate the volume increment $\Delta V(t)$ in the time interval Δt. When the size of the assembly reaches a threshold value, the vesicle divides into two daughter cells, transferring the compositional information (Segrè et al., 2000). From Segrè et al. (1998)

Chapter 2

Reflexively Autocatalytic and Food-generated sets

Recently, a formal definition of ASs has been proposed in the context of graph theory by the RAF theory (Hordijk and Steel, 2004; Hordijk et al., 2011). This allowed to overcome some limits associated with ASs, and to make evident their relevance in the context of the origin of life. In particular, RAF theory has successfully proved that ASs (or *RAF sets*, using the nomenclature of RAF theory) are highly likely to exist in a catalytic reaction system (Hordijk and Steel, 2004; Mossel and Steel, 2005; Hordijk et al., 2011; Hordijk and Steel, 2012a; Vasas et al., 2012), and RAF sets have been detected in the metabolic networks of Escherichia Coli (Sousa et al., 2015) and ancient anaerobic autotrophs (Xavier et al., 2020). Notice, moreover, that the notion or RAF sets is related to other network models of biochemical systems (Steel et al., 2013; Hordijk and Steel, 2017; Steel et al., 2019; Villani et al., 2014; Blokhuis et al., 2020), and it is easily connectable to autopoietic systems (Hordijk and Steel, 2015). Finally, RAF theory shows that RAF sets are usually composed by RAF subsets, (Hordijk et al., 2018b; Hordijk and Steel, 2012b, 2014), and it has been argued that (some of) these subsets could be the elementary units on which natural selection may act (Hordijk and Steel, 2014, 2012b; Vasas et al., 2012; Hordijk et al., 2018b,a). In the next sections, we present the RAF theory and some of the relevant results it has provided.

2.1 Basic theory: definition of RAF sets and the RAF algorithm

Within the framework of RAF theory (Hordijk and Steel, 2004; Hordijk et al., 2011), a network of interacting species is represented by a *Catalytic Reaction System* (CRS) (Lohn et al., 1998; Hordijk and Steel, 2004, 2017), that is a tuple (S, R, C, F) such that:

- S is the set of chemical species;

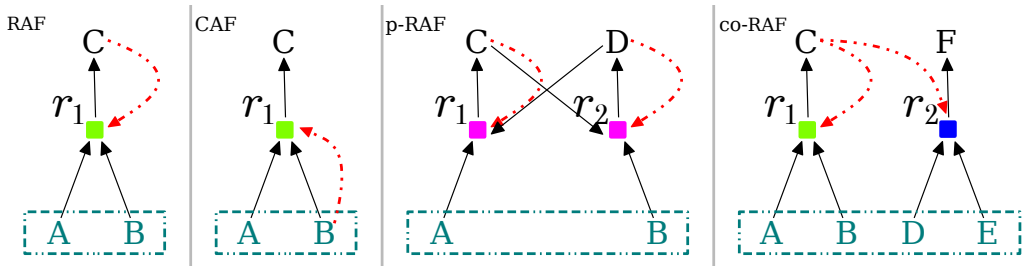

Figure 2.1. Example of RAF sets and similar structures introduced in Section 2.1. Species are represented by letters (dark-green for food-species, black for non-food species). The food set is surrounded by a dark-green dashed rectangle. Reactions are displayed by coloured squares. A black arrow emerging from a letter towards a square (from a square pointing at a letter) indicates the corresponding species is a source (a product) for that reaction. Red dashed arrows indicate catalyses. First panel: a RAF set consisting of the single reaction r_1 : A + B $\longrightarrow$ C and the catalysis (C, r_1). Notice that the F-generated property (Def. 1) is not longer satisfied if the food set is reduced, that is, if species A or species B (or both) are not considered as food-species. On the other hand, the reflexively autocatalytic property (Def. 1) is not longer satisfied if the catalysis set C is empty. Second panel: a CAF set consisting of the single reaction r_1 : A + B $\longrightarrow$ C and the catalysis (B, r_1). Notice that, contrary to what is shown in the first panel, in this case both the reactants and the catalyst of r_1 are available before the reaction occurs. Third panel: a p-RAF set consisting of the reactions $\{r_1$: A + D $\longrightarrow$ C, r_2 : B + C $\longrightarrow$ D$\}$ and the catalyses $\{(C, r_1), (D, r_2)\}$. Notice that this set of reactions does not satisfies the F-generated property (Def. 1), that is, it is not a RAF set. Fourth panel: a co-RAF set consisting of the reaction r_2 : D + E $\longrightarrow$ F and the catalysis (C, r_2). This set is not a RAF set, while the larger set of reactions $\{r_1$: A + B $\longrightarrow$ C, r_2 : D + E $\longrightarrow$ F$\}$, with catalyses $\{(C, r_1), (C, r_2)\}$, it is.

- R is the set of reactions, $\rho \rightarrow \pi$, where $\rho, \pi \subset S$ are the *reactants* and *products* of a reaction, respectively;
- C is the *catalysis* set, that is, a set of pairs $\{(s, r) : s \in S, r \in R\}$ indicating the species s as the *catalyst* of reaction r[1];
- $F \subset S$ is the *food* set, that is, a distinguished subset of S such that each species $s \in F$ is assumed to be available from the environment.

Let R' be a subset of R. The *closure* $cl_{R'}(F)$ is defined to be the (unique) minimal subset of S that contains F, together with all the species that can be produced from F by repeated applications of reactions in R'. Note that $cl_{R'}(F)$ is well defined and finite (Hordijk and Steel, 2004). In RAF theory, the notion of ASs is represented by the RAF sets.

Definition 1 (RAF set) *Given a CRS (S, R, C, F), a RAF set is a set of reactions $R' \subseteq R$ (and associated chemical species) that satisfies the following properties (Hordijk and Steel, 2004; Hordijk et al., 2011):*

i. Reflexively autocatalytic: for each reaction $r \in R'$ there exists at least one species $s \in cl_{R'}(F)$ such that $(s, r) \in C$;

ii. F-generated: for each reaction $r : \rho \rightarrow \pi, r \in R'$ and for each species $s \in S$ such that $s \in \rho$, it is $s \in cl_{R'}(F)$.

Thus, a RAF set is a set of reactions able to catalytically produce all its reactants starting from a suitable food set. Figure 2.1 shows an example of a RAF set. Authors in Hordijk and Steel (2004); Hordijk et al. (2011) show that, if a CRS has a RAF set, then it has a unique maximal RAF set which contains all other RAF sets. The maximal RAF set is denoted *maxRAF* set. Moreover, they introduce a polynomial time algorithm able to detect (if present) the maxRAF set of a generic CRS (S, R, C, F):

Algorithm 1 *(RAF algorithm, Hordijk et al. (2011))*

1. *Start with the complete set of reactions R and the food set F;*
2. *Compute the closure of the food set $cl_R(F)$ relative to the current set of reactions R;*
3. *For each reaction $r \in R$ for which (1) all catalysts, or (2) one or more reactants, are not in $cl_R(F)$, remove r from R;*
4. *Repeat steps 2 and 3 until no more reactions can be removed.*

[1]Notice that the catalyst s of a catalysis $(s, r) \in C$ is not required to be a reactant species of r.

If the resulting reaction set R' is empty, there is no RAF set in (S, R, C, F); otherwise, R' is the maxRAF set. The overall running time of the algorithm is $O(|R|^2 \log |R|)$ (worst-case), and, in practice, it is sub-quadratic on average (Hordijk and Steel, 2004; Hordijk et al., 2011). Note that the concept of a RAF set is related to other approaches to the formal description of metabolic networks (Steel et al., 2013; Hordijk and Steel, 2017, 2018), such as *(M,R)* systems (Rosen, 1991), *Chemical Organization Theory* (Dittrich and Speroni Di Fenizio, 2007) and *Hypercycles* (Eigen and Schuster, 1979). In particular, the latter are a special case of the more general notion of RAF set, with the additional constraint that all molecule types in the set must catalyse their own formation in addition to the formation of the other molecule types (Hordijk and Steel, 2017, 2018). Moreover, RAF sets are connected with the formalisation of ASs introduced in Jain and Krishna (1998) (Villani et al., 2014; Steel et al., 2019). Finally, other notions, similar to that of the RAF set, have been introduced by the RAF theory: the *Constructively Autocatalytic and F-generated* (CAF) sets (Mossel and Steel, 2005), the *pseudo-RAF* (or p-RAF) sets and the *co-RAF* sets (Steel et al., 2013). In particular, given a CRS (S, R, C, F), we call a subset $R' \neq \emptyset$ of R:

- CAF: if R' can be ordered, $r_1, r_2, \cdots, r_k$, so that, for each $i \geq 1$, each reactant of r_i and at least one catalyst of r_i is contained in the food set and/or is a product of an earlier reaction in the sequence (Steel et al., 2020);

- p-RAF: if for each $r \in R'$, each of the reactants of r and at least one catalyst of r are contained in $F \cup \pi(R')$, where $\pi(R')$ denotes the products of reactions in R' (Steel et al., 2020);

- co-RAF: if R' is a non-empty set for which there exists some RAF R'' set for (S, R, C, F), which is disjoint from R' and such that $R' \cup R''$ forms a RAF set for (S, R, C, F) (Steel et al., 2013).

Examples of a CAF set, a p-RAF set and a co-RAF set are shown in Figure 2.1. Informally, a CAF set is a (RAF) set of reactions that can take place on the condition that both their reactants and at least one catalyst are already made available by the occurrence of other catalysed reactions, starting from the food set F. Note that, due to these more restrictive requirements, CAF sets are less likely to appear in a chemical reaction system than RAF sets (Mossel and Steel, 2005). Furthermore, the structure of CAF sets is less "rich" than that one of the RAF sets (Mossel and Steel, 2005). A p-RAF set, instead, is not necessarily a RAF set. In fact, even if p-RAF sets satisfy some of the properties of RAF sets, they may not be able to build themselves up from the food set only. This peculiarity makes p-RAF sets not completely suitable as systems at the origin of life (Steel et al., 2020). Finally, co-RAF sets may not have a structure able to form RAF sets by themselves, but their (disjoint) union with other RAF sets can form a larger RAF set. In this case, a co-RAF set can be

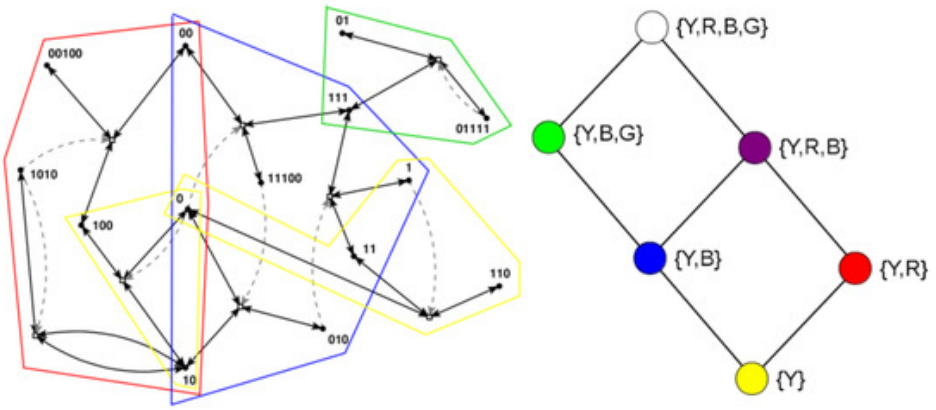

Figure 2.2. Closed RAF sets example. Left: an example of a RAF set. Black dots represent the chemical species, white boxes represent reactions. Each dot is labeled with a bit string, corresponding to a molecule type of the BPM (see Section 2.3). A black arrow emerging from a dot towards a box (from a box pointing at a dot) indicates the corresponding molecule is a reactant (a product) for that reaction. Dashed gray arrows indicate catalyses. Coloured polygons indicate some of the RAF subsets (the closed RAF subsets, see Section 2.2). Right: the six closed RAF sets within the RAF example and their mutual subset relationships. From Hordijk et al. (2018a).

viewed as the "periphery" of its associated RAF set, i.e., the RAF set can form and sustain both itself and the associated co-RAF set (Vasas et al., 2012; Steel et al., 2013).

It is important to underline that the definition of RAF (CAF, p-RAF, co-RAF) sets lies in the context of graph theory, and does not consider the dynamics underlying the reaction network. In particular, the set of catalyses C introduces a relationship between reactions and catalyst species, but does not give information on the specific (dynamical) catalytic process. Therefore, given a reaction $r : \rho \to \pi$ and a catalysis (s, r), the dynamics of the catalysed reaction could be modeled, for instance, either through considering a single reaction $r' : \rho + s \to \pi + s$ whose rate is proportional to the product of the concentrations of the reactants and the catalyst, or taking into account intermediate reactions involving ad-hoc introduced enzymatic species. We will return to the dynamical aspects of RAF sets in Part II, while in the next section we present some results regarding their structure.

2.2 The structure of RAF sets

RAF theory has shown that RAF sets usually have a complex structure, with the largest maxRAF set containing several *subRAF* sets (Hordijk et al., 2012; Steel et al., 2013). In particular, it is possible to identify two classes of subRAF sets that constitute a maxRAF set: the *irreducible RAF* (irrRAF) sets and the *closed RAF* sets. An irrRAF set is a subRAF set that cannot be reduced any further without losing the RAF property, i.e., removing any single reaction from an irrRAF set generates a set of reactions that is not a RAF set (Hordijk

and Steel, 2004). Given a CRS (S, R, C, F), the following result holds:

Theorem 1 *Hordijk et al. (2012)*

i. There exist RAF sets R' for which the number of irreducible RAF subsets is exponential in the number of molecules and reactions in R'.

ii. For any RAF set R', the number of maximal proper subRAF sets of R' can never exceed $|R'|$.

iii. Given a catalytic reaction system (S, R, C, F) and a RAF set $R' \subseteq R$, there exist polynomial time algorithms that solve the following problems:

(a) generate a list of all the maximal proper subRAF sets of R';

(b) determine whether or not R' is the union of two proper subRAF sets, and if so find all such pairs of subRAF sets;

(c) for any given non-empty subset of R', determine whether that subset is contained in every subRAF set of R'.

Thus, constructing an irrRAF set for (S, R, C, F) can be carried out in polynomial time; however, finding the smallest irrRAF set is, in general, NP-hard (Steel et al., 2013). The number of irrRAF sets, in fact, can grow exponentially with the size of (S, R, C, F) (Hordijk et al., 2012). This is, in principle, a significant result for the relevance of RAF sets in the context of the origin of life, each subRAF set being potentially connected with a biological unit capable of Darwinian evolution (Hordijk and Steel, 2014; Nghe et al., 2015). Nevertheless, it has been suggested that the actual elementary units on which natural selection can act could be the closed RAF sets (Hordijk and Steel, 2014; Smith et al., 2014; Hordijk et al., 2018b).

Definition 2 (Closed RAF set) *Given a CRS (S, R, C, F), a subset R' of R is said to be a closed RAF set if (Smith et al., 2014):*

i. R' is a RAF set;

ii. for each r such that all its reactants and at least one catalyst are either part of the set F or are produced by a reaction from R', it is $r \in R'$.

Figure 2.2 shows an example of a RAF set and the closed RAF sets contained in it. Note that the maxRAF set is always a closed RAF set (Smith et al., 2014). The importance of closed RAF sets is mainly due to their connection with the chemical organisation theory. In particular, the authors in Hordijk et al. (2018b) have shown that closed RAF sets are *chemical organizations* (the converse is not necessarily true)[2]. This suggests that closed

[2]Note that the connection between closed RAF sets and chemical organizations can be used to detect closed RAF sets in a generic CRS (Hordijk et al., 2018b).

RAF sets can be associated with the attractors of the dynamics of a CRS, thus being the relevant biological units within that CRS. In fact, given a reaction networks (S, R), where S is a set of molecule types and R is a set of reactions, that is, pairs of multisets over S indicating reactants and products, a chemical organisation $O \subseteq S$ is a set of molecule types that is (Dittrich and Speroni Di Fenizio, 2007):

- closed: none of the reactions that can be applied using only molecules from O generates any molecules that are not already in O;
- self-maintaining: let R_O be the set of reactions that can be applied using only molecules from O; then, all molecules in O that are consumed by reactions in R_O can be produced by reactions from R_O at a non-negative rate while all reactions in R_O have a strictly positive flux.

In particular, let ∇ be the *stoichiometric matrix* for the system, i.e., a matrix formed from the stoichiometric coefficients of each reaction, with rows indexed by molecules and columns by reactions (we will return on this definition in Section 5.3). The self-maintenance condition requires the existence of a flux vector J with strictly positive entries for which it is:

$$\nabla J \geq 0. \tag{2.1}$$

Therefore, if the dynamics of the system is governed by a differential equation of the form $\dot{c} = \nabla J(c(t))$, where $c(t)$ represents the state of the system at time t, then the molecular types with positive concentrations form a chemical organization (Dittrich and Speroni Di Fenizio, 2007; Peter and Dittrich, 2011). It is important to note, however, that not all chemical organisations are stable. In particular, taking dynamics into account, molecular species can disappear even if belonging to a chemical organisation (Dittrich and Speroni Di Fenizio, 2007).

2.3 The occurrence of RAF sets

A fundamental property that an AS must satisfy is the ability to form spontaneously. RAF theory has shown that RAF sets emerge in random chemical systems once a sufficiently complex suite of molecules and reactions is achieved. In particular, it has been shown that a (chemically plausible) linear growth rate in the level of catalysis, i.e., the expected number of reactions that each molecule catalyses, is sufficient for RAF sets to occur with high probability in a simple chemical reaction model based on polymer ligation and cleavage (Hordijk and Steel, 2004; Mossel and Steel, 2005; Hordijk et al., 2011; Vasas et al., 2012). To see this result, let $S = S(n)$ be the set of sequences of length at most n over the alphabet set $\{0, 1, \cdots, k-1\}$, and let F (the food set) be a distinguished subset of S consisting of all species of length less than or equal to a fixed length l_f, that is, $F = S(l_f), l_f < n$. Let $R(n)$ be

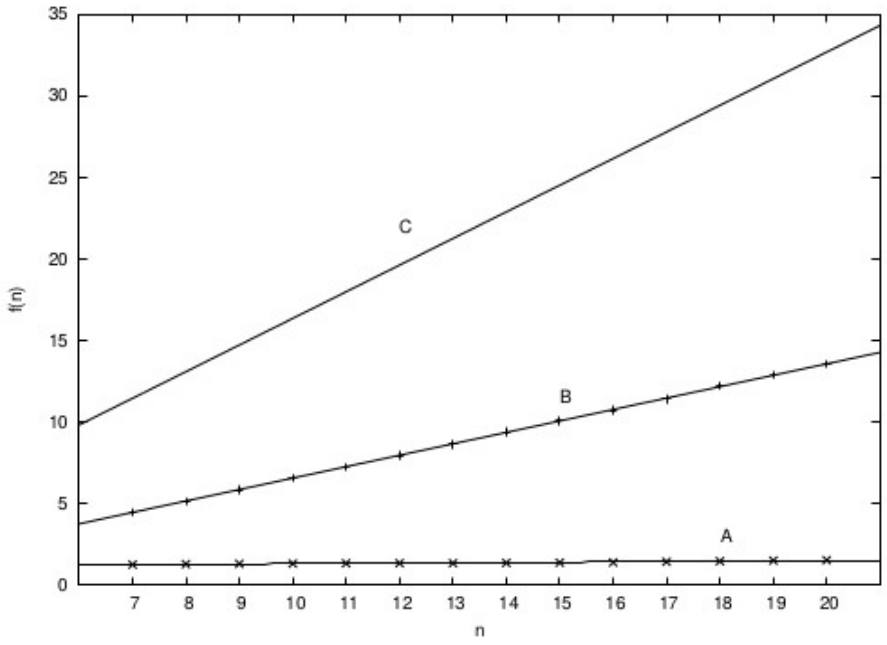

Figure 2.3. Required levels of catalysis for the occurrence of RAF sets in the BPM. See Section 2.3 for further details. On the x-axis: length n of the largest molecules in the system. On the y-axis: average level of catalysis $f(n)$ for which RAF sets occurring with high probability in a number of instances of the BPM, with the probability of catalysis not depending on chemical species. A: computational case for any RAF sets. B: computational case for all-molecule RAF sets. C: theoretical case for all-molecule RAF sets. From Hordijk et al. (2011).

the reaction set consisting of concatenation of two sequences resulting in a longer sequence (condensation), and cutting of a sequence into two smaller ones (cleavage). Finally, let each molecule $s \in S$ catalyse any given reaction $r \in R$ with probability $p(s)$. Notice that this chemical reaction model, to which we refer with the symbol $Q(n)$, is a generalisation of the *Binary Polymer Model* (BPM) introduced by Kauffman (1986) (the BPM is obtained from $Q(n)$ by imposing $k = 2$, see Section 3.3 for further details). Due to the random choice of the catalysis set, $Q(n)$ is usually referred to as a *random catalytic reaction system* (Hordijk and Steel, 2004). Let $P(n)$ be the probability that there exists a RAF set in $Q(n)$ that involves all molecule types, and let $f(n, s)$ denote the expected number of reactions that each molecule catalyses:

$$f(n, s) = p(s)|R(n)|. \tag{2.2}$$

The following result holds:

Theorem 2 *(Mossel and Steel, 2005) Consider a random catalytic reaction system $Q(n)$. Let $P(n)$ be the probability that there exists a RAF set in $Q(n)$ that involves all molecule types. Suppose that $f(n, s) \geq \lambda n$ for all $s \in S$, where $\lambda > \ln(k)$. Then,*

$$P(n) \geq 1 - \frac{k(ke^{-\lambda})^{l_f}}{1 - ke^{-\lambda}} \quad (\rightarrow 1 \text{ as } \lambda \rightarrow \infty). \tag{2.3}$$

Similar results are obtained in numerical simulations (Hordijk and Steel, 2004; Hordijk et al., 2011). In particular, setting $k = l_f = 2$, the authors of Hordijk et al. (2011) compare the required levels of catalysis for RAF sets to occur in $Q(n)$ with high probability for three cases:

A) Computational case for any RAF set;

B) Computational case for RAF sets that involve all molecule types in S;

C) Theoretical case for RAF sets that involve all molecule types in S.

The obtained data are shown in Figure 2.3 (see Hordijk et al. (2011) for simulations details). Table 2.1 presents the linear relations estimated from the simulation data or calculated from the theoretical analysis (from Hordijk et al. (2011)). Notice the discrepancy between the computational (cases *A*, *B*) and theoretical (case *C*) results: although the theoretically predicted level of catalysis grows fairly quickly, the actual value grows very slowly. Therefore, even for large systems, a RAF set occurs with high probability if each molecule catalyses (on average) between one and two reactions at least, which is a chemically highly plausible condition (Hordijk et al., 2011). Moreover, the conditions necessary for the emergence of RAF sets are compatible with those of chemical systems, both as regards the required molecular complexity, and in the case of more realistic models which introduce, for instance, a template-based catalysis (Hordijk et al., 2011). In conclusion, it is reasonable to

Table 2.1. The empirical (cases A and B) and theoretical (case C) linear relations.

A	$f(n) =$	1.0970 $0.0189n$	+
B	$f(n) =$	0.4736 $0.7012n$	+
C	$f(n) =$	$1.6339n$	

assume that RAF sets appear in (minimal) models of polymer chemistry (Hordijk et al., 2011; Vasas et al., 2012).

2.4 Biological relevance of RAF sets

We conclude this chapter by showing interesting results that directly connect RAF sets with real metabolic networks. Authors in Sousa et al. (2015) have shown that the best-studied metabolic network of *Escherichia coli* contains a RAF set. By applying the RAF algorithm, they have shown that the 98% of the full reaction network of the bacterium constitutes a (max)RAF set, consisting of 1787 reactions (only 39 reactions of the full network are not part of the maxRAF set) and about 1200 associated molecule types (Sousa et al., 2015). Table 2.2 shows the reactions (grouped in functional categories) that form the maxRAF sets. Remarkably, such an analysis pointed out the crucial role of metals and molecules such as ATP as obligatory autocatalytic metabolites, constraining the requirements for spontaneous chemical evolution (Sousa et al., 2015).

RAF structures are present, moreover, in the metabolism of ancient prokaryotic species (Xavier et al., 2020). In particular, RAF sets have been detected both in the metabolism of the acetogenic bacterium *Moorella thermoacetica* and the methanogenic archaeon *Methanococcus maripaludis*. Figure 2.4 shows the reactions (grouped, again, in functional categories) that constitute the RAF sets found. Notice that methanogens and acetogens are supposed to reflect the ancestral state of microbial physiology in the bacteria and archaea (see Xavier et al. (2020) for details and references). The intersection of the two RAF sets allows to identify a primordial network preceding the methanogen and the acetogen, able to produce fundamental organic molecules such as amino acids and nucleotides, starting from a simple food set. Using the words of the authors, "as far back as we could look in metabolic evolution, RAF sets were found". Moreover, the analysis carried out on the detected RAF sets indicates that the size and the complexity of such networks can be increased by the incorporation of organic cofactors (Xavier et al., 2020). To summarise, the existence of RAF sets within real metabolic networks, and in particular within the metabolism of ancient anaerobic autotrophs, suggests that ASs are at the basis of the emergence of metabolism, possibly preceding RNA in the chemical evolution at the origin of life (Hordijk et al., 2010;

Table 2.2. The number of reactions per functional category in the maxRAF sets within the metabolic network of Escherichia coli. From Sousa et al. (2015).

Functional category	Reactions
Alanine and Aspartate Metabolism	11
Alternate Carbon Metabolism	217
Anaplerotic Reactions	11
Arginine and Proline Metabolism	45
Cell Envelope Biosynthesis	135
Citric Acid Cycle	23
Cofactor and Prosthetic Group Biosynthesis	235
Cysteine Metabolism	13
Folate Metabolism	11
Glutamate Metabolism	6
Glycerophospholipid Metabolism	150
Glycine and Serine Metabolism	17
Glycolysis/Gluconeogenesis	34
Glyoxylate Metabolism	4
Histidine Metabolism	12
Inorganic Ion Metabolism	32
Lipopolysaccharide Biosynthesis / Recycling	39
Membrane Lipid Metabolism	78
Methionine Metabolism	16
Methylglyoxal Metabolism	10
Murein Recycling	20
Nitrogen Metabolism	13
Nucleotide Salvage Pathway	173
Oxidative Phosphorylation	65
Pentose Phosphate Pathway	19
Purine and Pyrimidine Biosynthesis	35
Pyruvate Metabolism	23
Threonine and Lysine Metabolism	25
Tyrosine, Tryptophan, and Phenylalanine Metabolism	29
Unassigned	21
Valine, Leucine, and Isoleucine Metabolism	23
tRNA Charging	23
Catalysts Reaction	219
Total	1787

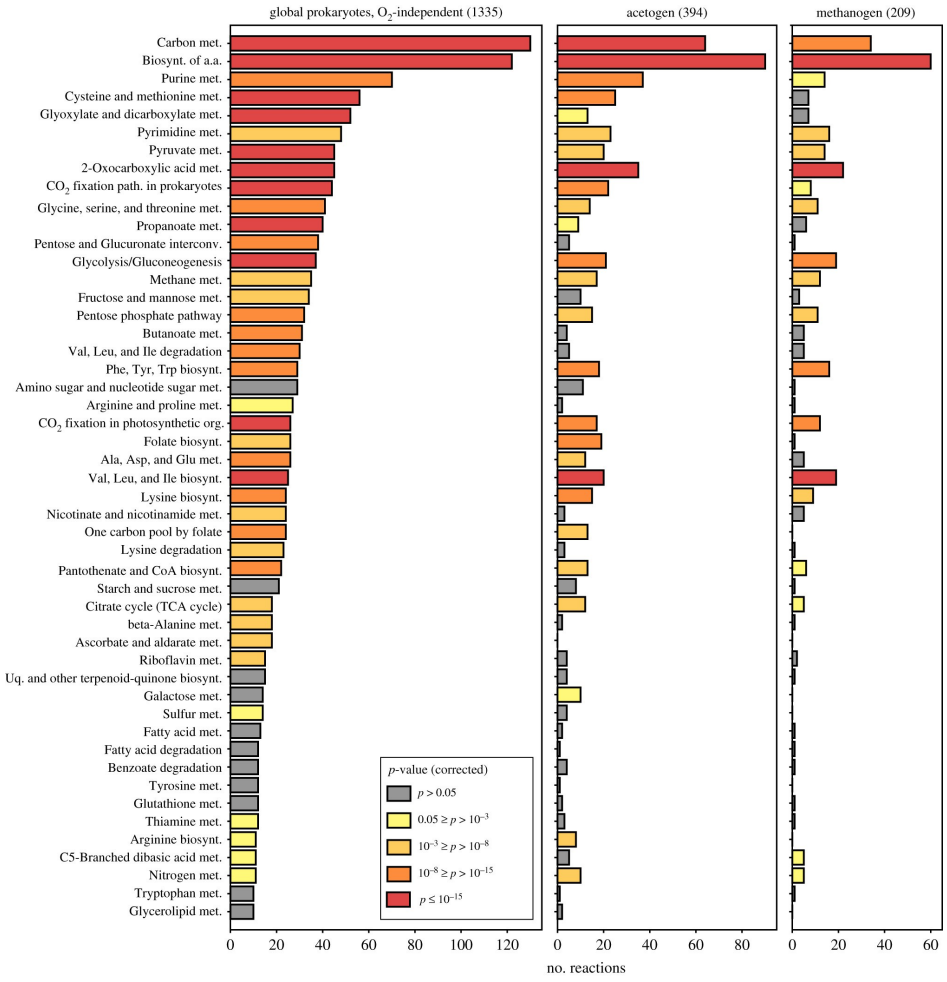

Figure 2.4. The number of reactions per functional category for three maxRAF sets within the global O2-independent prokaryotic network, acetogen (Ace) and methanogen (Met). From Xavier et al. (2020).

Vasas et al., 2012; Hordijk et al., 2018b; Xavier et al., 2020).

Part II

Dynamics of RAF sets: self-reproduction and evolvability

Summary

The RAF theory shows that RAF sets have a realistic probability to exist in a generic CRS, and it has been shown that RAF sets are present in real chemical systems (see Section 2.3 and Section 2.4). In this part, we discuss their dynamical behaviour. In particular, we address the issue of the emergence of a RAF set, that is, its dynamical appearance. This aspect is closely related to self-reproduction. Indeed, the dynamical emergence of a RAF set implies the production of the components of the network via the chemical reactions of the network itself. The dynamical behaviour of RAF sets is connected also with their *evolvability*, i.e., the capacity of experiencing adaptive evolution. Adaptive evolution pertains to the collection of evolutionary changes that are beneficial for survival and reproduction in a given environment. It has been argued that the autocatalytic subsets present within the structure of a maxRAF set could be the elementary units on which natural selection can act (Hordijk and Steel, 2014; Vasas et al., 2012; Hordijk et al., 2018a): the availability of spontaneous reactions would allow the occurrence of mutations and, consequently, the appearance of novel autocatalytic subsets with different dynamical behaviours; their simultaneous existence would then result in competition and selection. In particular, it has been suggested that the closed RAF sets could be the relevant units for adaptive evolution (Smith et al., 2014; Hordijk et al., 2018b,a).

However, the actual evolvability of ASs has been criticised (Vasas et al., 2010, 2012), and first numerical results show that the asymptotic dynamics of simple RAF sets eventually reaches the state in which all the reactions of the maxRAF set occur catalytically (Vasas et al., 2012; Hordijk et al., 2018a). In this state, all the elementary autocatalytic units coexist without effectively competing with each other, thus leaving no room for adaptive evolution (Vasas et al., 2012, 2010; Hordijk et al., 2018a). The evolvability of RAF sets can be restored by embedding them into compartments and allowing the sharing of resources and the exchange of chemical molecules (Vasas et al., 2012; Hordijk et al., 2018a; Kauffman, 2011; Serra and Villani, 2019). For instance, through numerical simulations, it has been observed that RAF sets enclosed in semipermeable protocells can reach different asymptotic states (Serra and Villani, 2019), and that spatially separated RAF sets consuming the same food source can give rise to different combinations of competing autocatalytic subsets (Hordijk et al., 2018a), suggesting that the evolvability of RAF sets is related to the interactions among RAF sets themselves (see Figure 2.5). In Chapter 3 we investigate this latter point, while in Chapter 4 we study more generally the connection between the topology and the dynamics of RAF sets.

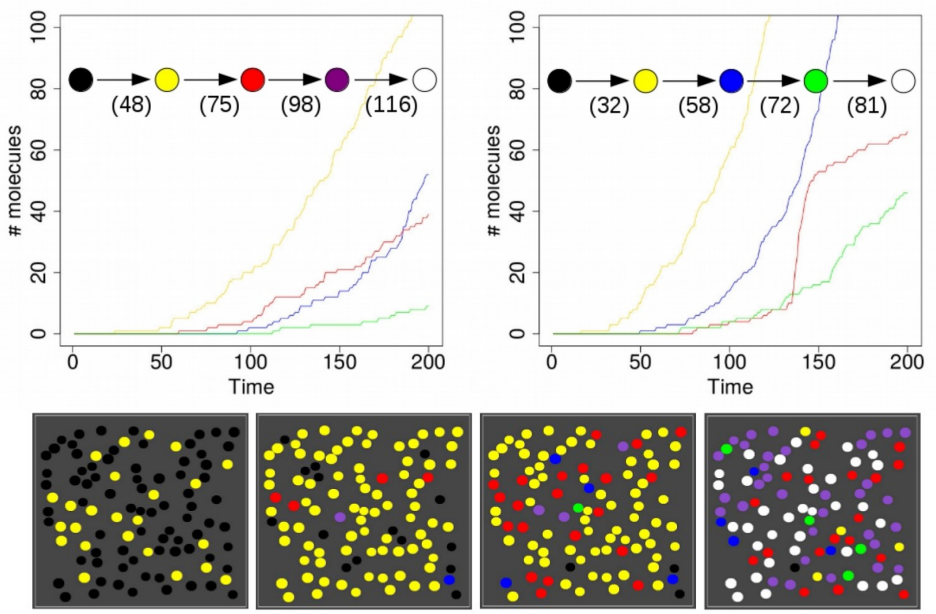

Figure 2.5. Dynamics of simple RAF sets. Each color corresponds to an emerged closed RAF set. Above: two simulation runs of a RAF set within a single compartment. The stochasticity of the simulations results in different intermediate states, but eventually the maxRAF set always emerges (white circle). Below: dynamics of a population of compartments embedding copies of the same RAF set. Different states are reached by different compartments. The RAF set used in the simulations is shown in Figure 2.2. Adapted from Hordijk et al. (2018a).

Chapter 3

Impact of composition on the dynamics of RAF sets

3.1 Introduction

In this chapter we study the role of various interactions among RAF sets, in order to understand how these interactions affect the emergent dynamics. To this aim, we use the Stochastic Petri nets formalism (Molloy, 1982; Haas, 2006) to represent and evolve RAF sets. Furthermore, we introduce some composition operations acting on nets, which correspond to different interactions among RAF sets. In this framework, assuming that the entire maxRAF set always emerges in an isolated RAF set, our goal is to find some composition operations under which the dynamical appearance of the maxRAF set is not invariant. This means that the corresponding interaction causes only some of the maxRAF subsets to emerge, allowing the existence of multiple long-term behaviours required for the evolvability of RAF sets.

The chapter is organised as follows. In Section 3.2 we introduce the definitions of Stochastic Petri nets. In Section 3.3 we describe the model we use to evolve nets and we introduce the composition operations. In Section 3.4 we present and analyse the results obtained by simulating the dynamics of various composed RAF sets. Finally, in Section 3.5 we discuss the conclusions.

3.2 Background: Stochastic Petri nets

A *Petri net* consists of (see Petri and Reisig (2008) for further details):

– a finite set of places P;

– a finite set of transitions W;

– functions $b, e : P \times W \to \mathbb{N}$.

Here $b(p, w)$ and $e(p, w)$ are the number of edges from place p to transition w and from transition w to place p, respectively. The sets $b(w) \subset P$ and $e(w) \subset P$ are the sets of places connected to transition w by at least one edge. A *marking* X of a Petri net is a map $X : P \to \mathbb{N}$ that assigns to each place a discrete number of marks called *tokens*. In fact, a marking X identifies a state of the system in the space of possible configurations of tokens available in each place. With x_p we indicate the number of tokens of place p available in marking X. Firing a transition w consumes $b(p, w)$ tokens from each of its input places $p \in b(w)$, and produces $e(p', w)$ tokens in each of its output places $p' \in e(w)$. For each marking X, a transition w is *enabled* (it may fire) if there are enough tokens in its input places making the consumption possible. This shall occur, if and only if $X(p) \geq b(p, w)$, $\forall p \in P$. A *Stochastic Petri net* (SPN) (Molloy, 1982; Haas, 2006) is a Petri net for which each transition is equipped with a (possibly marking-dependent) rate for the exponentially distributed transition firing times. λ denotes the set of firing rates of a SPN. Note that the evolution of a SPN with exponentially distributed transition rates is isomorphic to continuous-time Markov chain (Molloy, 1982; Grimmett, 2020).

Petri net formalism provides a suitable environment for studying the composition of networks, with both a computational and theoretical approach; the latter, in particular, in the context of category theory (Baez and Pollard, 2017). Moreover, this formalism can describe nets with different dynamics (Vazquez and Silva, 2011). Finally, Petri nets can be used to model *cellular automata* (Von Neumann, 1966; Schaller and Svozil, 2009), which in turn are powerful tools for studying the phenomena of self-reproduction and cellular self-assembly (Ishida, 2014). These characteristics make the model we introduce easily generalisable, and suitable for future studies on the composition of AS in different contexts.

3.3 The model

3.3.1 Building the net

Given a CRS (S, R, C, F) (or, in particular, a set of reactions and associated species that is a RAF set), we build a SPN by adding a place p for each species $s \in S$ and a transition w for each reaction $r \in R$ such that $b(w) = \rho(r)$ and $e(w) = \pi(r)$, where $\rho(r)$ and $\pi(r)$ are the sets of reactants and products species of r, respectively. Moreover, for each catalysis $(s, r) \in C$ we add a transition w such that $b(w) = \rho(r) \cup s$ and $e(w) = \pi(r) \cup s$. Finally, let 0 be a pseudo-species representing the environment. For each $s \in F$, we add a transition i_s such that $b(i_s) = 0$ and $e(i_s) = s$, that is, i_s is an input transition producing a food species. Furthermore, we introduce outflow transitions o_s such that $b(o_s) = s$ and $e(o_s) = 0$. Thus, the SPN is a flow reactor that allows inflow and outflow of species from and towards the

environment. Hereafter, we use S and R to indicate both species and reactions of a CRS and places and transitions of a SPN.

The rates $\lambda(r)$ associated with each transition r are marking dependent rates:

$$\lambda(r) = h_r(X)\lambda_r. \tag{3.1}$$

Here, λ_r is a fixed constant depending on the type of its corresponding reaction in the CRS ($\lambda_r = \{\lambda_s, \lambda_c, \lambda_i, \lambda_o\}$ in which each λ_r specifies spontaneous, catalysed, inflowing and outflowing reactions, respectively) and $h_r(M)$ is a value proportional to the number of combinations of tokens available in the input places of transition r in the state X. Thus, explicitly, we shall have:

$$h_r(X) = \frac{\prod_j b(j,r)}{V^{|b(r)|-1}} \prod_j \binom{x_j}{b(j,r)}, \tag{3.2}$$

where V is an arbitrary constant that takes into account the volume of the system and the product is among all the input places of transition r. We set functions b and e such that the inflowing transitions do not consume tokens of the pseudo-species 0 and produce a fixed value of tokens of the food species, while the outflowing transitions consume a token of the outflowing species and do not produce tokens of the pseudo-species 0. Thus, the rate of outflowing transitions is proportional to the amount of tokens of the outflowing species, while the rate of inflowing transitions is independent of the state of the system. It is noteworthy that the inflowing of food elements still remains a stochastic event. We add inflowing transitions for species not belonging to the originary food set F (setting the rate of such a transition equal to zero), if required for the purpose of composition between nets (see Section 3.3.2). The dynamics of the obtained SPN is described by the stochastic mass action kinetics, that is the classical dynamics used to represent chemical reactions, assuming a well-stirred system (Anderson and Kurtz, 2011).

The CRSs used in this work are generated according to the BPM (Kauffman, 1986). The BPM produces a CRS where the species set S consists of all bit strings up to (and including) a maximum length N, and the reaction set R consists of condensation and cleavage reactions. Condensation reaction is a concatenation of two bit strings resulting in a longer string, and cleavage reaction cuts a bit string into two smaller ones. The food set is represented by all species with a length less than or equal to a fixed length l_f (we set $l_f = 2$), and each species can be a catalyst of each reaction with a certain probability fixed a priori. We chose to only allow the condensation reactions to occur in the system. Therefore, we focus on CRSs with irreversible reactions only. Notice, however, that the technique we use is applicable in the case where also cleavage reactions are allowed[1], that is, when all reac-

[1] Although the composition rules we have introduced can be applied with no differences to CRSs with both irreversible and reversible reactions, including cleavage reactions would produce networks, in principle,

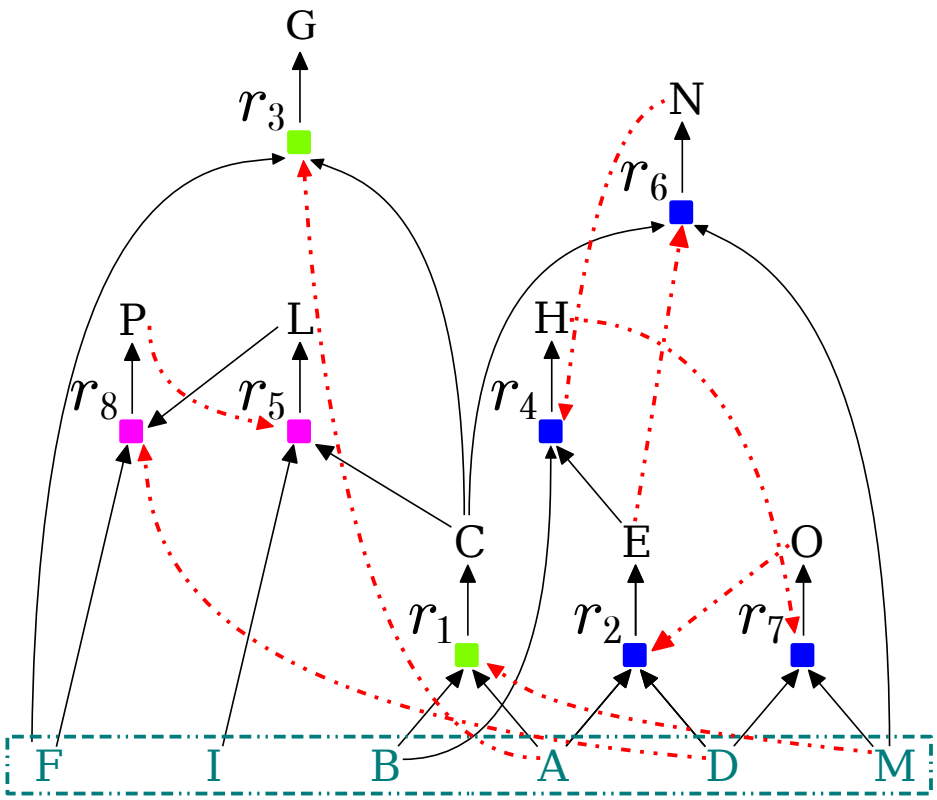

Figure 3.1. RAF set example. Species are represented by letters (dark-green for food-species, black for non-food species). The food set is surrounded by a dark-green dashed rectangle. Reactions are displayed by coloured squares. A black arrow emerging from a letter towards a square (from a square pointing at a letter) indicates the corresponding species is a source (a product) for that reaction. Red dashed arrows indicate catalyses. The maxRAF set consists of three closed RAF sets: $R^{(1)} = \{r_1, r_3\}$ (green squares), $R^{(2)} = \{r_1, r_3, r_5, r_8\}$ (magenta and green squares), $R^{(3)} = \{r_1, r_3, r_2, r_4, r_6, r_7\}$ (blue and green squares).

tions are reversible. In fact, none of the operations we introduce in Section 3.3.2 is affected by the reversibility of the network.

With this limitation, all the spontaneous reactions of our model are binary reactions (i.e., reactions with two reactants, possibly of the same species type), while all the catalysed reactions are ternary reactions. Even if ternary reactions are rare, they can represent a first approximation of two or more elemental reactions, such as the sequence of reactions of an enzyme catalysis (Gillespie, 2007).

Figure 3.1 shows an example of a RAF set and its constituent closed RAF sets, used in our analysis. We exemplify our point by introducing a set of species $S = \{A, B, C, D, E, F, G, H, I, L, M, N, O, P\}$ and a food set $F = \{A, B, D, F, I, M\}$. In this

exhibiting different dynamics with respect to systems with condensation reactions only, since a network with reversible reactions can have different topology with respect to the equivalent irreversible network (Feinberg, 1995). We will return on this aspect in Chapter 4.

example, the RAF set is composed of the following reactions (a species above the arrow of a reaction indicates the catalyst associated with that reaction):

$$r_1 : \mathrm{A} + \mathrm{B} \xrightarrow{\mathrm{M}} \mathrm{C}$$
$$r_2 : \mathrm{A} + \mathrm{D} \xrightarrow{\mathrm{O}} \mathrm{E}$$
$$r_3 : \mathrm{C} + \mathrm{F} \xrightarrow{\mathrm{A}} \mathrm{G}$$
$$r_4 : \mathrm{B} + \mathrm{E} \xrightarrow{\mathrm{N}} \mathrm{H}$$
$$r_5 : \mathrm{C} + \mathrm{I} \xrightarrow{\mathrm{P}} \mathrm{L}$$
$$r_6 : \mathrm{C} + \mathrm{M} \xrightarrow{\mathrm{E}} \mathrm{N}$$
$$r_7 : \mathrm{D} + \mathrm{M} \xrightarrow{\mathrm{H}} \mathrm{O}$$
$$r_8 : \mathrm{F} + \mathrm{L} \xrightarrow{\mathrm{D}} \mathrm{P}$$

The maxRAF set consists of three closed RAF sets: $R^{(1)} = \{r_1, r_3\}$, $R^{(2)} = \{r_1, r_3, r_5, r_8\}$, $R^{(3)} = \{r_1, r_3, r_2, r_4, r_6, r_7\}$. Notice that the closed RAF set $R^{(1)} = \{r_1, r_3\}$ is also a CAF set (Mossel and Steel, 2005). The full list of the simulated reactions is the following:

$r_1 : \mathrm{A} + \mathrm{B} \longrightarrow \mathrm{C}$	$r'_1 : \mathrm{A} + \mathrm{B} + \mathrm{M} \longrightarrow \mathrm{C} + \mathrm{M}$	$i_A : 0 \longrightarrow \mathrm{A}$	$o_A : \mathrm{A} \longrightarrow 0$
$r_2 : \mathrm{A} + \mathrm{D} \longrightarrow \mathrm{E}$	$r'_2 : \mathrm{A} + \mathrm{D} + \mathrm{O} \longrightarrow \mathrm{E} + \mathrm{O}$	$i_B : 0 \longrightarrow \mathrm{B}$	$o_B : \mathrm{B} \longrightarrow 0$
$r_3 : \mathrm{C} + \mathrm{F} \longrightarrow \mathrm{G}$	$r'_3 : \mathrm{C} + \mathrm{F} + \mathrm{A} \longrightarrow \mathrm{G} + \mathrm{A}$	$i_D : 0 \longrightarrow \mathrm{D}$	$o_D : \mathrm{D} \longrightarrow 0$
$r_4 : \mathrm{B} + \mathrm{E} \longrightarrow \mathrm{H}$	$r'_4 : \mathrm{B} + \mathrm{E} + \mathrm{N} \longrightarrow \mathrm{H} + \mathrm{N}$	$i_F : 0 \longrightarrow \mathrm{F}$	$o_F : \mathrm{F} \longrightarrow 0$
$r_5 : \mathrm{C} + \mathrm{I} \longrightarrow \mathrm{L}$	$r'_5 : \mathrm{C} + \mathrm{I} + \mathrm{P} \longrightarrow \mathrm{L} + \mathrm{P}$	$i_I : 0 \longrightarrow \mathrm{I}$	$o_I : \mathrm{I} \longrightarrow 0$
$r_6 : \mathrm{C} + \mathrm{M} \longrightarrow \mathrm{N}$	$r'_6 : \mathrm{C} + \mathrm{M} + \mathrm{E} \longrightarrow \mathrm{N} + \mathrm{E}$	$i_M : 0 \longrightarrow \mathrm{M}$	$o_M : \mathrm{M} \longrightarrow 0$
$r_7 : \mathrm{D} + \mathrm{M} \longrightarrow \mathrm{O}$	$r'_7 : \mathrm{D} + \mathrm{M} + \mathrm{H} \longrightarrow \mathrm{O} + \mathrm{H}$		
$r_8 : \mathrm{F} + \mathrm{L} \longrightarrow \mathrm{P}$	$r'_8 : \mathrm{F} + \mathrm{L} + \mathrm{D} \longrightarrow \mathrm{P} + \mathrm{D}$		

3.3.2 Composition

We model interactions between CRSs as composition operations[2] between SPNs. First, notice that RAF sets satisfy the following conditions (hereafter, we refer to these as the *inclusion conditions*) (Hordijk and Steel, 2004):

[2]For an in-depth formal description of compositional rules among graphs representing chemical systems, see Andersen et al. (2018).

- if R'_1 is RAF in (S_1, R_1, C_1, F_1), it is RAF also in (S_2, R_2, C_2, F_2), if conditions $S_1 \subseteq S_2,\ R_1 \subseteq R_2,\ C_1 \subseteq C_2,\ F_1 \subseteq F_2$ are satisfied;
- if R'_1 is RAF (S_1, R_1, C_1, F_1) and R'_2 is RAF in (S_2, R_2, C_2, F_2), then $R'_1 \cup R'_2$ is RAF in $(S_1 \cup S_2, R_1 \cup R_2, C_1 \cup C_2, F_1 \cup F_2)$.

Thus, if composition does not remove species from the food set or reactions belonging to a RAF set, it will not have any impact on its RAF property. However, the dynamical behaviour of the composed system can be, generally, different from that of the starting one.

Let $(S_1, R_1, b_1, e_1, \lambda_1)$ and $(S_2, R_2, b_2, e_2, \lambda_2)$ be two SPNs and let I, O be subsets of their inflowing and outflowing transitions sets. Let $\sim$ be the equivalence relation such that $s \sim s'$ if $i_s \in I$ and $o_{s'} \in O$ for some choice of I, O. $S_\sim$ denotes the set of places identified by relation $\sim$. We define the following composition operations (a possible bio-inspired interpretation will be provided below):

$\mathrm{CO_I}$:

$$(S_1, S_2) \to S_* = S_1 \cup S_2;$$
$$(R_1, R_2) \to R_* = (R_1 \cup R_2 \cup R_I) \setminus (O_1 \cup I_2);$$
$$(b_1, b_2) \to b_* = b_1 \cup b_2 \cup b_I;$$
$$(e_1, e_2) \to e_* = e_1 \cup e_2 \cup e_I;$$
$$(\lambda_1, \lambda_2) \to \lambda_* = \lambda_1 \cup \lambda_2 \cup \lambda_I;$$
$$R_I := \{r \,|\, b(r) = s,\ e(r) = s',\ \forall\ s \in S_1, s' \in S_2 \text{ such that } s \sim s'\};$$
$$\lambda_I := \{\lambda(r) \,|\, \lambda(r) = h_r(X)\lambda_f,\ \forall\ r \in R_I\}.$$

$\mathrm{CO_{II}}$:

$$(S_1, S_2) \to S_* = S_1 \cup S_2;$$
$$(R_1, R_2) \to R_* = (R_1 \cup R_2 \cup R_{II}) \setminus (O_1 \cup I_2);$$
$$(b_1, b_2) \to b_* = b_1 \cup b_2 \cup b_{II};$$
$$(e_1, e_2) \to e_* = e_1 \cup e_2 \cup e_{II};$$
$$(\lambda_1, \lambda_2) \to \lambda_* = \lambda_1 \cup \lambda_2 \cup \lambda_{II};$$
$$R_{II} := \{r \,|\, b(r) = b(r'),\ e(r) = b(r''),\ \forall\ r'' \in R_2 \text{ such that } b(r'') \subset S_\sim,\ b(r') \sim b(r'')\};$$
$$\lambda_{II} := \{\lambda(r) \,|\, \lambda(r) = h_r(X)\lambda_f,\ \forall\ r \in R_{II}\}.$$

$\mathrm{CO_{III}}$:

$$(S_1, S_2) \to S_* = \{S_1 \sqcup S_2\}/\sim;$$
$$(R_1, R_2) \to R_* = R_1 \cup R_2;$$
$$(b_1, b_2) \to b_* = b_1 \cup b_2;$$
$$(e_1, e_2) \to e_* = e_1 \cup e_2;$$
$$(\lambda_1, \lambda_2) \to \lambda_* = \lambda_1 \cup \lambda_2.$$

Here λ_f is a constant value and $(S_*, R_*, b_*, e_*, \lambda_*)$ is the composed SPN. To summarise, all the composition operations we define relate a set of places S that are input for outflowing transitions of a SPN, together with a set of places S' that are input for inflowing transitions of another SPN. The formal addition of inflowing transitions for places not belonging to the food set enlarges the possible composition operations between SPNs.

Given a set $S_\sim$, operation CO_I adds a transition from S to S' for each pair of places in $S_\sim$, while operation CO_{II} adds a transition from S to S' for each combination of places that appears as input of a transition in the inflowing net. Each combination corresponds to the definition of complex [3] in the framework of chemical reaction networks (Feinberg, 1995). In fact, given a set of chemical species, a complex is defined as a member of the vector space generated by the species that provide the inputs (or the outputs) of a reaction (Feinberg, 1995; Anderson and Kurtz, 2011). We will return on this notion in Chapter 4.

Both operations CO_I and CO_{II} introduce a flux of species from one net to another. The composite network can therefore be seen as the union of two separate networks that evolve in parallel, communicating only via (asymmetrical) exchange of chemical species. This could be, for instance, the case of two spatially separated protocells, one of which can release molecules towards the other. According to this interpretation, the flowing rate λ_f is a parameter that encompasses the characteristics of the flow process (for example, cell permeability). Operation CO_{III}, instead, merges each pair of places in $S_\sim$, allowing transitions of the two original SPNs to operate on the glued set of places. Composing nets via operation CO_{III} actually produces a new single network. In this case, one can think of composite net as the result of mutations that enlarge a network (for instance, net 1), introducing new possible reactions and, consequently, new chemical species (corresponding to net 2).

It is worth to underline that, if there exists a $s \in S_\sim$ such that $s \in F$, operations CO_I and CO_{II} can actually modify the RAF property of net 2. In particular, if transitions $r \in R_{(I,II)}$ are assumed to be spontaneous transitions ($\lambda_f < \lambda_c$), net 2 could not be catalytically produced starting from the food set F. In this case, the composed net contains a RAF set R' such that $R_1 \subseteq R' \subset (R_1 \cup R_2)$, with $R_1 = R'$ if $F \subseteq S_\sim$. Instead, if transitions $r \in R_{(I,II)}$ are assumed to be (auto) catalysed transitions ($\lambda_f \geq \lambda_c$), the whole composed net shall be a RAF set.

3.4 Results and Discussion

In this section, we present the results regarding the impact of composition on the dynamics of RAF sets as follows: we first introduce the characteristics of simulations and the quan-

[3] Note that complexes play a major role in the framework of chemical reaction networks theory. For instance, the deficiency theorems (Feinberg, 1995) are able to predict whether the dynamics of a large class of networks will have a stationary distribution, starting from the topology of the reaction graph having complexes as nodes. See Chapter 4 for further details

tities taken into account, while in Section 3.4.1 we present results for the non-interacting nets, in order to have a reference model for the interacting cases, presented in Section 3.4.2.

Starting from different instances of the BPM with $N < 8$, we use the RAF algorithm introduced in Hordijk et al. (2011) (see Section 2.1) in order to detect and select three different RAF sets, each of which contains more than one closed RAF set. Notice that, even if different RAF sets have the same species set S, the set of reactions R will be different; i.e., various RAF sets have different chemistry. The RAF sets identified through this procedure constitute the collection on which we will carry out the study. Even if such a small collection cannot be taken as a solid statistical basis, it is still sufficient for providing us with interesting information. We duplicate each RAF set and let it interact with its copy by switching to representation of RAF set as an SPN and using one of the composition operations introduced above. We simulated the dynamics of the system using the standard Gillespie algorithm (Gillespie, 1976, 1977), setting the volume of the system at $V = 1$ (arbitrary units). For each simulation, we perform 100 independent runs of 10^6 time steps. One of the necessary conditions for a RAF set is the ability to produce itself starting from the elements of the food set. Indeed, the initial state of the SPN is set such that:

$$\begin{cases} x_s(t=0) = x_0 \text{ if } s \in F; \\ x_s(t=0) = 0 \text{ otherwise.} \end{cases} \tag{3.3}$$

Here x_0 is an arbitrary constant. The values of x_0, λ_c, λ_i and λ_o are set such that the number of tokens of food places at $t \to \infty$ is equal to 10^5, for an SPN with inflow, outflow and all (and only) binary transitions having, as input, food places only (and firing rate λ_c). The value of λ_s is fixed at $\lambda_s = \lambda_c/10$, while λ_f varies such that $\lambda_f \in [\lambda_c 10^{-1}, \lambda_c 10^6]$. It is noteworthy that the values of these parameters are not taken from "in vivo" data, but they have phenomenological motivations. Thus, although we can reasonably generalise the characteristics of the dynamics, quantities such as the species' production rate or the time evolution of the concentrations may differ from those in other similar stochastic simulations (Hordijk and Steel, 2012a; Hordijk et al., 2018a).

We focus our attention on the effective appearance of a maxRAF set during the evolution of the system. In particular, we introduce the following quantities:

1) $M_s(t) = \sum_s \frac{1}{1+x_s(t)}$, $\forall s \notin F$;

2) $\tau_i = \min\{t \,|\, n(r) \geq i, \forall r \in R\}$.

Here $n(r)$ is the number of executions of transition r, and R is the maxRAF set. Notice that the natural condition $x_s(t) \geq 0$ implies that each term contributing to the computation of $M_s(t)$ can assume, at most, the value one. Both $M_s(t)$ and τ_i are calculated for each single net that forms the composed net. Let $m_M = \overline{M_s(t)}$ be the mean value of $M_s(t)$ with respect to time for large t, that is, $m_M = 1/t \int_0^t M_s(t')dt'$, $t \gg 1$. If all the non-food

species of a maxRAF set are efficiently produced, then $M_s(t) \to 0$ for large t and $m_M \approx 0$. However, the definition of a RAF set does not ensure that all the species associated with such a set are present in large amount during the evolution of the system. For instance, a non-food species that is a source for a transition of a RAF set could be continuously consumed by that transition as soon as it is produced, resulting in a fluctuating evolution of its number of tokens. For this reason, we consider a less restrictive condition than $m_M \approx 0$ for the emergence of a maxRAF set. In particular, for large t, we require a strictly positive concentration for all non-food species and a high concentration for most of them. This implies that the relation $\frac{1}{1+x_s} < 1$ holds for all the terms contributing to the calculation of M_s, and that the relation $\frac{1}{1+x_s} \approx 0$ holds for most of them. Thus, we introduce the following condition:

$$m_M < 1. \tag{3.4}$$

We assume that, if condition (3.4) holds, the entire maxRAF set emerges.

Notice, moreover, that different growing rates among species of a RAF set correspond to different effective firing rates of the transitions. Therefore, even if a maxRAF set R appears, the time τ necessary to perform all the transition of R can exhibit different slopes during the evolution of the net, based on the various effective rates of subsets of R. We use the slope m_τ of the straight line $y_\tau(i) = m_\tau i + q_\tau$ that approximates τ_i for $i \to \infty$ in order to compare the efficiency of the (total) self-reproduction of different RAF sets. We summarise the results obtained from the simulated composition operations and the different RAF sets of our collection through a scatter plot showing the values (m_M, m_τ) averaged over independent runs (Figure 3.7).

3.4.1 Non interacting nets

We start investigating the non interacting nets by simulating the evolution of three isolated RAF sets that constitute the collection, in order to obtain the dynamics that will be a basis for comparison for the evolution of the composite nets. Figure 3.2 shows the time evolution of the number of tokens of non-food species for the isolated RAF set represented in Figure 3.1. Hereafter, we refer to this simulation as "reference", since it will be used as a benchmark for the other simulations. It is evident that, after a transient time of approximately 0.06 time units, all the species associated with the RAF set grow in number, with the exception of species C: C is the only species in the set to be a source for more than one transition (Figure 3.1). The green line in Figure 3.3 shows the corresponding trend of $M_s(t)$. As expected, after the same transient time of $\approx$ 0.06 time units, $M_s(t)$ decreases down to values close to zero, the entire maxRAF set appears and condition (3.4) is satisfied (Figure 3.7).

We find that the asymptotic dynamics of simple isolated RAF sets is not affected by changing the initial state (notice that this is not the case, for instance, in the simulations

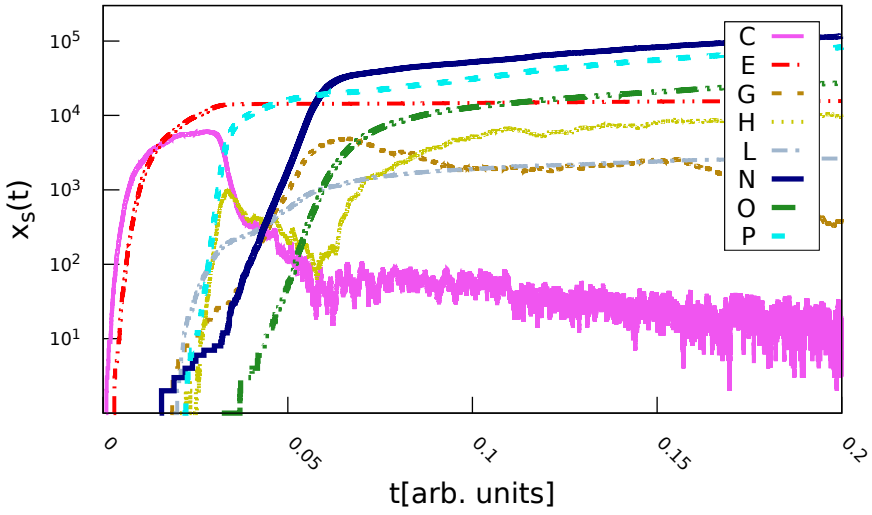

Figure 3.2. Isolated RAF set. Number of tokens over time of non-food species obtained in a simulation run of the isolated RAF set shown in Figure 3.1. After a transient time of $t \approx 0.006$ (arbitrary units) all the species are present in a large amount, with the exception of the species C which is repeatedly consumed by more than one reaction of the RAF set.

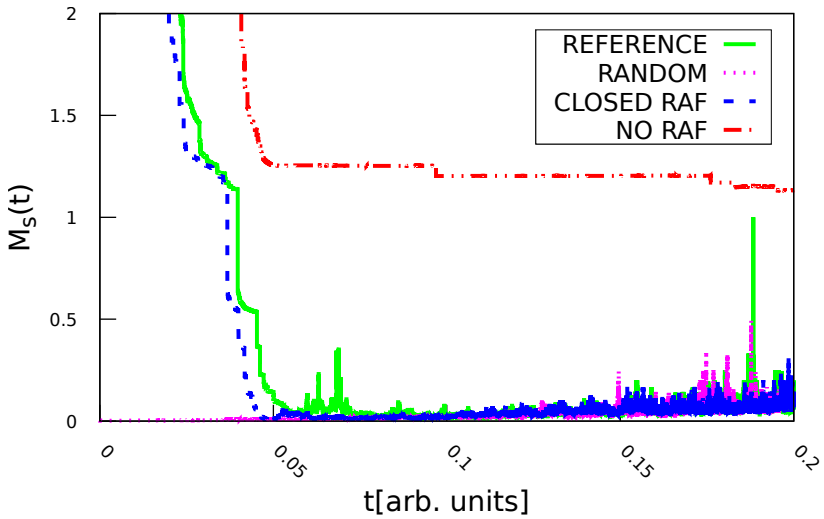

Figure 3.3. Total production of non-food species by isolated nets. $M_s(t)$ obtained in a simulation run of the isolated RAF set shown in Figure 3.1 for different initial conditions: solid green line (reference simulation): $x_s(t = 0) = 100$ if $s \in F$, $x_s(t = 0) = 0$ otherwise; dotted magenta line: $x_s(t = 0) = 100$ if $s \in F$, $x_s(t = 0) = rand(0, 10^4)$ otherwise; dashed blue line: $x_s(t = 0) = 100$ if $s \in F$, $x_s(t = 0) = 10^4$ if $s \in \{E, H, N, O\}$, $x_s(t = 0) = 0$ otherwise. After a transient time of $t \approx 0.006$ (arbitrary units) $M_s(t)$ always takes values close to zero, indicating that the maxRAF set has emerged for all the different tested configurations. Dash-dotted red line: net that failed to be a RAF set, obtained by switching off the catalysis $(D, 8)$ in the RAF set shown in Figure 3.1. In this case, $M_s(t)$ is always greater than 1, indicating that more than one non-food species is not efficiently generated by transitions of the system, or that at least one of them is not produced at all.

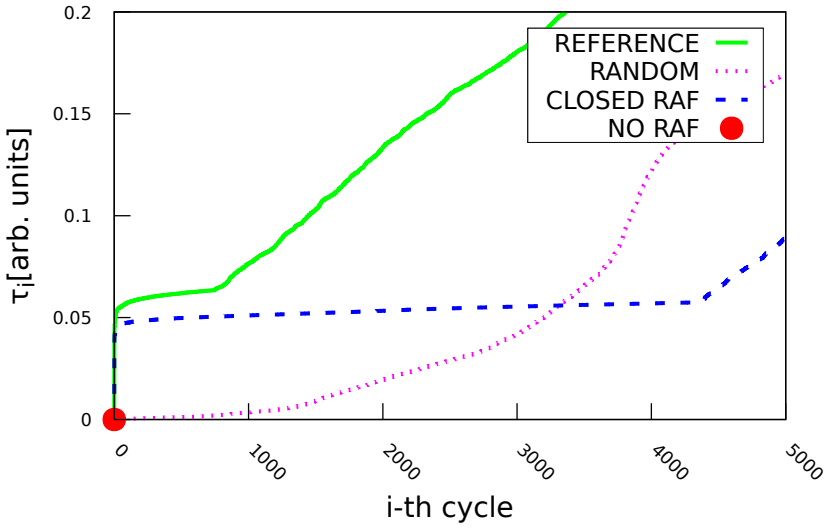

Figure 3.4. Cycles of transitions completed by isolated nets. τ_i obtained for the isolated RAF set shown in Figure 3.1 with different initial conditions: solid green line (reference simulation): $x_s(t=0) = 100$ if $s \in F$, $x_s(t=0) = 0$ otherwise; dotted magenta line: $x_s(t=0) = 100$ if $s \in F$, $x_s(t=0) = rand(0, 10^4)$ otherwise; dashed blue line: $x_s(t=0) = 100$ if $s \in F$, $x_s(t=0) = 10^4$ if $s \in \{E, H, N, O\}$, $x_s(t=0) = 0$ otherwise. The similar slope of τ_i for $t \to \infty$ associated with different tested configurations indicates that, after a transient time, the efficiency of performing all the transitions of the RAF set does not depend on the initial conditions. Red circle: the net that failed to be a RAF set, obtained by switching off the catalysis $(D, 8)$ in the RAF set shown in Figure 3.1. In this case, the net is not able to perform all its transitions.

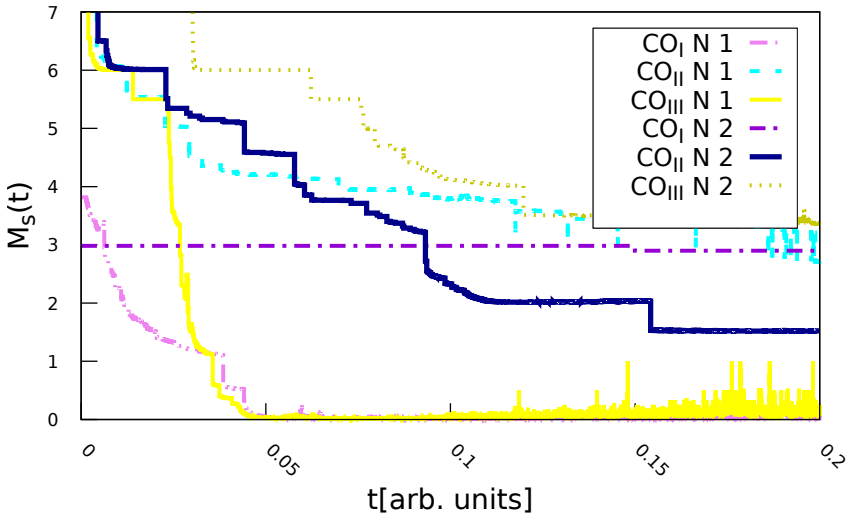

Figure 3.5. Total production of non-food species by composite nets. $M_s(t)$ is obtained for two copies of the RAF set shown in Figure 3.1 with different composition operations. For each composite net, two $M_s(t)$ are calculated, each from the species associated with the original copies. Dash-dotted magenta line: operation CO_I, net 1, $\lambda_f = 10^5\lambda_c$. Dashed cyan line: operation CO_{II}, net 1, $\lambda_f = 10^5\lambda_c$. Solid yellow line: operation CO_{III}, net 1. Dash-dotted violet line: operation CO_I, net 2, $\lambda_f = 10^5\lambda_c$. Solid blue line: operation CO_{II}, net 2, $\lambda_f = 10^5\lambda_c$. Dotted dark-yellow line: operation CO_{III}, net 2, delayed. For all composite operations, $M_s(t)$ of net 2 does not satisfy the condition stated by Eq. (3.4) that results in the emergence of the maxRAF set. For operation CO_{II}, both the maxRAF sets of net 1 and net 2 do not emerge.

performed in Serra and Villani (2019)). This is obvious from Figure 3.3 and Figure 3.4 by comparing the trends of $M_s(t)$ and τ_i obtained for the same RAF set for various initial conditions. In particular, we perform different simulations by setting $x_s(t = 0)$ equal to a random number less than 10^4 for all non-food species of the maxRAF set, and by setting $x_s(t = 0) = 10^4$ for only those species associated with a particular closed RAF set. For all the RAF sets in the collection, the resulting values of m_M and m_τ are in agreement with those corresponding to the initial conditions described by Eq. (3.3) (Figure 3.7). Conversely, the dynamics emerging in a net that failed to be a RAF set is significantly different (Figure 3.3 and Figure 3.4, red lines).

These results suggest once again that simple RAF sets have an effective advantage in self-reproduction over non-RAF set. Also, the structure of RAF sets alone is not sufficient to guarantee the presence and the dynamical selectability of different long-term behaviours. Using the dynamics of isolated RAF sets as reference, we can now move on to the dynamics of composed RAF sets.

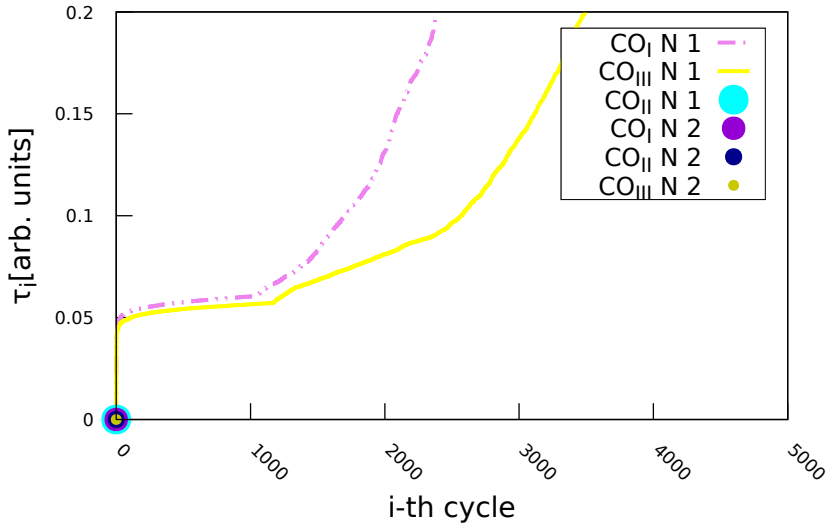

Figure 3.6. Cycles of transitions completed by composite nets. τ_i is obtained for two copies of the RAF set shown in Figure 3.1 with different composition operations. For each composite net, two τ_i are calculated, each from the transitions associated with the original copies. Dash-dotted magenta line: operation CO_I, net 1, $\lambda_f = 10^5\lambda_c$. Solid yellow line: operation CO_{III}, net 1. Large cyan circle: operation CO_{II}, net 1, $\lambda_f = 10^5\lambda_c$. Intermediate violet circle: operation CO_I, net 2, $\lambda_f = 10^5\lambda_c$. Intermediate blue circle: operation CO_{II}, net 2, $\lambda_f = 10^5\lambda_c$. Small dark-yellow circle: operation CO_{III}, net 2, delayed. For all composite operations, net 2 is not able to execute all its transitions. For operation CO_{II}, both net 1 and net 2 do not perform a complete cycle of transition of the RAF set.

3.4.2 Composite nets

In order to compose nets, we choose five different sets $S_\sim$: the set of places belonging to the food set, the set of places non belonging to the food set, the set of places corresponding to the molecules of length $l = l_f + 1$ and $l \leq l_f + 1$ of the BPM and the set of places that are not input places for spontaneous transitions (not selected for operation $\mathrm{CO_{II}}$). We compose copies of the RAF sets according to the composition operations CO_I, CO_{II} and CO_{III}. The initial states of the nets are set according to Eq. (3.3). Moreover, for operation CO_{III}, simulations are performed in which the transitions belonging to net 2 cannot proceed for a certain time interval of 10^4 time steps. Hereafter, we refer to this particular configuration as the "delayed configuration".

We find that composition operations do not have any impact on the emergence of the maxRAF sets for any choice of $S_\sim$ that does not include food species (Figure 3.7). However, a primordial form of biological interactions can be established; namely, facilitation and cheating. In particular, in nets composed through operations CO_I and CO_{II}, inflowing of external species can facilitate the appearance and the sustenance of a RAF set, improving its production efficiency. At the same time, withdrawing species produced by a RAF set can counteract its production. These aspects are well highlighted by various trends of the generated m_τ due to different conditions.

On the other hand, as expected, composition operations involving the food set have a major role on the emergence of the maxRAF set. Figure 3.5 and Figure 3.6 show the behaviour of $M_s(t)$ and τ_i associated with two RAF sets that are composed by operations CO_I, CO_{II} and CO_{III} for $S_\sim = F$. Similar trends are obtained from the composition of the other RAF sets in our collection. Results show that operations CO_I and CO_{II} prevent the entire maxRAF set in at least one of the two copies from emerging. In particular, we find that, if the rate λ_f of transitions allowing the flux of food elements from net 1 to net 2 is low enough ($\lambda_f < 10^6 \lambda_c$), operation CO_I prevents the emergence of the maxRAF set in net 2, while net 1 exhibits the same dynamics of the isolated net, as can be concluded from Figure 3.7. On the other hand, for the same composition operation, if the rate λ_f is sufficiently high ($\lambda_f \geq 10^6 \lambda_c$), the flow of food elements is such that the maxRAF set of net 1 does not contain available resources to perform all its transitions, while net 2 evolves as it is isolated and able to draw food directly from the environment (Figure 3.7). For operation CO_{II}, we have achieved significantly different results. In this case, we find different threshold values $\lambda_f = (\lambda_{f1}, \lambda_{f2})$ (depending on the specific RAF set of the collection) such that the emergence of the maxRAF set in net 2 is prevented for $\lambda_f \leq \lambda_{f1}$, while the opposite situation is obtained for $\lambda_f \geq \lambda_{f2}$. Moreover, for intermediate values $\lambda_{f1} < \lambda_f < \lambda_{f2}$, no maxRAF set emerges but only some of the closed RAF sets (Figure 3.5 and Figure 3.6). Therefore, for this range of values, the flux of species is such that both nets 1 and 2 have enough food elements to fire transitions and perform (complementary) subsets of the maxRAF set,

namely, the closed RAF sets. Furthermore, the stochastic nature of the flow process allows the emergence of different closed RAF sets in each run, hence showing the possible selectability of asymptotic dynamics for composite nets.

The observed dynamics lead to some important considerations: first, it is clear that the actual availability of resources is a crucial element in the dynamical realisation of a RAF set, and the rate at which food elements enter the net is as relevant as the definition of the food set itself, as expected. Moreover, the differences emerging due to the impact of the CO_I and CO_{II} operations suggest that the complexes play an important role in the dynamics of the RAF sets, even if they are defined starting from the single species. We will investigate these points in Chapter 4. Finally, as previously observed in (Hordijk et al., 2018a), biological interactions different from competition among RAF sets are plausible.

It is also intriguing that an effective competition can emerge if two nets share the same food, as in case of composition operation CO_{III} and $S_\sim$. In particular, we observed that in the delayed configuration, the presence of the maxRAF of net 1 prevents the emergence of the maxRAF of net 2. In fact, once the maxRAF of net 1 has had enough time to appear, the number of tokens of its associated species increases. Since the effective rate of a transition is proportional to the number of tokens of its sources, species of net 1 have an higher chance of reacting with respect to their counterparts belonging to the delayed net 2. Most of the food elements are therefore consumed by transitions of net 1. Once activated, only some of the transitions of net 2 are able to be performed efficiently, leading to the emergence of only some of the closed RAF sets which constitute the maxRAF set of net 2. Different runs show that the emerging closed RAF sets can vary due to the stochastic nature of the system evolution, thus guaranteeing the selectability of the different long-term behaviours and meeting the basic requirements for evolutionary processes (Vasas et al., 2012; Hordijk and Steel, 2014; Hordijk et al., 2018a).

This result is in contrast with the previous ones where it has been observed that isolated RAF sets are not able to experiment different asymptotic dynamics. In fact, composing two RAF sets using operation CO_{III} produces a composite net in which all transitions form a (larger) RAF set (see the inclusion conditions, Section 3.3.2), and the effect of the delay can be seen as a selection of a particular initial state. However, the same composite net is not able to produce competition if the delay is not introduced. Also, an effective competition between closed RAF sets has not been observed in an isolated net with initial conditions containing RAF sets already emerged at time $t = 0$ (Figure 3.7, Figure 3.3 and Figure 3.4).

We suggest that key elements for this form of competition are both the structure of the composite RAF set and the particular choice of initial conditions. In fact, in nets composed by operation CO_{III} and $S_\sim = F$, each transition that consumes at least one food species as a source or a catalyst, always has at least one competitor represented by its copy. By contrast, the hierarchical structure of RAF sets does not guarantee such a level of compe-

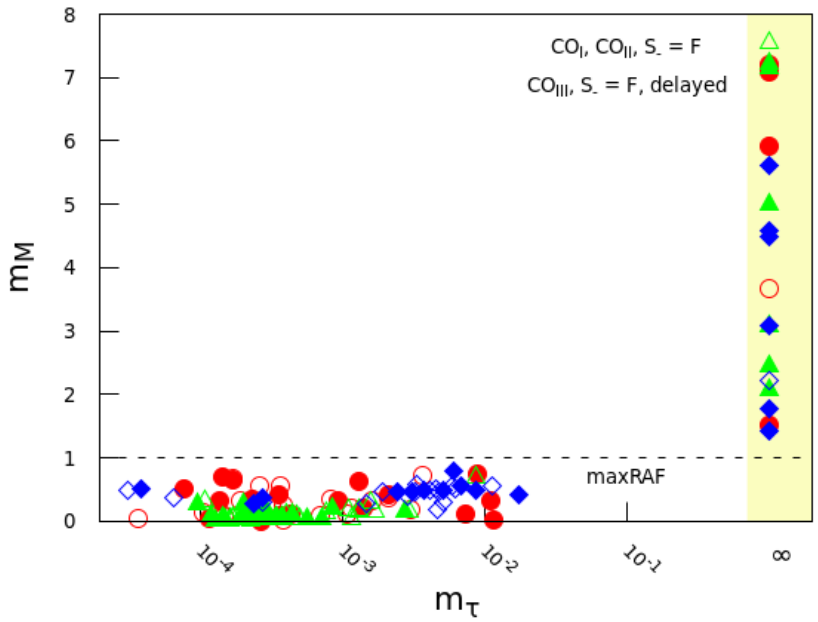

Figure 3.7. Impact of composition operations on the emergence of the maxRAF set. On the x-axis: slope m_τ of the straight line fitting τ_i for $t \to \infty$. On the y-axis: $m_M = \overline{M_s(t)}$, where $\overline{\cdots}$ is the average over time for $t \to \infty$. Notice that both values shown for m_τ and m_M are obtained by further averaging these quantities over 100 independent runs. For each run, both m_τ and m_M are calculated for $t \geq \frac{5}{6} t_f$, where t_f signifies the end of the simulation run. Green triangles: RAF set 1 (Figure 3.1). Red circles: RAF set 2. Blue squares: RAF set 3. Empty points: net 1. Filled points: net 2. Yellow shaded region indicates values corresponding to $m_\tau \to \infty$, obtained for composition operations CO_I, CO_{II}, CO_{III} (delayed) and $S_\sim = F$.

tition between different close RAF sets. Moreover, the delay brings the system into a state that promotes the formation of some subsets of the RAF set. The system can hardly reach this state only through random fluctuations. The results presented in this section show that these two conditions allow RAF sets to have different accessible asymptotic dynamics.

3.5 Discussion and conclusions

In this chapter we studied the impact of composition operations on the dynamics of simple RAF sets. This allowed us to test whether the interactions among RAF sets permit different long-term dynamical behaviour of the RAF sets themselves, that is a necessary condition for evolvability. To this aim, we generated various RAF sets starting from different instances of the BPM and represent RAF sets as SPNs. Moreover, we introduced composition operations that, acting on SPNs, correspond to interactions among RAF sets. We found that, if the composition operations do not involve the food species of a RAF set, the dynamics of the system always reaches a state in which all the composed RAF sets

appear. However, how fast the RAF sets emerge and their efficiency in self-reproduction depend on the exchange of species, showing that the composition operations can give rise to interactions with ecological features.

On the other hand, composition operations involving food species hinder the appearance of, at least, one of the two original RAF sets, giving rise to possible different long-term behaviours. In particular, if the food species can be exchanged between one RAF set and another, as the case of composition operations CO_I and CO_{II}, the emergence of the maxRAF set of the starting nets depends on the rate of the exchange transitions (the flow). For sufficiently low rates, only the RAF set capable of acquiring food directly from the environment is able to form. Conversely, for sufficiently high rates the elements of the food are exchanged in such portions to allow only the receiving RAF set to appear. Furthermore, if complexes of a reaction are involved in the exchange and not individual species (as in the case of the composition operation CO_{II}), we found an intermediate interval of flow rate values within which the exchange of food elements between the nets allows the emergence of just some of the closed RAF sets that constitute the starting maxRAF sets. For these intermediate flow rates, therefore, the necessary evolvability conditions are met. Finally, we found that only some closed RAF sets within a maxRAF set can appear if the maxRAF set shares the food species with its copy that has already fully emerged. The latter is a relevant result, since sharing the same food set by two RAF sets produces a maxRAF set that is the union of the two starting RAF sets. The dynamics observed in this case shows that different long-term behaviours are possible for a single RAF set, at least as long as the system is in a particular initial state and the subsets of the RAF set compete with each other for each reaction that needs food elements.

In previous works it was theorised that separate RAF networks could compete for shared resources (Hordijk and Steel, 2014; Vasas et al., 2012; Kauffman, 2011), and a competitive dynamics was observed in spatially separate RAF sets (Hordijk et al., 2018a). Results presented in this chapter confirm the possible evolvability of a system of RAF sets separated into compartments. We also noticed that isolated (composite) RAF sets can experience different asymptotic dynamics. However, since all the simple (tested) isolated RAF sets experience the emergence of the entire maxRAF set, the definition of the RAF sets does not seem to be sufficient for implying dynamics with multiple selectable long-term behaviours. We will return on this aspect in Chapter 4. Moreover, in the future it might be interesting to extend our analysis to a larger ensemble of RAF sets, as well as to study the composition of RAF sets enclosed in protocells, investigating how the coupling between internal networks and boundaries affects the global dynamics of the system.

Chapter 4

Long-term behaviours of RAF sets

4.1 Introduction

As observed in previous chapters and in early numerical results (Vasas et al., 2012; Hordijk et al., 2018a; Serra and Villani, 2019; Ravoni, 2020a), the conditions a graph must satisfy to be a RAF set (see Section 2.1) are not sufficient to strictly constrain its dynamics, and the system may not exhibit the features necessary to self-reproduction and evolvability. Actually, the connection between the topology of a RAF set and its dynamics is not yet fully understood (Filisetti et al., 2011; Serra and Villani, 2019; Hordijk and Steel, 2018, 2012a). In this chapter we make a first attempt to solve this issue, by studying RAF sets through the formalism of the *Chemical Reaction Network* (CRN) theory[1] (Feinberg, 2019). The CRN theory offers powerful tools that allow to connect the topology of a network with its dynamical behaviour, for a large class of network dynamics (Feinberg, 2019, 1987, 1995; Ellison, 1998; Ellison et al., 2012). Note that the CRN theory usually deals with the study of real-world chemical systems. Starting from the results of the CRN theory, we identify which conditions on the structure of RAF sets are useful for predicting their long-term behaviours. In particular, we investigate which conditions determine a dynamics with desired properties for systems at the origin of life (e.g., self-maintenance, concentrations growth, homeostasis), adding new elements in the scenario previously proposed for the evolvability of RAF sets (Hordijk et al., 2018a; Vasas et al., 2012).

The chapter is organised as follows. In Section 4.2 we recall notions of the CRN theory useful for our study. In Section 4.3 we show our representation of RAF sets in terms of CNRs. In Section 4.4 we introduce motifs in the structure of RAF sets that are connected with long-term behaviours of the networks, and we provide an illustrative example of evolvability of RAF sets by numerically simulating the dynamics. Finally, in Section 4.5

[1] Recently Andersen et al. (2020) and Blokhuis et al. (2020) have defined and classified autocatalytic structures based on general stoichiometric conditions in CRNs. We are currently investigating the connection between these structures and the RAF sets, focusing mainly on the (RAF) motifs we introduce in Section 4.4.

we discuss the conclusions.

4.2 Background: Chemical Reaction Networks (CRNs) and the Deficiency Zero Theorem

In this section we recall some useful definitions and we introduce the *Deficiency Zero Theorem* (DZT) (Feinberg, 1987, 1995). An interested reader can find a detailed discussion of the CRN theory in (Feinberg, 2019). Let $\mathcal{S}$ denote the set of chemical *species*, $\mathcal{N} = \{\nu_i, \nu_i' : i = 1, \cdots, r,\ \nu_j \neq \nu_i'\}$ the set of *complexes*, that is, the members of the vector space $\mathbb{R}^S_{>0}$ generated by the species that provide the inputs and the outputs of a reaction. We denote with $\nu(s)$ the s-th component of the vector ν, that is, the *stoichiometric coefficient* of species s in the complex ν. Let $\mathcal{R} = \{\nu_i \to \nu_i' : i = 1, \cdots, r\}$ be the set of *reactions*, that is, the set of relations among complexes. For each reaction $\nu_i \to \nu_i' \in \mathcal{R}$, the component $\nu_i(s)$ indicates the number of molecules of the s-th chemical species consumed by the i-th reaction, while the component $\nu_i'(s)$ indicates the number of molecules of the s-th species produced by the i-th reaction. A CRN is a triple $(\mathcal{S}, \mathcal{N}, \mathcal{R})$. Note that it is possible to consider *open* CRNs introducing pseudo reactions such as $0 \to \nu$ and $\nu \to 0$, where 0 is called the *zero complex* and it is the zero vector of $\mathbb{R}^{\mathcal{S}}$.

We denote with $\mathcal{G}$ the directed graph with complexes as nodes and reactions $\nu_i \to \nu_i'$ as directed edges. The connected components of $\mathcal{G}$ are called the *linkage classes* of the CRN. A *strong-linkage class* is a strongly connected linkage class. A *terminal strong-linkage class* is a strong-linkage class containing no complex that is a source for an edge pointing to a different strong-linkage class. Note that a complex not involved in any reaction is a terminal strong-linkage class. A CRN is said to be *weakly reversible* if each linkage class in $\mathcal{G}$ is a strong-linkage class, or, equivalently, if each linkage class is a terminal strong-linkage class. The *reaction vectors* for a CRN are the members of the set $\{\nu_i' - \nu_i \in \mathbb{R}^{\mathcal{S}} | \nu_i \to \nu_i' \in \mathcal{R}\}$. The span generated by the reaction vectors is called the *stoichiometric subspace* of the network, and its dimension is denoted by d. The *deficiency* of a CRN is:

$$\delta = n - l - d, \tag{4.1}$$

where n and l are the number of complexes and linkage classes, respectively. Note that the dimension d of the span of two networks with the same complexes and the same linkage classes is the same. This implies that the two networks have the same deficiency δ, and that it results $\delta \geq 0$ (Feinberg, 1995).

In the following, we refer to *mass-action systems*, that are CRNs taken together with an element $\kappa \in \mathbb{R}^{\mathcal{R}}_{>0}$. The number $\kappa_{\nu \to \nu'}$ is the rate constant for the reaction $\nu_i \to \nu_i' \in \mathcal{R}$. Hereafter, we use $\mathcal{G}$ to indicate both a CRN, its associated directed graph and the resulting

mass-action system. The *species-formation rate function* for a mass-action system is the function $f(\cdot, \kappa) : \mathbb{R}^{\mathcal{S}}_{\geq 0} \to \mathbb{R}^{\mathcal{S}}$ defined by:

$$f(c, \kappa) = \sum_{\nu \to \nu'} \kappa_{\nu \to \nu'} c^{\nu} (\nu' - \nu), \tag{4.2}$$

where c is the (time-dependent) vector of species concentration and c^{ν} is defined as:

$$c^{\nu} := \prod_{s \in \mathcal{S}} c(s)^{\nu(s)}. \tag{4.3}$$

Here $c(s)$ is the concentration of species s. The dynamics of $\mathcal{G}$ is described by the equation:

$$\dot{c} = f(c, \kappa), \tag{4.4}$$

where the point indicates the time derivative. Eq. 4.4 corresponds to a set of ordinary differential equations (ODEs) that describe the time evolution of concentration of each species in S. Indeed, it is natural to define a *positive equilibrium* as an element $c \in \mathbb{R}^{\mathcal{S}}_{>0}$ such that $f(c, \kappa) = 0$. A positive equilibrium is then a steady state of the mass-action system characterized by a positive concentration and a zero net production rate for every species of the CRN. Note that the term "equilibrium" used in this context does not refer to thermodynamic equilibrium, but rather to a general steady state. A necessary condition for the existence of a positive equilibrium for a mass-action system is the existence of a *positive vector* $\alpha \in \mathbb{R}^{\mathcal{R}}_{>0}$ such that (Feinberg, 1995):

$$\sum_{\nu \to \nu'} \alpha_{\nu \to \nu'} (\nu' - \nu) = 0. \tag{4.5}$$

If exists α such that Eq. 4.5 is satisfied, we say that the network's reaction vectors are positively dependent. Note that weak reversibility is a sufficient (but not necessary) condition for the existence of a positive equilibrium (Boros, 2019; Feinberg, 1995).

The DZT provided a connection between the topology of a network, expressed in terms of its deficiency, and the existence and the uniqueness of steady states for the associated mass-action system (Feinberg, 1987, 1995). In fact, the DZT does much more, and its results can be applied to a broad class of kinetics systems. However, in this work we limit our attention on a specific result (again, see (Feinberg, 2019) for a comprehensive illustration of the theorem and its application). In particular, we will use the following statement:

Theorem 3 (The deficiency zero theorem) *Let $(\mathcal{S}, \mathcal{N}, \mathcal{R})$ be a reaction network of deficiency zero.*

1. *If the network is weakly reversible, the resulting mass-action system admits precisely*

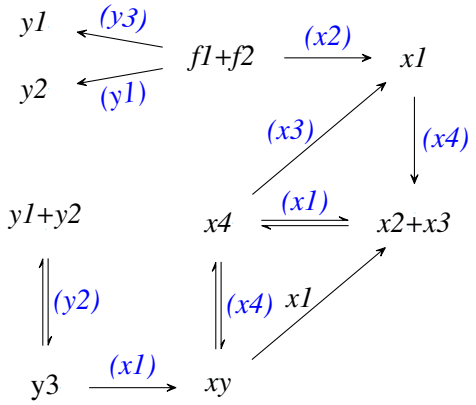

Figure 4.1. Example of a RAF set as a CRN. Complexes are represented by black letters (the letter f indicates food species), reactions by arrows. Blue letters in brackets indicate catalysts. The entire reaction network is a RAF set. Two closed RAF sets are present within the RAF set, namely: $R^{(1)} = \{f1{+}f2 \xrightarrow{(x2)} x1,\ x1 \xrightarrow{(x4)} x2{+}x3,\ x2{+}x3 \overset{(x1)}{\rightleftharpoons} x4,\ x4 \xrightarrow{(x3)} x1,\ x4 \overset{(x4)}{\rightleftharpoons} xy\}$ and $R^{(2)} = \{f1{+}f2 \xrightarrow{(y3)} y1,\ f1{+}f2 \xrightarrow{(y1)} y2,\ y2{+}y3 \overset{(y2)}{\rightleftharpoons} y3\}$.

one positive equilibrium for each initial condition, no matter what (positive) rate constants are assigned to the reactions .

2. *If the network is not weakly reversible, there can be no assignment of (positive) rate constants such that the resulting mass-action system admits the existence of a positive equilibrium (the network's reaction vectors are not positively dependent).*

4.3 Reflexively Autocatalytic and Food-generated CRNs

In this section we study RAF sets in the context of CRN theory. Figure 4.1 shows an example of a RAF set in this framework. Our first step is to represent F-generated sets in terms of CRNs (Section 4.3.1). In particular, we focus our attention on zero deficiency CRNs (this restriction is dropped when we introduce catalysis, see Section 4.3.2). We open the system to the inflow of matter by introducing pseudo reactions that produce species of the food set. We consider both reversible and irreversible reactions and allow only elementary reactions (i.e., reactions involving one or two chemical species as reactants) to occur. Finally, in Section 4.3.2 we introduce the notion of catalysis within the framework of the CRN theory.

In RAF theory, a catalyst is a species able, with its presence, to facilitate (i.e. accelerate) the proceeding of a reaction (Hordijk and Steel, 2004). However, in real systems, catalysed reactions usually involve one or more intermediate complexes and can exhibit various dynamical behaviours (Michaelis and Menten, 1913; Ricard and Cornish-Bowden, 1987). We define catalysis within CRNs by introducing an enzymatic mechanism such that a catalysed reactions consumes a catalyst x and a substrate s to form an intermediate

complex e, which in turn releases product species and the original catalyst x:

$$s + x \underset{\kappa_{-1}}{\overset{\kappa_1}{\rightleftharpoons}} \mathrm{e} \underset{\kappa_{-2}}{\overset{\kappa_2}{\rightleftharpoons}} p + x \tag{4.6}$$

where $\kappa_{-2} = 0$ for irreversible reactions. Note that this modeling is the common *Michaelis-Menten scheme* (Michaelis and Menten, 1913), extensively used to describe enzymatic processes, and that this modelisation has already been used to simulate RAF sets dynamics (Serra and Villani, 2019). Furthermore, we assume that, due to its highly reactivity, the intermediate complex e reaches a quasi-equilibrium state very quickly, compared to the characteristic evolutionary time scale of other species. Therefore, the derivative in Eq. 4.4 relating to the intermediate complex can be set quasi equal to zero:

$$\dot{c}(e) \approx 0. \tag{4.7}$$

We refer to Eq. 4.7 as the *quasi steady-state* (QSS) assumption. It is important to underline that the QSS assumption is at the basis of the *quasi steady-state approximations* (QSSAs) (Briggs and Haldane, 1925; Borghans et al., 1996; Tzafriri, 2003; Tzafriri and Edelman, 2004), that are theoretical tools widely used to study enzymatic reactions. In particular, the QSSAs start from the QSS assumption in order to derive algebraic relations among intermediate complexes and the other reactants, reducing the number of ODEs that describe the evolution of the system. Interested readers can consult, for example, Bersani et al. (2015) to learn more about these approaches.

The applicability of the QSSAs depends on the the initial conditions and the parameters describing the system. If their conditions of validity are not satisfied, the use of these approximations leads to a wrong description of the dynamics of interest (see, for instance, Flach and Schnell (2006); Pedersen et al. (2007)). However, as shown in Borghans et al. (1996); Bersani et al. (2015); Tzafriri (2003); Tzafriri and Edelman (2004), the so-called *total quasi steady-state approximation* (tQSSA) is able to accurately reproduce the dynamics of enzymatic reactions for a wide range of parameters. In particular, it holds whenever it is (Tzafriri, 2003; Tzafriri and Edelman, 2004):

$$\frac{\kappa_{-1} + \kappa_2}{\kappa_1} >> 1, \tag{4.8}$$

$$\frac{\kappa_{-1} + \kappa_2}{\kappa_1} >> \frac{\kappa_2}{\kappa_1}, \tag{4.9}$$

$$\frac{\kappa_{-2}}{\kappa_1} << 1. \tag{4.10}$$

Therefore, for these values of the rate constants we can be reasonably confident that the QSS assumption (Eq. 4.7) is valid. This assumption allows us to provide a relation between the topology of the CRN without catalysis and the corresponding dynamics including en-

zymatic processes (Appendix A).

4.3.1 Food-generated CRNs

Let F be a set of *chemostatted* chemical species, that is, a set of species whose concentration is controlled by the environment. Given a CRN $\mathcal{G} = (\mathcal{S}, \mathcal{N}, \mathcal{R})$, we consider $F \subset S$ to be the food set of $\mathcal{G}$. As in RAF theory, we say that $\mathcal{G} = (\mathcal{S}, \mathcal{N}, \mathcal{R})$ is an *F-generated CRN* if, for a certain set $F \subset S$ and for each $s \in \mathcal{S}$, there exists a sequence of reactions $(\nu'_0 - \nu_0), (\nu'_1 - \nu_1), \ldots, (\nu'_i - \nu_i)$ such that:

i. $\nu'_i(s) \neq 0$;

ii. $\nu_0(s') = 0 \Leftrightarrow s' \in F$;

iii. $\forall s' \in \mathcal{S} \setminus F$ such that $\nu_j(s') \neq 0$, $j = 1, \ldots, i$, exists $k < j$ such that $\nu'_k(s') \neq 0$.

Let $\mathcal{G} = (\mathcal{S}, \mathcal{N}, \mathcal{R})$ be an F-generated CRN. We say that $\mathcal{G}$ is *minimal* if the following condition holds:

$$\forall(\nu, \mu) \in \mathcal{N}\ \exists s \in \mathcal{S} \mid \mu \neq \nu \Rightarrow \nu(s) \neq 0, \mu(s) = 0, \tag{4.11}$$

that is, a F-generated CRN $\mathcal{G}$ is minimal if all its complexes contain at least one species that does not appear in any other complex of the network. It can be shown that a minimal F-generated CRN is a zero deficiency network. In fact, let $\mathcal{G}'$ be a minimal F-generated CRN having just one linkage class that connects all its n complexes through exactly $n - 1$ reactions. From Eq. 4.11 it follows that the reaction vectors $(\nu' - \nu)$ are linearly independent. It follows that $d_{\mathcal{G}'} = n - 1$, and it is $\delta_{\mathcal{G}'} = 0$. Let $\mathcal{G}$ be a CRN obtained from $\mathcal{G}'$ by removing exactly m reactions. Note that $\mathcal{G}$ is again minimal. It results that $l_{\mathcal{G}} = 1 + m$, $d_{\mathcal{G}} = n - 1 - m$, and $\delta_{\mathcal{G}} = 0$. From the arbitrary choice of m and the equivalence of the deficiency for CRNs having the same complexes and the same linkage classes (Feinberg, 1995), it follows that each CRN satisfying Eq. 4.11 is a deficiency zero network.

In order to model the chemostatting of species in F, we introduce pseudo reactions for each species $f \in F$ such that:

$$0 \underset{o_f}{\overset{\iota_f}{\rightleftharpoons}} f \tag{4.12}$$

where ι_f and o_f are the rate constants for reactions $0 \to f$ and $f \to 0$, respectively. We denote with $\mathcal{G}_F = (\mathcal{S}_F, \mathcal{N}_F, \mathcal{R}_F)$ the CRN such that $\mathcal{S}_F = F$, $\mathcal{N}_F = F \cup 0$ (where 0 is the zero complex) and $\mathcal{R}_F$ is the set of the pseudo reactions. Note that for each pair of reaction vectors $(\nu'_i - 0), (\nu'_j - 0) \in \mathcal{R}_F$, for $i \neq j$, it is $(\nu'_i - 0) \cdot (\nu'_j - 0) = 0$, where $\cdot$ is the scalar product. Thus, it results $d_{\mathcal{G}_F} = |F|$ and $\delta_{\mathcal{G}_F} = 0$, that is, $\mathcal{G}_F$ is a (weakly) reversible zero deficiency CRN. The DZT states that $\mathcal{G}_F$ admits exactly one steady state. In particular,

for each $f \in F$, the positive equilibrium is given by $c(f) = \iota_f / o_f$. Therefore, $c(f)$ is the concentration that the species f would reach if only pseudo reactions are included.

Given a CRN $\mathcal{G}' = (\mathcal{S}', \mathcal{N}', \mathcal{R}')$ and a food set $F \subset \mathcal{S}'$, the equivalent *open CRN* $\mathcal{G}$ of $\mathcal{G}'$ is obtained from $\mathcal{G}'$ by adding $\mathcal{G}_F$, such that it is $\mathcal{G} = (\mathcal{S}, \mathcal{N}, \mathcal{R})$, where $\mathcal{S} = \mathcal{S}'$, $\mathcal{N} = \mathcal{N}' \cup \mathcal{N}_F$ and $\mathcal{R} = \mathcal{R}' \cup \mathcal{R}_F$. Note that, in general, the addition of $\mathcal{G}_F$ to $\mathcal{G}'$ changes the topology of $\mathcal{G}'$; for instance, $\mathcal{G}_F$ can connect separated linkage classes of $\mathcal{G}'$. Moreover, the introduction of various chemostatted chemical species affects the dynamical behaviour of the network and its thermodynamic properties (Polettini and Esposito, 2014; Rao and Esposito, 2016, 2018). In this chapter, we focus our attention on CRNs having no complexes including both food and non-food species, and we do not allow food species to be catalysts. Therefore, for each complexes $\nu \in \mathcal{N}$ and species $s \in \mathcal{S}$ it is:

$$\nu(f) \neq 0, \nu(s) \neq 0 \Rightarrow s \in F \tag{4.13}$$

$$(s, \nu \rightarrow \nu') \in C \Rightarrow s \notin F, \tag{4.14}$$

where f denotes a food species. We will investigate the impact of chemostatting on network dynamics if Eq. 4.13 and Eq. 4.14 are not satisfied in a future work.

4.3.2 Addition of catalysis

In this section we introduce a procedure to include catalysis within a CRN. In RAF theory, a catalysis is a pair (x, r) indicating that species x catalyses reaction r. As previously indicated, in our model we add a catalysis as a substrate-catalyst interaction that produces a *substrate-catalyst complex*. In particular, for a monomolecular reaction $s_1 \rightarrow p$ catalysed by a molecule x, we assume that the species s_1 reacts with the catalyst x to form the substrate-catalyst complex e, which can perform the inverse reaction or release the product p and the catalyst x. Similarly, for a bimolecular reaction $s_1 + s_2 \rightarrow p$ catalysed by x, we assume that one reactant, says s_2, is the substrate that reacts with x to produce e^*, while the other reactant, s_2, reacts with e^* producing e, that eventually releases x and products p. Figure 4.2 sketched the procedure.

Note that the substrate-catalyst complexes e, e^*, e^{**} (Figure 4.2) are considered as different complexes, that is:

$$(e_i \cdot e_j), (e_i^* \cdot e_j^*), (e_i^{**} \cdot e_j^{**}) \neq 0 \Leftrightarrow i = j \tag{4.15}$$

$$e_i \cdot e_j^* = e_i \cdot e_k^{**} = e_j^* \cdot e_k^{**} = 0 \ \forall i, j, k. \tag{4.16}$$

Moreover, it is important to underline that original spontaneous reactions are still present in the network with addition of catalysis. Given a CRN $\mathcal{G}$ and a set of catalyses C, we call $\mathcal{G}_C$ the CRN obtained from $\mathcal{G}$ by adding reactions for each catalysis in C according to the

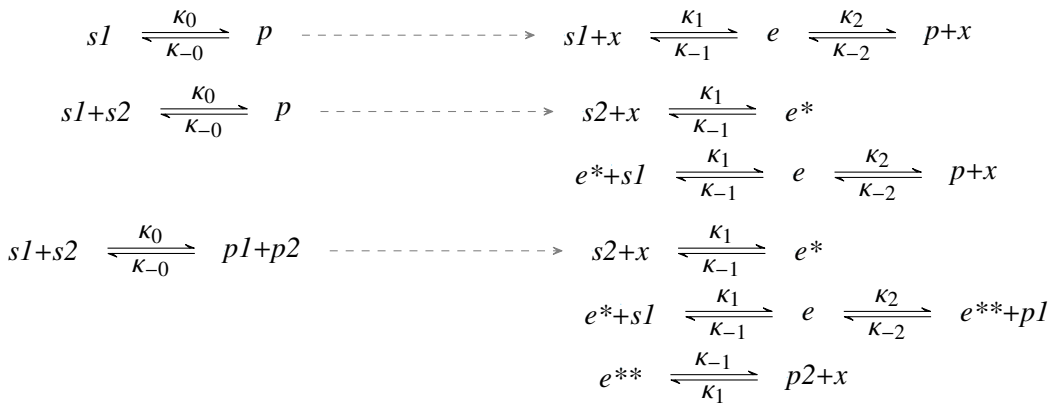

Figure 4.2. Catalysis scheme. The dashed gray arrows associate spontaneous reactions (terms on the left) with the corresponding catalysed reactions (terms on the right). Catalyses associated with irreversible reactions can be obtained from the first two catalyses of the scheme by setting κ_{-0} and κ_{-2} equal to zero. Note that for irreversible reactions, p is in turn a complex, i.e., it can be constituted by one or more chemical species. The associated ODEs are shown in Appendix A.

scheme of Figure 4.2. Therefore, $\mathcal{G}_C$ represents the "real" mass-action system underlying a CRN to which a set of catalyses is associated.

As in RAF theory, given a F-generated CRN $\mathcal{G} = (\mathcal{S}, \mathcal{N}, \mathcal{R})$ and a set of catalyses $C = \{(s, \nu \to \nu') : s \in \mathcal{S}, \nu \to \nu' \in \mathcal{R}\}$, we say that $\mathcal{G}$ is a *RAF CRN* if, for each reaction $\nu \to \nu' \in \mathcal{R}$, there exists at least one species $s \in \mathcal{S}$ such that $(s, \nu \to \nu') \in C$; we say that a RAF CRN is a *closed RAF CRN* if, for each reaction $\nu \to \nu'$ such that all its reactants and at least one catalyst are either part of the set F or are produced by a reaction from $\mathcal{R}$, it is $\nu \to \nu' \in \mathcal{R}$; finally, we say that a closed RAF CRN is a *minimal closed RAF CRN* if it does not contain any other closed RAF CRNs.

4.4 Long-term behaviour

In this section, we identify motifs in the topology of a minimal closed RAF CRN $\mathcal{G}$ that allow to predict the dynamics of its associated network $\mathcal{G}_C$ (note that, although not specified, we are considering open CRNs). Usually, adding catalysis increases the deficiency of a CRN, and higher deficiency theories are necessary in order to study the steady states of the network (Feinberg, 1995; Ellison, 1998).

However, the topology of the zero deficiency CRN $\mathcal{G}$ provides some information on the dynamics of $\mathcal{G}_C$, at least if Eq. 4.7 holds (see Appendix A for more details). In fact, the relation among complexes provided by $\mathcal{G}$ does not change in $\mathcal{G}_C$: the terms $\alpha_{\nu\to\nu'}(\nu - \nu')$ in the sum of Eq. 4.4 for the two networks, differ only in the values of $\alpha_{\nu\to\nu'}$, with $\alpha_{\mathcal{G}_C} > \alpha_{\mathcal{G}}$ (Appendix A). This implies, for instance, that if $\mathcal{G}$ is not weakly reversible, thanks to the DZT we can say that the reaction vectors of $\mathcal{G}_C$ are not positively dependent; on the other

hand, if $\mathcal{G}$ is weakly reversible, $\mathcal{G}_C$ admits the existence of a positive equilibrium. Nevertheless, it is worth to underline that $\mathcal{G}$ and $\mathcal{G}_C$ are not equivalent. In particular, if the QSS assumption does not hold, they can exhibit very different dynamics. For example, consider the CRN shown in Figure 4.3a. The network without catalysis $\mathcal{G}$ is a weakly reversible zero deficiency network, and it admits exactly one positive equilibrium for each choice of initial condition. Conversely, by analysing the associated CRN $\mathcal{G}_C$ through the *CRN Toolbox* (Ellison et al., 2012) without explicitly assume Eq. 4.7 as valid, we find that $\mathcal{G}_C$ admits the existence of multiple stationary solutions starting from the same initial conditions, for an appropriate choice of the rate constants κ. Moreover, weak reversibility is not a precondition for the existence of positive equilibria in CRNs having nonzero deficiency (Boros, 2019; Feinberg, 1995). For instance, let us consider the following one deficiency CRN:

$$2\,\mathrm{x}_1 \underset{\kappa_-}{\overset{\kappa_+}{\rightleftharpoons}} \mathrm{x}_1 + \mathrm{x}_2 \xrightarrow{\kappa_+} 2\,\mathrm{x}_2. \tag{4.17}$$

The network is not weakly reversible. However, it admits positive equilibria whenever it is $\kappa_+ = 1$ and $\kappa_- > 1$ (Feinberg, 1995). By focusing on minimal CRNs and making the QSS assumption, we ensure the validity of the connection shown above between the dynamics of a CRN with spontaneous reactions only and that of its counterpart which includes catalyses.

We use these results in order to predict the dynamics of the mass-action system $\mathcal{G}_C$ associated with a RAF CRN $\mathcal{G}$. In particular, let $\mathcal{G}$ be a minimal closed RAF CRN, and let $\mathcal{G}_-$ be the CRN obtained from $\mathcal{G}$ by removing all the reactions $\nu_0 \to \nu'$, where the complex ν_0 contains (only) food species. We define:

i. *Fully connected* (FC) motif: $\mathcal{G}$ is a FC motif if it is a weakly reversible CRN;

ii. *Non connected* (NC) motif: $\mathcal{G}$ is a NC motif if both $\mathcal{G}$ and $\mathcal{G}_-$ are not weakly reversible CRNs;

iii. *Core connected* (CC) motif: $\mathcal{G}$ is a CC motif if it is not a weakly reversible CRN and $\mathcal{G}_-$ is a weakly reversible CRN.

Figure 4.3 shows examples of the three motifs. They exhibit dynamics with different characteristics (Figure 4.4a). In particular, we focus our attention on three dynamical properties of the concentrations of species that constitute a motif:

i. *homeostasis*: the ratio among concentrations of all the species is constant over time ;

ii. *continuous growth*: the concentrations of all the species increase in time;

iii. *self-conservation*: if the inflow of matter towards the CRN is interrupted, the concentrations of all the species do not decrease in time .

Note that these are desired features for a system at the basis of the origin of life. For instance, homeostasis is considered to be a fundamental property connected with self-maintenance of an organism; a growth of species concentration is necessary for self-replication, and self-conservation prevents the decay of the system in case of insufficient resources (Luisi, 2006; Varela, 2000).

We argue that FC motif exhibits homeostasis, NC motif exhibits none of the properties and CC motif exhibits continuous growth and self-conservation. It is important to underline that we are referring to long-term dynamics of the networks and not to their transient behaviour.

In fact, FC motif admits the existence of a positive equilibrium for the concentration of all its chemical species, meaning that, for $t \to \infty$, the ratio $c(s)/c(s')$ is constant for each pair $s, s' \in \mathcal{S}$ (Figure 4.4a). However, if the inflow rate ι_f is set equal to zero for each $f \in F$, the resulting network is no more weakly-reversible. In particular, there is a terminal strong-linkage class (i.e., the zero complex) that is an *absorbing linkage class*, meaning that, once the flow of matter falls in it, it can no longer leave it. Therefore, the matter consumed by reactions involving the species of the CRN is not replaced, the species concentrations decrease and the network is not self-conservative (Figure 4.4a).

On the other hand, NC motif contains an absorbing linkage class involving a strict subset $\mathcal{S}'$ of $\mathcal{S}$, both in case of $\iota_f > 0$ and $\iota_f = 0$. As a result, species in $\mathcal{S}'$ increase their concentrations at the expense of other species $s \notin \mathcal{S}'$. Thus, even if a subset of $\mathcal{S}$ can experience continuous growth, the whole NC motif does not satisfy any of the properties listed above (Figure 4.4a).

By definition, instead, all the non-food species of a CC motif belong to a weakly reversible (sub)network that is absorbing for the inflowing matter coming from the environment. This implies that, if $\iota_f > 0$, each non-food species is reached by a positive flow of matter (continuous growth); on the other hand, if $\iota_f = 0$, the matter is redistributed among non-food species and does not escape from the CRN (self-conservation). Note that a CC motif could exhibit homeostasis, depending on the fine details of its topology.

4.4.1 An illustrative example of evolvability of RAF sets

In this section we present illustrative examples on how the detected motifs (Section 4.4) impact the long-term dynamics of a (larger) RAF CRN. We start our study by simulating the dynamics of a RAF CRN constituted by three different closed RAF CRNs that share the same food set F. The closed RAF CRNs correspond to the different motifs we have introduced in Figure 4.3.

Figure 4.4b shows the dynamics of this particular network: as expected, the resulting dynamics is substantially equivalent to that shown by the non composed motifs (Figure 4.4a, $\iota_f > 0$). In fact, letting the motifs share the food set does not affect their structures,

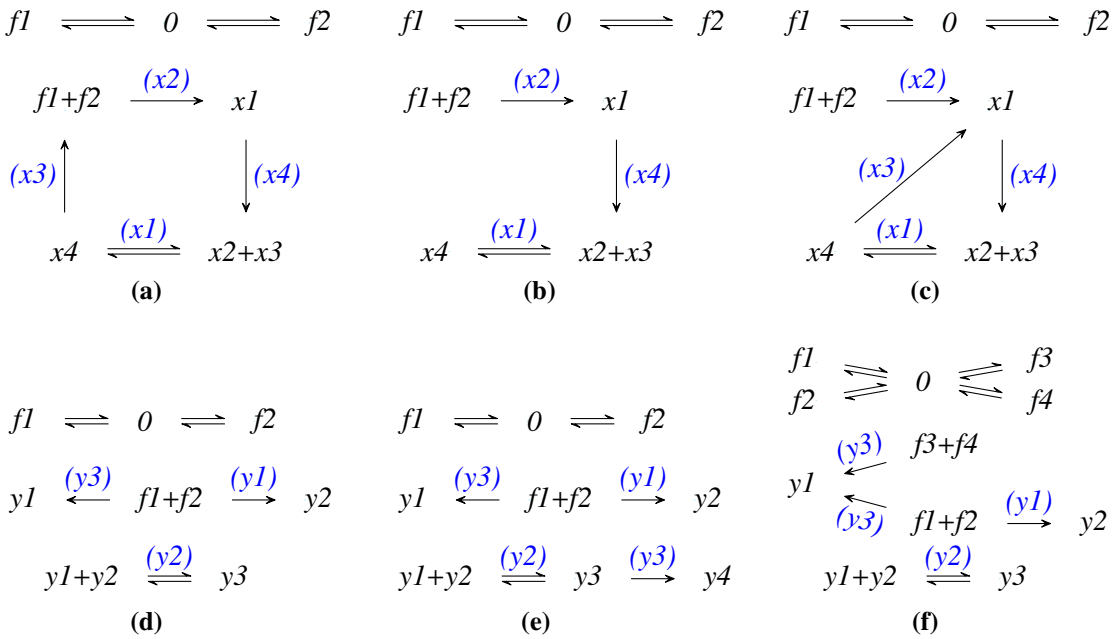

Figure 4.3. Examples of motifs. Complexes are represented by black letters (the letter f indicates food species), reactions by arrows. Blue letters in brackets indicate catalysts. (a) FC motif: the CRN is weakly reversible. (b,e) NC motif: the CRN is not weakly reversible, and there is not a weakly reversible (sub)network that includes all the non-food species. (c,d,f) CC motif: the CRN is not weakly reversible, and there is a weakly reversible (sub)network that includes all the non-food species. Note that all the motifs are closed RAF CRNs.

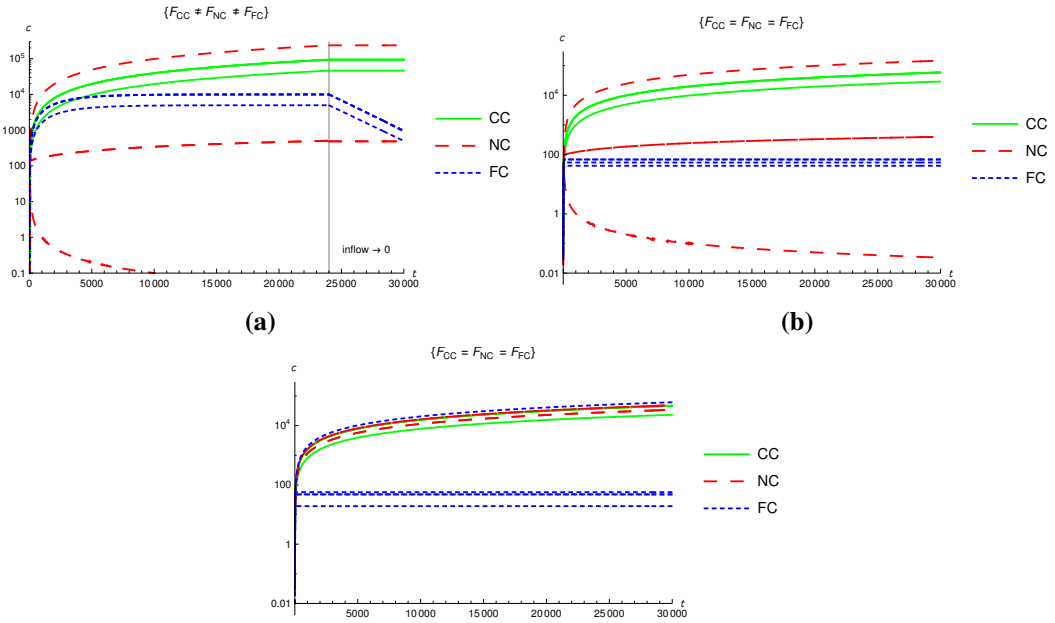

Figure 4.4. Dynamics of motifs. On the x-axis: time steps t. On the y-axis: species concentration c. (a) Dynamics of the three isolated motifs introduced in Figure 4.3a, Figure 4.3b and Figure 4.3c. For $t > 24000$ the inflow rate ι_f is set equal to 0 for each pseudo reaction $0 \xrightarrow{\iota_f} f$. (b) Dynamics of the three motifs introduced in Figure 4.3a, Figure 4.3b and Figure 4.3c, that draw from the same food set $F = \{f1, f2\}$. (c) Resulting dynamics after mutations that change the FC motif of Figure 4.3a in a NC motif, and the NC motif of Figure 4.3b in a CC motif. The plotted curves are obtained by numerically solving the ODEs associated with the CRNs (Eq. 4.4), setting $\iota_f = 10$, $o_f = 10^{-2}$, $\kappa_0 = \kappa_{-0} = 10^{-3}$, $\kappa_1 = 10$, $\kappa_{-1} = 10^7$, $\kappa_2 = 10^4$, $\kappa_{-2} = 10^{-1}$, and an initial concentration of $c_0 = 10^{-2}$ for all the species.

nor does significantly change the ODEs describing the dynamics (apart from a change in the equilibrium constants of FC motif). Therefore, the overall dynamics of the network is given by the union of the dynamics of the single motifs.

However, introducing new reactions among species can have a major role in the resulting dynamics of the network. For instance, adding the reaction $x4 \xrightarrow{(x1)} x5$ to the FC motif of Figure 4.3a changes it into a NC motif. At the same time, adding the reaction $x4 \xrightarrow{(x4)} x1$ to the NC motif of Figure 4.3b changes it into a CC motif. The dynamics of the overall network, in fact, is the result of the evolution of a FC motif and two CC motifs (Figure 4.4c). This is an example of a general case: it is always possible to pass from one motif to another by adding (or removing) one or more reactions.

This last point has important consequences for the evolvability of RAF sets. In fact, we can interpret the characteristic dynamical behaviour of a motif as its phenotype, and the (random) addition of a new reaction as a mutation. In this framework, the examples of Figure 4.4b and Figure 4.4c show that closed RAF CRNs can acquire (or lose) dynamical properties that can be, potentially, picked by natural selection. As further evidence to support this observation, in Figure 4.5 we show different frames of an hypothetical evolution of a RAF CRN in which mutations occur. In particular, the starting network is formed by two closed RAF CRNs that share the same food set $F = \{f1, f2\}$. The closed RAF CRNs are indicated with letters X (CC motif shown in Figure 4.3c) and Y (CC motif shown in Figure 4.3d), respectively. Initially, both the closed RAF CRNs show a continuous growth of species concentrations, with similar growing rates (Figure 4.5a). However, the addition of a new reaction in the network allows Y to draw resources from a supplementary source compared to X, represented by the food elements $f3$ and $f4$ (Figure 4.3f). Consequently, this favorable mutation provides an advantage for Y, which is able to grow faster than X (Figure 4.5b). At the same time, as previously observed, an unfavorable mutation (Figure 4.3e) can decrease the efficiency of a network's self-reproduction (Figure 4.5c). Finally, note that a mutation introducing a connection between X and Y can have major effects on their dynamics. In particular, consider the RAF CRN shown in Figure 4.1: it can be built starting from the networks of Figure 4.3c and Figure 4.3d, by adding the production of the species xy. This latter expansion of the network can be interpreted, for instance, as the result of a mutation that allows species $x4$ to produce species xy in a reversible way, and species $x1$ to catalyse the irreversible production of species xy starting from species $y3$. Therefore, thanks to a favorable mutation, one motif can steal resources from the other. The dynamics of the resulting RAF CRN is shown in Figure 4.5d: due to the mutation, the closed RAF CRN X' (the symbol X' indicates the network X to which the reaction $x4 \xrightarrow{(x4)} xy$ is added) is an absorbing linkage class in which the flow of matter of the net Y falls; consequently, network X' still shows a continuous growth in species concentrations, while Y dynamically disappears.

In this section, we have shown how the presence of motifs FC, NC and CC within the structure of a RAF CRN affects the dynamics of the system. Moreover, the examples we have introduced suggest that closed RAF CRNs could be the elementary units that experience adaptive evolution. Regarding this issue, it is important to underline two points. First, note that we are dealing with a deterministic model. This approximation does not allow to directly simulate neither the spontaneous appearance of novelty, nor the probabilistic effects, that are characteristics of systems with few elements. However, recent numerical simulations have shown how these stochastic processes can determine both a dependence on different initial conditions (for instance, deriving from an inhomogeneous distribution of resources, or from random events, such as the division of a protocell), and an actual competition among closed RAF CRNs (Hordijk et al., 2018a; Serra and Villani, 2019; Ravoni, 2020a). Therefore, the addition of stochastic elements to the RAF CRN model introduced in this chapter should reproduce the scenario proposed in (Vasas et al., 2012; Hordijk et al., 2018a; Ravoni, 2020a) for the evolvability of a population of compartmentalised RAF sets. Moreover, it is very important to note that our results show that a RAF CRN does not always fully emerge in the long-term dynamics, and that an actual competition can therefore occur also among subsets of the same RAF network.

In the future, it would be interesting to study the stochastic dynamics of the identified motifs, as well as the role of the QSS assumption and other hypotheses made in this chapter on the dynamics of the networks.

4.5 Discussion and conclusions

In this chapter we studied the long-term behaviours of RAF sets, particularly focusing on those systems that are considered to be the building blocks from which life emerged. For this purpose, we represented RAF sets in terms of CRNs, and we used CRN theory to predict the dynamics of the networks starting from their topology. Our main result is the identification of additional topological conditions compared to the one introduced by the RAF theory, which allowed us to predict the dynamics of the system and to identify networks with interesting dynamical properties. To our knowledge, this is the first time that the actual dynamics of RAF sets have been successfully connected with their topology.

Furthermore, starting from their structure, we displayed that not all the subsets of a RAF network eventually dynamically emerge, contrary to what has been observed in previous works, where too simple CRNs were considered (Hordijk et al., 2018a; Ravoni, 2020a). These results show that the increase of complexity of a RAF set significantly affects the emergent dynamics, supporting the potential evolvability of RAF sets and their importance in the transition from inanimate to living matter.

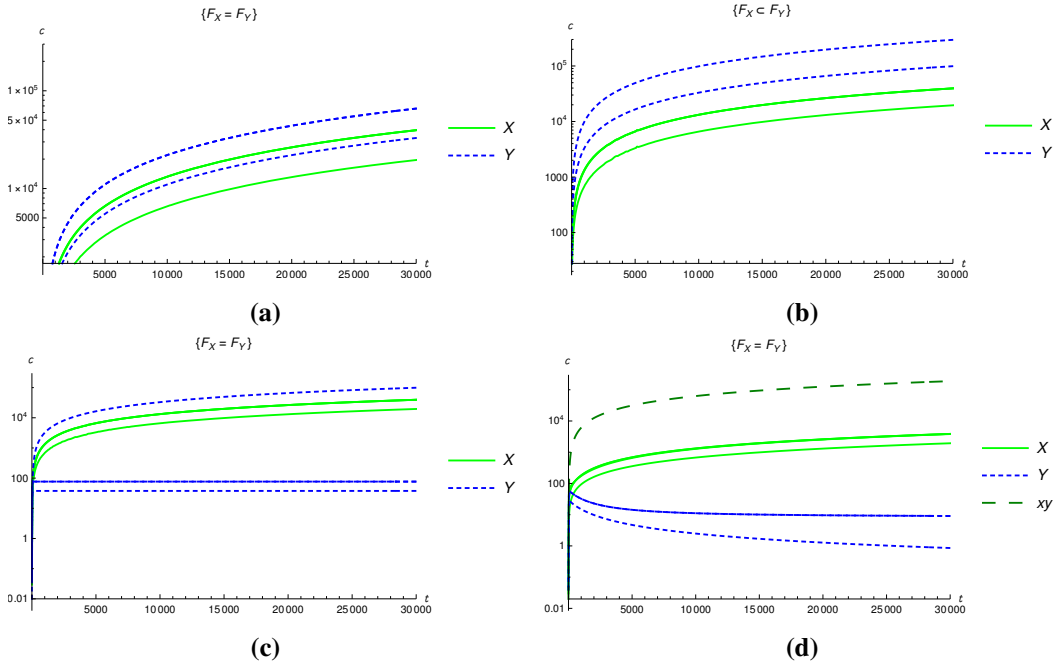

Figure 4.5. Evolution of a RAF CRN induced by mutations. On the x-axis: time steps t. On the y-axis: species concentration c. (a) Dynamics of a RAF CRN constituted by the CC motif of Figure 4.3c (X) and the CC motif of Figure 4.3d (Y), that draw from the same food set $F = \{f1, f2\}$. (b) A favorable mutation allows Y to draws resources from the expanded set $\{f1, f2, f3, f4\}$ (Figure 4.3f), resulting in a higher self-reproduction rate. (c) A unfavorable mutation changes Y in a NC motif (Figure 4.3e), preventing from its continuous growth. (d) A mutation allows X to steal matter from Y, causing the dynamical disappearance of Y (the CRN associated with this dynamics is shown in Figure 4.1). The plotted curves are obtained by numerically solving the ODEs associated with the CRNs (Eq. 4.4), setting $\iota_f = 10$, $o_f = 10^{-2}$, $\kappa_0 = \kappa_{-0} = 10^{-3}$, $\kappa_1 = 10$, $\kappa_{-1} = 10^7$, $\kappa_2 = 10^4$, $\kappa_{-2} = 10^{-1}$, and an initial concentration of $c_0 = 10^{-2}$ for all the species.

Part III

Thermodynamics of RAF sets

Summary

To our knowledge, the thermodynamic properties of RAF sets have not yet been investigated. In this part, we try to address this topic. Starting from the work of Prigogine and Nicolis (see, for example, Prigogine and Nicolis (1971)), it has been suggested that the peculiarities of living systems derive from the nonequilibrium thermodynamic state in which they are (Walker, 2017). However, classical thermodynamics does not provide a coherent treatment of systems far from equilibrium, such as living organisms (England, 2015; Marsland and England, 2017). Furthermore, the idea that thermodynamics alone can explain life is criticised by many authors (see, for instance, Luisi (2006); Walker (2017)). Nevertheless, recent works on nonequilibrium thermodynamics applied to biological and living systems, have shown that a thermodynamic approach can actually lead to relevant results in the study of life (Gnesotto et al., 2018; England, 2013; Perunov et al., 2016; Marsland and England, 2017; Sarkar and England, 2019; Penocchio et al., 2019). For instance, a comprehensive thermodynamic description of chemical networks has been provided in several works (Schmiedl and Seifert, 2007; Polettini and Esposito, 2014; Polettini et al., 2015; Rao and Esposito, 2016, 2018), and it has been shown that stochastic thermodynamics can be used to represent self-replication processes (England, 2013). By using the recent results on nonequilibrium thermodynamics of CRNs, in Chapter 6 we address the issue of thermodynamics of RAF sets. In particular, we focus on the relation between the RAF sets topology and thermodynamic properties, such as dissipation and energy storage. First, however, in Chapter 5 we introduce some general thermodynamic notions, and results obtained for replicating systems (Section 5.2) and generic chemical networks (Section 5.3).

Chapter 5

Brief introduction to nonequilibrium thermodynamics

5.1 Traditional thermodynamics

As previously stressed, living systems are open systems that exchange energy and matter with the environment, operating far from the thermodynamic equilibrium. Therefore, nonequilibrium thermodynamics is an essential tool in order to provide a suitable description of such systems. From the 1950's, Onsager, Prigogine and others started to build a mathematical apparatus in order to find general principles able to represent the nonequilibrium processes near the equilibrium, as classical thermodynamics did for equilibrium situation (Prigogine, 1947; Onsager, 1931; De Groot, 1962). In recent years, general properties of processes arbitrarily far from equilibrium have been detected, especially thanks to the emergent field of so-called *stochastic thermodynamics* (see, for instance, Seifert (2012) for a review). Here, we introduce a very brief description of some results suitable for the study of RAF sets, that we accomplish in Chapter 6.

The thermodynamic state of a system is characterised by thermodynamic variables, such as energy, number of particles, volume. A thermodynamic system is said to be *isolated* if it cannot exchange matter and energy, *closed* if it can exchange only energy with the environment and *open* if it can exchange both energy and matter. A closed system eventually evolves towards the so-called *equilibrium state*, that is a stationary state in which there are not fluxes of matter and energy within the system.

Classical thermodynamics deals with transformations that change the state of a thermodynamic system. A transformation that goes from a state i to a state j is said to be *reversible* if it is possible to reverse it and bring the system back from state j to state i, without causing any change in the surrounding environment. Reversible transformations are ideal processes that take place over an infinitely long time, during which the system is

always in a state of thermodynamic equilibrium. Real thermodynamic transformations are *irreversible* processes.

The first law of thermodynamics states that the change of the energy dU during a thermodynamic transformation in time dt does not depend on the particular transformation, but only on the initial and the final state that the transformation connects. In particular, for a cyclic thermodynamic transformation it is:

$$\oint dU = 0. \tag{5.1}$$

For a closed system, the change of the energy dU is related with the amount of work δW and heat δQ exchanged with the environment, according to the relation:

$$dU = \delta W + \delta Q. \tag{5.2}$$

Notably, on the contrary of the internal energy, the changes δW and δQ depend on the particular transformation.

For a cyclic reversible transformation, it results that also the quantity $\delta Q/T$ does not change:

$$\oint \frac{\delta Q}{T} = 0, \tag{5.3}$$

where T is the Kelvin temperature of the system. Therefore, it is possible to introduce another state variable S, called *entropy*, such that for a reversible transformation it is:

$$dS = \frac{\delta Q}{T}. \tag{5.4}$$

The second law of thermodynamics states that the total (system and environment) entropy difference between equilibrium states can never be negative:

$$\Delta S_{tot} \geq 0. \tag{5.5}$$

It is useful to assume that the environment surrounding the system is represented by a thermal bath or *reservoir*, that is, a thermodynamic system that maintains itself in an equilibrium state at temperature T, regardless the amount of heat exchanging with the system. Therefore, Eq. 5.5 can be written as:

$$dS_{tot} = dS + dS_r = dS + \frac{\delta Q_r}{T}, \tag{5.6}$$

where S_r is the entropy of the reservoir and $\delta Q_r = -\delta Q$.

Prigogine has introduced the hypothesis of *local equilibrium* (Kondepudi and Prigogine, 2014), according to which a system out of equilibrium can be viewed as constituted by sub-

systems that can be considered in thermodynamic equilibrium. The local equilibrium hypothesis finds its justification in the different time scales between microscopic and macroscopic processes. This assumption makes the entropy a well-defined quantity even for irreversible transformations. In particular, it is possible to decompose the change of the entropy dS of a system into two contributions, namely the *entropy production* dS_i and the *entropy flow* dS_e (Kondepudi and Prigogine, 2014), such that it is:

$$dS = dS_i + dS_e. \tag{5.7}$$

The term dS_e takes into account the exchange with the environment, while the term dS_i is associated with the irreversible processes inside the system. Consider again an ideal thermal reservoir, in which no irreversible processes are assumed to take place. The entropy flow of the system dS_e is opposite to the the entropy change of the reservoir. It results $dS_i = dS_{tot}$. Therefore, the second law for a non-isolated system exchanging a reversible entropy flow with its environment can be written as (Kondepudi and Prigogine, 2014):

$$dS = dS_i + dS_e, \quad dS_i \geq 0, \tag{5.8}$$

or, equivalently:

$$\frac{dS}{dt} = \Sigma + \frac{dS_e}{dt}, \quad \Sigma \geq 0, \tag{5.9}$$

where Σ is the *entropy production rate* (EPR). At the steady state it is $dS/dt = 0$. If the steady state is a thermodynamic equilibrium state, the terms Σ and dS_e/dt vanish individually, while a *nonequilibrium steady state* is characterised by a non-vanishing EPR Σ, that is exactly canceled by the term dS_e/dt (Kondepudi and Prigogine, 2014).

For systems sufficiently close to equilibrium, where *thermodynamic forces* (i.e., gradients of thermodynamic parameters) and associated fluxes exhibit a linear relationships, it has been shown that the *principle of minimum entropy production* (Prigogine, 1947) holds. In particular, let us express the EPR in terms of thermodynamic forces F_i and fluxes J_i (Kondepudi and Prigogine, 2014):

$$\Sigma = \sum_i F_i J_i. \tag{5.10}$$

At equilibrium, it is $F_i = 0$ and $J_i = 0$. Linear irreversible thermodynamics assumes that (Kondepudi and Prigogine, 2014):

$$J_i = \sum_j L_{ij} F_j, \tag{5.11}$$

where the matrix elements L_{ij} satisfy the *Onsager reciprocity relations* (Onsager, 1931):

$$L_{ij} = L_{ji}, \tag{5.12}$$

and the diagonal elements L_{ii} are positive according to the second law of thermodynamics. The principle of minimum entropy production states that, in the linear regime where the relations in Eq. 5.11 hold, the EPR Σ assumes a minimum value in correspondence with the nonequilibrium steady state (Prigogine, 1947; Kondepudi and Prigogine, 2014).

For thermodynamic systems arbitrarily far from equilibrium, the results of linear irreversible thermodynamics are no longer valid. However, in recent years stochastic thermodynamics has proved to be a powerful tool for the study of nonequilibrium processes (Seifert, 2012; Van den Broeck, 2013). The theory of stochastic thermodynamics is built on top of stochastic dynamics. This formalism allows, for example, to derive fluctuation theorems that constrain the probability distributions for work, to generalise a fluctuation-dissipation theorem involving entropy production for nonequilibrium steady states, and to introduce thermodynamic quantities and formulate thermodynamic laws at the level of stochastic trajectory.

In this thesis we will not deal in detail with stochastic thermodynamics. However, in Section 5.2 we show a possible application of it to biological systems, in particular to self-replicating systems, as provided in England (2013). In Section 5.3, instead, we introduce a description of the nonequilibrium thermodynamics of CRNs, as provided in Polettini and Esposito (2014); Rao and Esposito (2016, 2018). Next, in Chapter 6, we use these results to study the thermodynamics of RAF sets.

5.2 Stochastic thermodynamics and self-replication

In this section, we report the results obtained in England (2013) as an example of a stochastic thermodynamics approach to the description of biological processes. Let us consider a driven system in equilibrium with a heat bath of inverse temperature $\beta = 1/(\kappa_B T)$ (where κ_B is the Boltzmann constant expressed in natural units), whose dynamics is stochastic and Markovian (Grimmett, 2020). Let i, j denote two microstates of the system. It is possible to show that the following *fluctuation theorem* holds (see Crooks (1999); Sevick et al. (2008); Seifert (2012) for more details):

$$\frac{\pi(i \to j)}{\pi(j \to i)} = e^{\beta \Delta Q(i \to j)}, \tag{5.13}$$

where $\pi(i \to j)$ and $\pi(j \to i)$ are the probabilities of the transition from i to j in a forward direction, and of the reverse path from j to i, respectively, and $\Delta Q(i \to j)$ is the heat released into the bath over the trajectory from the microstate i to microstate j. Eq. 5.13

expresses a relationship between heat and irreversibility: the more a process is irreversible (i.e., the larger the probability of a forward trajectory is than its time-reverse), the more heat is dissipated into the surrounding bath.

In England (2013) the author uses Eq. 5.13 in order to study the irreversible process of cellular replication. To this aim, coarse-grained variables are introduced, allowing the study of the macroscopic irreversibility of the system starting from the microscopic rule of Eq. 5.13. In particular, two (arbitrary) macrostates are considered: the macrostate I, in which a single living cell is present, and the macrostate II, consisting of two living cells. A conditional probability $p(i|I)$ can be associated to macrostate I, where $p(i|I)$ is the probability that the system is in a microstate i, if it is observed in the macrostate I. Analogously, if the system is observed in the macrostate II, a conditional probability $p(j|II)$ is assumed to describe the probability of the system to be in microstate j (England, 2013). By integrating over the ensembles, the probabilities of transitions between macrostates are obtained. In particular, let $\pi(I \to II)$ denote the probability that a system prepared in the macrostate I is observed in macrostate II after time τ, and $\pi(II \to I)$ denote the probability that the system returns in the macrostate I after another time interval τ. It results (England, 2013):

$$\pi(I \to II) = \int_{II} dj \int_{I} di \; p(i|I)\pi(i \to j), \tag{5.14}$$

and

$$\pi(II \to I) = \int_{I} di \int_{II} dj \; p(j|II)\pi(j \to i). \tag{5.15}$$

Therefore, the macroscopic description of the irreversibility of spontaneous propagation from I to II is given by:

$$\frac{\pi(I \to II)}{\pi(II \to I)} = \Big\langle \frac{\langle e^{-\beta \Delta Q_{ij}} \rangle_{i \to j}}{e^{ln[\frac{p(i|I)}{p(j|II)}]}} \Big\rangle_{I \to II}, \tag{5.16}$$

where $\Big\langle \cdots \Big\rangle_{I \to II}$ denotes an average over all paths from some microstate i in the macrostate I to some microstate j in the macrostate II.

Let $S \equiv -\sum_i p_i \ln p_i$ be the (Shannon) entropy for each ensemble associated with a macrostate, and $\Delta S_{int} \equiv S_{II} - S_I$ be the internal entropy change for the forward transition $I \to II$. Eq. 5.16 can be rearranged in order to obtain a generalisation of the second law of thermodynamics, constraining the irreversibility of macroscopic processes (England, 2013)

$$\beta \langle \Delta Q \rangle_{I \to II} + ln\Big[\frac{\pi(II \to I)}{\pi(I \to II)}\Big] + \Delta S_{int} \geq 0. \tag{5.17}$$

Note that, if I and II are the same macrostate containing all the micro states i, Eq. 5.17 reduces to the constrain of the second law of thermodynamics. On the other hand, for an irreversible transition $I \to II$, Eq. 5.17 sets a stricter bound: the more irreversible the

macroscopic process, the larger the minimum entropy production (England, 2013).

In order to apply Eq. 5.17 to self-replication, consider a population of replicators living at inverse temperature β. Let g and δ be the replication and decay rates, respectively, such that the probability in an infinitesimal period of time dt that a replicator gives birth is $\pi(I \to II) = gdt$, while the probability of a replicator decaying is $\pi(II \to I) = \delta dt$. By replacing these probabilities in Eq. 5.17 and assuming $g > \delta$, the following expression is obtained for the maximum net growth rate of a self-replicator (England, 2013):

$$g_{max} - \delta = \delta(e^{\beta\Delta q + \Delta s_{int}} - 1). \tag{5.18}$$

Here, Δs_{int} and Δq are the change of the internal entropy of the system and the average amount of heat released into the surrounding by the formation of a new replicator, respectively. Eq. 5.18 carries relevant biological information, such as the connection between the reproductive fitness of a replicator and its ability to exploit sources of energy, or the thermodynamic benefit of the simplest replicators (England, 2013). However, it is important to note that the framework introduced in England (2013) is not specific to living systems, and it was suggested that approaches based solely on dissipative processes and entropy production may not be sufficient to adequately understand the peculiarities underlying life (Walker, 2017). Nevertheless, thanks to the results shown above and obtained in other recent works, the general theory of nonequilibrium physics is proposed as a suitable framework for the study of life and its origin (Gnesotto et al., 2018).

5.3 Nonequilibrium thermodynamics of CRNs

5.3.1 Further notions on CRNs

In this section, we introduce the nonequilibrium thermodynamics of CRNs, based on the description established in Polettini and Esposito (2014); Rao and Esposito (2016, 2018). We focus our attention on specific quantities and results. For a more detailed discussion, please refer to the original works. Further notions on CRNs are needed in addition to those already provided in Section 4.2. We define a CRN as a triple $\mathcal{G} = (\mathcal{S}, \mathcal{N}, \mathcal{R})$, where $\mathcal{S}$ is the set of chemical species, $\mathcal{N} = \{\nu\}$ is the set of complexes and $\mathcal{R} = \{\nu \to \nu'\}$ is the set of reactions. The information about interactions among species can be enclosed in the *stoichiometric matrix* ∇, i.e., a $|\mathcal{N}| \times |\mathcal{R}|$ matrix where the element $\nabla(s, r)$, denoted by $\nabla_r(s)$, is the integer stoichiometric coefficient (positive for products and negative for reactants) of species s in reaction r. Note that the stoichiometric matrix ∇ can be written as (Horn and Jackson, 1972; Horn, 1972; Van der Schaft et al., 2015):

$$\nabla = ZM, \tag{5.19}$$

where Z is the *complex composition matrix*, i.e., a $|\mathcal{S}| \times |\mathcal{N}|$ matrix such that the element $Z(s, \nu)$ is the stoichiometric number of species s in the complex ν, and M is the $|\mathcal{N}| \times |\mathcal{R}|$ incidence matrix of the graph having complexes as nodes and reactions as edges.

We refer to mass-action systems (see Section 4.2 for details). Moreover, we focus on reversible CRNs, that is, CRNs in which each reaction $r_+ : \nu \to \nu'$ has a corresponding reverse reaction $r_- : \nu' \to \nu$. We use r as the index of pairs of forward-backward reactions. It is possible to define net concentration currents J_r along a pair of reversible reactions r, such that:

$$J_r = \kappa_{r_+} c^{\nu} - \kappa_{r_-} c^{\nu'}, \tag{5.20}$$

where $\kappa_{r_+} > 0$ ($\kappa_{r_-} > 0$) is the positive rate constant for the reaction r_+ (r_-), c is the vector of molar concentrations of chemical species, and c^{ν} is defined as:

$$c^{\nu} := \prod_{s \in \mathcal{S}} c(s)^{\nu(s)}. \tag{5.21}$$

With this notation, the set of ODEs describing the time evolution of concentrations of species in $\mathcal{S}$, Eq. 4.4, can be written as a continuity equation for the concentration (Polettini and Esposito, 2014; Rao and Esposito, 2016):

$$\dot{c} = \nabla J, \tag{5.22}$$

and *steady states* c^* are characterised by:

$$\nabla J^* = 0. \tag{5.23}$$

A mass-action system is called *complex balanced* if it admits a steady state c^* for which it is (Horn and Jackson, 1972; Horn, 1972; Feinberg, 1972):

$$M J^* = 0. \tag{5.24}$$

Therefore, a mass-action is complex balanced if, at each complex, the current inflow is exactly balanced by the current outflow. If a mass-action system admits a complex balanced steady state, then every other steady state is complex balanced (Horn and Jackson, 1972). Note that a mass-action system in which the underlying CRN is a reversible deficiency zero CRN, is always complex balanced (Horn and Jackson, 1972; Horn, 1972; Feinberg, 1972).

Furthermore, a mass-action system is called *detailed balanced* if it admits a (equilibrium) steady state c^* that satisfies the detailed-balance property (Lewis, 1925; Aris, 1965, 1968; Kondepudi and Prigogine, 2014; Rao and Esposito, 2016):

$$J_{eq} = 0, \tag{5.25}$$

that is, if all the current vanishes. For a mass-action system, Eq. 5.25 can be expressed as (Rao and Esposito, 2016):

$$\frac{\kappa_{r+}}{\kappa_{r-}} = \frac{(c_{eq})^{\nu'}}{(c_{eq})^{\nu}}, \forall r : \nu \rightleftharpoons \nu'. \tag{5.26}$$

To be thermodynamically consistent, a closed CRN must be detailed balanced. Therefore, Eq. 5.26 is a constraint that the rate constants must satisfy. It represent a property that holds regardless the network state, and is called *local detailed balanced* (Rao and Esposito, 2016).

Detailed balanced mass-action systems are a subclass of complex balanced mass-action systems (Feinberg, 1989; Dickenstein and Millán, 2011; Müller and Joshi, 2020). In particular, a reversible deficiency zero CRN governed by mass-action kinetics is detailed balanced if it satisfies $(|\mathcal{R}|/2-|\mathcal{N}|+l)$ *circuit conditions* (see Feinberg (1989) for details), where l is the number of linkage classes introduced in Section 4.2. Note that $(|\mathcal{R}|/2 - |\mathcal{N}| + l)$ is the *cycle rank* (Berge, 1962), that is, the minimum number of edges that must be removed from the undirect graph associated with the CRN to break all its cycles. It follows that, if $\mathcal{G}$ is a mass-action system in which the underlying CRN is a reversible deficiency zero CRN, and such that $|\mathcal{R}|/2 - |\mathcal{N}| + l = 0$, then $\mathcal{G}$ is detailed balanced for all the values of the rate constants (Feinberg, 1989).

5.3.2 Chemostatting, (broken) conservation laws and (emergent) cycles

We refer to a reservoir controlling the concentration of chemical species as the *chemostat*, and the controlled species are said to be *chemostatted*. We denote with $F = \{f\} \subset \mathcal{S}$ the set of chemostatted chemical species, and with $c_F := \{c(f), f \in F\}$ the corresponding concentrations. Note that concentrations c_F are not dynamical variables. Indeed, it is $\dot{c}_F = 0$ in case of a nondriven open CRN, and $c_F \equiv c_F[g(t)]$ in case of a driven open CRN, where $g(t)$ is a time-dependent protocol governing the change over time of the chemostatted concentrations. The set of internal (non-chemostatted) species is denoted by X, such that it is $\mathcal{S} = X \cup F$. We say that $\mathcal{G}$ is a closed CRN if $F \equiv \emptyset$, and that it is an open CRN otherwise.

Let $\mathcal{G}$ be a closed CRN. A *conservation law* λ is a vector in coker(∇) (Alberty, 2003; Polettini and Esposito, 2014; Rao and Esposito, 2016, 2018):

$$\lambda\nabla = 0. \tag{5.27}$$

From Eq. 5.22 and Eq. 5.27, it follows that vectors in coker(∇) identify conserved quantities called *components*, $\mathcal{H} = \sum_{s\in\mathcal{S}} \lambda(s)c(s)$ (Alberty, 2003). Indeed it is:

$$\dot{\mathcal{H}} = \lambda\dot{c} = \lambda\nabla J = 0. \tag{5.28}$$

Furthermore, a vector γ in $\ker(\nabla)$ is called a *cycle* (Polettini and Esposito, 2014; Rao and Esposito, 2016, 2018):

$$\nabla\gamma = 0. \tag{5.29}$$

A cycle γ represents a transformation that brings the system back to the same state (in the space of concentrations) to which the transformation is applied, the entries of γ being the number of times each reaction must occur during the cycle. From Eq. 5.23, it follows that steady state currents J^* belong to $\ker(\nabla)$. Therefore, they can be expressed as linear combinations of sets of cycles that are basis vectors for $\ker(\nabla)$ (Polettini and Esposito, 2014).

Consider now an open CRN $\mathcal{G}$. Its stoichiometric matrix ∇ can be parted such that (Polettini and Esposito, 2014):

$$\nabla = \Big(\frac{s \in X}{s \in F}\Big). \tag{5.30}$$

The stoichiometric matrices related to internal and chemostatted species are indicated with ∇^X and ∇^F, respectively. The concentrations of internal species change according to:

$$\dot{c}_X = \nabla^X J, \tag{5.31}$$

while for the chemostatted species it is:

$$\frac{đc_F}{đt} = \nabla^F J + I, \tag{5.32}$$

where I is the vector of the external currents for the inflow and the outflow of chemostatted species, and the symbol $\frac{đ}{đt}$ indicates a non-exact time derivative. Therefore, a steady state of an open mass-action system is characterised by (Polettini and Esposito, 2014; Rao and Esposito, 2016):

$$\begin{aligned} \nabla^X J^* &= 0 \\ \nabla^F J^* + I^* &= 0, \end{aligned} \tag{5.33}$$

where $I^* \neq 0$ for nonequilibrium steady states.

Passing from a closed CRN to an open CRN by chemostatting chemical species can either break conservation laws or generate *emergent cycles*, i.e., transfers of chemicals among chemostats that do not change the internal state of the CRN (Polettini and Esposito, 2014). A *broken conservation law* λ_b is characterised by (Polettini and Esposito, 2014; Rao

and Esposito, 2016):

$$\begin{aligned} \lambda_b \nabla &= 0, \\ \sum_{s \in X} \lambda_b(s) \nabla_r^X(s) &\neq 0, \text{ for some } r \in \mathcal{R}. \end{aligned} \tag{5.34}$$

Note that the component related to a broken conservation law is no longer a conserved quantity. An emergent cycle γ_e is characterised by (Polettini and Esposito, 2014; Rao and Esposito, 2016):

$$\begin{aligned} \nabla^X \gamma_e &= 0, \\ \nabla^F \gamma_e &\neq 0. \end{aligned} \tag{5.35}$$

Notably, assuming that for each reaction $r \in \mathcal{R}$ the chemostatting procedure does not involve all the species taking part in r, from the rank-nullity theorem for the stoichiometric matrices ∇ and ∇^X it follows (Polettini and Esposito, 2014):

$$|F| = |\{\lambda_b\}| + |\{\gamma_e\}| \tag{5.36}$$

where $|F|$ is the number of chemostatted species, $|\{\lambda_b\}|$ is the number of broken conservation laws, and $|\{\gamma_e\}|$ is the number of emergent cycles.

5.3.3 Entropy production rate, nonequilibrium Gibbs free energy and chemical work

Here we introduce thermodynamic quantities associated with CRNs, as done in Polettini and Esposito (2014); Rao and Esposito (2016, 2018). Again, we encourage an interested reader to see the original works for an exhaustive discussion. Hereafter, we make the assumption of the local equilibrium (Kondepudi and Prigogine, 2014), meaning that the thermalisation is much faster than the reactions' time scales. Therefore, it is possible to define intensive thermodynamic variables and densities of extensive thermodynamic quantities. Let us consider a homogeneous reaction mixture at temperature T and pressure p, where T is the temperature of the thermal bath consisting of the solvent, and p is pressure of the environment. We assume that the solvent does not react with the solutes, and that its concentration c_0 is constant and almost equal to that of the entire solution. Then, the *chemical potential* of a species $s \in \mathcal{S}$ is (Alberty, 2003; Rao and Esposito, 2016):

$$\mu(s) = \mu_\circ(s) + RT \ln c(s), \tag{5.37}$$

where R is the gas constant, and $\mu_\circ(s)$ takes into account both the standard-state chemical potential of species s at temperature T, and the term deriving from the solvent $-RT \ln c_0$.

We denote with μ_F the chemical potentials of chemostatted species.

The *Gibbs free energies of reaction* is defined as (Kondepudi and Prigogine, 2014; Alberty, 2003):

$$\Delta G_r = \nabla_r^T \mu = -RT \ln \frac{J_{r+}}{J_{r-}}, \tag{5.38}$$

where ∇^T is the transpose of ∇ and the last equality is obtained by using the local detailed balance, Eq. 5.26. The term

$$\mathcal{A}_r = RT \ln \frac{J_{r+}}{J_{r-}} \tag{5.39}$$

is the *reaction affinity*, that expresses the fundamental force that acts on reaction r. The change of Gibbs free energy along emergent cycles can be expressed in terms of *cycle affinities* (Polettini and Esposito, 2014; Rao and Esposito, 2016):

$$\mathcal{A}_{\gamma_e} = -\sum_r \gamma_e(r) \Delta G_r = -\gamma_e (\nabla^F)^T \mu_F, \tag{5.40}$$

Note that if the cycle affinities do not vanish, the system has not reached an equilibrium steady state.

The rate of the Gibbs free energy decrease gives the EPR of the CRN (Kondepudi and Prigogine, 2014; Polettini and Esposito, 2014; Rao and Esposito, 2016):

$$T\Sigma = -\sum_r J_r \Delta G_r = RT \sum_r (J_{+r} - J_{-r}) \ln \frac{J_{+r}}{J_{-r}} \geq 0. \tag{5.41}$$

Note that the EPR is non-negative and vanishes at equilibrium steady states. Moreover, it can be decomposed in two contributions, obtaining (Polettini and Esposito, 2014; Rao and Esposito, 2016):

$$T\Sigma = T\Sigma_X + T\Sigma_F = -\sum_{s \in X} \mu(s) \dot{c}(s) - \sum_{f \in F} \mu(f) [\dot{c}(f) - I(f)], \tag{5.42}$$

that is, the EPR is the sum of a term ($T\Sigma_X$) that takes into account the changes of the internal species, and of another term ($\mathrm{T}\Sigma_F$) emerging from the chemostatting and that takes into account both the time-dependent driving of the chemostatted species, and the external currents I. Note that the first term vanishes at nonequilibrium steady states, while the latter does not. In particular, at nonequilibrium steady states one has (Polettini and Esposito, 2014; Rao and Esposito, 2016):

$$T\Sigma^* = I^* \mu_F = \sum_{\{\gamma_e\}} \gamma_e J^* \mathcal{A}_{\gamma_e}. \tag{5.43}$$

Eq. 5.43 shows that, at a steady state, the dissipation of an open CRN is related to chemostatting, in particular being due to the emergent cycles.

The *nonequilibrium Gibbs free energy* of a CRN can be expressed as (Rao and Esposito, 2016):

$$\tilde{G} = \sum_{s\in\mathcal{S}} [c(s)\mu(s) - RTc(s)] + \tilde{G}_0, \tag{5.44}$$

where the terms $-RT\sum_s c(s)$ and $\tilde{G}_0$ take into account the contribution of the solvent. The *chemical work rate* performed by a chemostat on the CRN can be expressed as (Rao and Esposito, 2016):

$$\dot{W}_c = I\mu_F. \tag{5.45}$$

The rate of change of nonequilibrium Gibbs free energy $d\tilde{G}/dt$, the chemical work rate and the EPR are related according to the following (Rao and Esposito, 2016):

$$T\Sigma = \dot{W}_c - \frac{d\tilde{G}}{dt} \geq 0. \tag{5.46}$$

Let us consider a transformation that drives the CRN from an initial state i to a final state j. By integrating Eq. 5.46, it results:

$$T\Delta\Sigma = W_c - \Delta\tilde{G} \geq 0. \tag{5.47}$$

The difference of nonequilibrium Gibbs free energy $\Delta\tilde{G} = \tilde{G}_f - \tilde{G}_i$ between the states f and i can be related to the difference of the Gibbs free energy between the two equilibrium states j_{eq} and i_{eq} obtained from j and i by closing the CRN. It results (Rao and Esposito, 2016):

$$\Delta\tilde{G} = \Delta\tilde{G}_{eq} + \Delta D, \tag{5.48}$$

where D is the *relative entropy* defined as:

$$D(j,i) = \sum_{s\in S} [c_j(s)\ln\frac{c_j(s)}{c_i(s)} - c_j(s) + c_i(s)] \geq 0, \tag{5.49}$$

and

$$\Delta D = D(f, f_{eq}) - D(i, i_{eq}). \tag{5.50}$$

The quantity

$$W_c - \Delta\tilde{G}_{eq} = RT\Delta D + \Delta\Sigma \tag{5.51}$$

represents the chemical work dissipated during a nonequilibrium transformation. Thanks to the non-negativity of the entropy production, it results (see the original work Rao and Esposito (2016) for details and discussion on such relation):

$$W_c - \Delta\tilde{G}_{eq} \geq RT\Delta D. \tag{5.52}$$

The nonequilibrium Gibbs free energy is minimised by the dynamics in closed CRNs (Rao and Esposito, 2016). However, for an open detailed balanced CRNs with chemostatted species, the proper thermodynamic potential that is minimised by the dynamics is the *semigrand Gibbs free energy* G, obtained from $\tilde{G}$ by subtracting the energetic contribution of the broken conservation laws (Rao and Esposito, 2016, 2018). First of all, note that the set of chemostatted species F can be decomposed into two groups, $F_\beta = \{f_\beta\}$ and $F_\alpha = \{f_\alpha\}$, such that the former is a minimal set of chemostatted species that break all the broken conservation laws, while the latter is constituted by the remaining chemostatted species. It is possible to build a nonsingular matrix whose entries are $\{\lambda_b^{f_\beta}\}$ (Rao and Esposito, 2016; Falasco et al., 2018; Rao and Esposito, 2018). The column vectors of this latter matrix are denoted by $\{\bar{\lambda}_b^{f_\beta}\}$. The semigrand Gibbs free energy G can be expressed as:

$$G = \tilde{G} - \sum_{\lambda_b} f_{\lambda_b} \mathcal{H}_{\lambda_b}, \tag{5.53}$$

where

$$f_{\lambda_b} = \mu_{F_\beta} \bar{\lambda}_b^{f_\beta}. \tag{5.54}$$

Moreover, it is possible to define the *fundamental nonconservative chemical forces* $\mathcal{F}_{F_\alpha}$ (Falasco et al., 2018; Rao and Esposito, 2018):

$$\mathcal{F}_{f_\alpha} = \mu_{f_\alpha} - \sum_{f_\beta} \mu_{f_\beta} \sum_{\{\lambda_b\}} \bar{\lambda}_b^{f_\beta} \lambda_b^{f_\alpha}. \tag{5.55}$$

The forces $\mathcal{F}_{F_\alpha}$ identify chemical potential gradients imposed by the chemostats. A CRN is detailed balanced if and only if $\mathcal{F}_{F_\alpha} = 0$ (Falasco et al., 2018; Rao and Esposito, 2018). For open nondriven CRNs, Eq. 5.46 can be rearranged as (Falasco et al., 2018; Rao and Esposito, 2018):

$$T\Sigma = \dot{W}_{nc} - \frac{dG}{dt} \geq 0, \tag{5.56}$$

where

$$\dot{W}_{nc} = \sum_{f_\alpha} I_{f_\alpha} \mathcal{F}_{f_\alpha} \tag{5.57}$$

is the nonconservative chemical work rate. By integrating Eq. 5.56 it results (Rao and Esposito, 2018):

$$T\Delta\Sigma = W_{nc} - \Delta G. \tag{5.58}$$

In the following chapter we use these results in order to study the thermodynamic efficiency of RAF sets.

Chapter 6

Thermodynamic efficiency of RAF sets

6.1 Introduction

The RAF theory rises in the framework of graph theory, and the first works on RAF sets focus mainly on the "static" properties of such systems, looking only partially at the dynamic aspects and leaving out the thermodynamic ones. In previous chapters, we investigate the dynamics of RAF sets, observing a rich variety of dynamical behaviours. In particular, we show that in some cases the dynamical properties of RAF sets are predictable from the networks topology. In this chapter, we focus on the thermodynamic features of RAF sets. To our knowledge, these have not yet been examined. Our goal is to find a connection between the thermodynamic efficiency of the system and the constraints that a network must satisfy to be a RAF sets. In particular, we use the formalism introduced in Polettini and Esposito (2014); Rao and Esposito (2016, 2018); Wachtel et al. (2018); Penocchio et al. (2019) (see Section 5.3) in order to investigate the role of the reflexively autocatalytic property (Def. 1) on the ability of the network to store the chemical work performed by the surrounding environment. We carried out a preliminary study of this issue through the introduction of a simple toy model, observing that the catalysis plays a major role in the thermodynamic efficiency of the networks. We are currently investigating also the relation between the F-generated property (Def. 1) and the efficiency of the system.

The chapter is organised as follows. In Section 6.2 we uniform the food set notion introduced in previous chapters with the one provided in (Polettini and Esposito, 2014; Rao and Esposito, 2016), and we establish a general set-up for our study. In Section 6.3 we introduce a toy model to investigate the thermodynamic properties of simple RAF sets, and numerically calculate their efficiency. Finally, in Section 6.4 we discuss some preliminary results and future developments.

6.2 General set-up

6.2.1 Chemostatting of RAF sets

Let $\mathcal{S}$ be a set of interacting chemical species. In RAF theory, the food set $F \subset \mathcal{S}$ is a distinguibile subset of species that collects the resources provided by the environment (Hordijk and Steel, 2004). In previous chapters, given a CRN $(\mathcal{S}, \mathcal{N}, \mathcal{R})$ and a food set F, we introduced pseudo reactions among the zero complex 0 and each species $f \in F$, in order to represent a flow of matter that controls the concentration of food species. Following Horn and Jackson (1972); Polettini and Esposito (2014); Rao and Esposito (2016), here we consider a species s', whose concentration is maintained costant by the action of the environment, as an *external species*. The external species do not appear in the CRN representation of interacting species: consider, for instance, the reactions $s' \to s_1$ and $s' + s_1 \to s_2$; if s' is an external species, then the actual reactions of the CRN are $0 \to s_1$ and $s_1 \to s_2$. The species s' is said to be *chemostatted*, that is, each molecule of s' consumed or produced by a reaction is introduced or withdrawn by the environment. Hereafter, we identify the food set F introduced in RAF theory as the set of external species of a CRN.

Let $\tilde{\mathcal{G}} = (\tilde{\mathcal{S}}, \tilde{\mathcal{N}}, \tilde{\mathcal{R}})$ be a closed CRN. It is $F = \emptyset$. Suppose now that the system is opened by chemostatting some (external) species $f \in \tilde{\mathcal{S}}$, and denote with $\mathcal{G}$ the CRN obtained from $\tilde{\mathcal{G}}$ after the chemostatting. The set $\{f\} \subset \tilde{\mathcal{S}}$ is the food set F of $\mathcal{G}$. We denote with $\mathcal{S} = \tilde{\mathcal{S}} \setminus F$ the set of internal species of $\mathcal{G}$, with $\mathcal{N} = \{\nu\}$ the set of complexes obtained from $\tilde{\mathcal{N}}$ by removing the food species in each complex $\tilde{\nu} \in \tilde{\mathcal{N}}$, that is, $\nu(s) = \tilde{\nu}(s)$ if $s \in \mathcal{S}$ and $\nu(f) = 0$ for each $f \in F$, and with $\mathcal{R}$ the set of reactions among complexes $\nu \in \mathcal{N}$. Note that, if $F \neq \emptyset$, then $\mathcal{N}$ includes the zero complex 0. We say that $\mathcal{G}$ is F-generated (Hordijk and Steel, 2004) if, given the set $\mathcal{S} = \tilde{\mathcal{S}} \setminus F$, there exists a sequence of reactions $(0 \to \nu'_0), (\nu_1 \to \nu'_1), \ldots, (\nu_i \to \nu'_i) \in \mathcal{R}$ for each species $s \in \mathcal{S}$ such that:

$\nu'_i(s) \neq 0$;

$\forall s' \in \mathcal{S}$ such that $\nu_j(s') \neq 0$, $j = 1, \ldots, i$, there exists $k < j$ such that $\nu'_k(s') \neq 0$.

The chemostatting procedure can modify the topology of a CRN, by making the complexes with external species "collapse" in others already present, and making new pathways emerge within the network (see Figure 6.1 for an example). Therefore, the dynamics of an open CRN is, generally, different from that of the correspondent closed CRN. In particular, let $\tilde{\mathcal{G}}$ be a closed CRN taken with mass-action kinetics, and let $\tilde{\kappa}$ be the vector of rate constants for the reactions of the network. The changes of the internal species of the open CRN $\mathcal{G}$ are described by the equation (Polettini and Esposito, 2014):

$$\dot{c} = \sum_{\nu \to \nu'} \kappa_{\nu \to \nu'} c^{\nu} (\nu' - \nu), \quad \kappa_{\nu \to \nu'} = \tilde{\kappa}_{\tilde{\nu} \to \tilde{\nu}'} \prod_{f \in F} c(f)^{\tilde{\nu}(f)}. \tag{6.1}$$

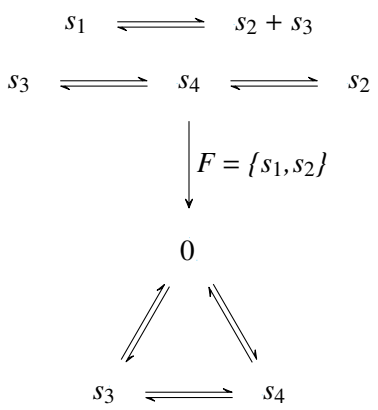

Figure 6.1. Chemostatting example. Above: the closed CRN $\tilde{\mathcal{G}}$ is constituted by the complexes $\{s_1, s_2 + s_3, s_3, s_4, s_2\}$. Below: the open CRN $\mathcal{G}$ is obtained from $\tilde{\mathcal{G}}$ by chemostatting species s_1 and s_2. In the open CRN, complexes s_1 and s_2 collapse in the zero complex 0, and the complex $s_2 + s_3$ becomes undistinguishable from complex s_3.

Moreover, as previously mentioned (see Section 5.3.2), the chemostatting of a chemical species can break a conservation law or lead to the emergence of a cycle that bears a cycle affinity, Eq. 5.40, generally nonvanishing at steady states (Polettini and Esposito, 2014). It follows that an open mass-action system $\mathcal{G}$ can reach nonequilibrium steady states with a non-zero EPR. Notice that, once a conservation law is established (such as the mass conservation for a closed CRN), at least two chemostatted species are necessary in order to drive the system out of equilibrium (Polettini and Esposito, 2014).

6.2.2 Thermodynamic efficiency

Let us consider an homogeneous reaction mixture at temperature T and pressure p, containing species undergoing elementary reactions. The reaction systems is represented by an open CRN $\mathcal{G} = (\mathcal{S}, \mathcal{N}, \mathcal{R})$, where the subset of species $F \subset \mathcal{S}$ is assumed to be chemostatted. The dynamics of the system is governed by the equations:

$$\begin{aligned} \dot{c}_X &= \nabla^X J, \\ \frac{đc_F}{đt} &= \nabla^F J + I = 0, \end{aligned} \tag{6.2}$$

where $c(s)$ is the vector of species concentrations, J is the vector of the reaction fluxes, Eq. 5.20, I is the vector of the external currents for the inflow and the outflow of chemostatted species, and ∇^X and ∇^F indicate the stoichiometric matrices related to internal and chemostatted species, respectively (see Section 5.3 for details). The chemical potential of each species $s \in \mathcal{S}$ is given by (Alberty, 2003):

$$\mu(s) = \mu_\circ(s) + RT \ln c(s), \tag{6.3}$$

where $\mu_\circ(s)$ takes into account both the standard-state chemical potential of species s, and the term deriving from the solvent. The rate constants of the CRN satisfy the local detailed balance, Eq. 5.26. The EPR is given by (Kondepudi and Prigogine, 2014; Polettini and Esposito, 2014; Rao and Esposito, 2016):

$$T\Sigma = -\sum_r RT(J_{+r} - J_{-r}) \ln \frac{J_{+r}}{J_{-r}} \geq 0. \tag{6.4}$$

If $F = \emptyset$, the (closed) CRN eventually reaches the equilibrium state, for which it is $T\Sigma = 0$. However, the chemostatting of species of the food set ($F \neq \emptyset$) can drive the system out of equilibrium. In particular, the chemical potential gradients imposed by the chemostats are associated with nonconservative chemical forces $\mathcal{F}_{F_\alpha}$, Eq. 5.55, and the fueling power performed on the system by the chemostats can be expressed as: (Rao and Esposito, 2018; Falasco et al., 2018; Penocchio et al., 2019):

$$\dot{W}_{nc} = \sum_{f_\alpha} I_{f_\alpha} \mathcal{F}_{f_\alpha}, \tag{6.5}$$

where $I_{f\alpha}$ is the external current of the chemostatted species f_α (see Section 5.3.3 for details). It results (Falasco et al., 2018; Rao and Esposito, 2018):

$$T\Sigma = \dot{W}_{nc} - \frac{dG}{dt}. \tag{6.6}$$

Here, G is the semigrand Gibbs free energy, Eq. 5.53. For some values of the concentrations of food species, the forces $\mathcal{F}_{F_\alpha}$ can vanish, and the open CRN reaches an equilibrium state, even in the presence of chemostatting. On the other hand, if $\mathcal{F}_{F_\alpha} \neq 0$, the system is driven towards a nonequilibrium steady state (Rao and Esposito, 2018; Falasco et al., 2018; Penocchio et al., 2019).

Following Penocchio et al. (2019), we assume an open CRN initially at equilibrium, that is brought out of equilibrium by increasing the concentration of a food species f_α (the fuel), with respect to a chemostatted species f_β (the waste), such that it is $\mathcal{F}_{f_\alpha} = \mu(f_\alpha) - \mu(f_\beta) > 0$. While reaching the nonequilibrium steady state, the system stores energy, quantified by the nonequilibrium free energy G. By integrating Eq. 6.6, it results (Penocchio et al., 2019):

$$W_{nc} = T\Delta\Sigma + \Delta G, \tag{6.7}$$

which links the work performed by the chemostats with the dissipated and the stored energy. The latter stabilises on a constant value once the nonequilibrium steady state is reached, and all the chemical work is then used by the system to preserve the accumulated energy. The

efficiency of the process can be defined as (Penocchio et al., 2019):

$$\eta = \frac{\Delta G}{W_{nc}} = 1 - \frac{T\Sigma}{W_{nc}}, \tag{6.8}$$

that reaches a maximum during the charging phase, and drops towards zero during the maintenance phase (Penocchio et al., 2019).

We are interested in how the catalysis of a RAF set affects the process of energy storage, quantified by the efficiency η. Let us consider a closed CRN $\tilde{\mathcal{G}} = (\tilde{\mathcal{S}}, \tilde{\mathcal{N}}, \tilde{\mathcal{R}})$, and let $C = \{(s, r), s \in \tilde{\mathcal{S}}, r \in \tilde{\mathcal{R}}\}$ be a set of catalyses, meaning that species s catalyses reaction r. We denote with $\tilde{\mathcal{G}}_C$ the full network obtained from $\tilde{\mathcal{G}}$ by adding reactions according to the scheme showed in Figure 4.2, for each catalysis in C. Note that, for each catalysis $(s, r) \in C, r : \nu \rightleftharpoons \nu'$, the stoichiometric matrix ∇_C of $\tilde{\mathcal{G}}_C$ contains m columns and $m - 1$ rows more than the stoichiometric matrix ∇ of the "spontaneous" CRN $\tilde{\mathcal{G}}$, where

$$m = \sum_{s \in \tilde{\mathcal{S}}} [\nu(s) + \nu'(s)]. \tag{6.9}$$

We denote with $\tilde{\mathcal{R}}_{(s,r_i)}$ the set of reactions introduced to represent the catalysis $(s, r) \in C$. It is:

$$r_i \perp r_j, r_j \perp r_k, \forall r_j, r_k \in \tilde{\mathcal{R}}_{(s,r)}, r_j \neq r_k; \tag{6.10}$$

$$\sum_{r_j \in \tilde{\mathcal{R}}_{(s,r)}} r_j = r_i, \tag{6.11}$$

where r_i is the i-th columns of the stoichiometric matrix ∇. These relations are obtained by using Eq. 4.15 and Eq. 4.16, that is, they are due to the assumption that each enzimatyc complex is different from the others. From Eq. 6.10 and Eq. 6.11 it follows that, for each catalysis $(s, r) \in C$, it is:

$$rk(\nabla_C) = rk(\nabla) + m - 1. \tag{6.12}$$

By using the rank-nullity theorem, it results:

$$\begin{aligned} |\lambda_C| &= |\lambda|, \\ |\gamma_C| &= |\gamma| + |C|, \end{aligned} \tag{6.13}$$

where λ_C, γ_C, λ, γ are the conservation laws and the cycles associated with ∇_C and ∇, respectively, and $|C|$ is the number of catalyses. Note that each of the $|C|$ cycles of the CRN $\tilde{\mathcal{G}}_C$ that is not present for $\tilde{\mathcal{G}}$, corresponds to a realisation of a spontaneous reaction in one direction and the associated catalysis, in the opposite direction. When species in the food set F of $\tilde{\mathcal{G}}$ are chemostatted, either conservation laws are broken, or new cycles emerge (Polettini and Esposito, 2014). However, the relations of Eq. 6.13 still hold: it follows that

the open CRN with catalyses has the same broken conservation laws (and emergent cycles) of the analogous CRN without catalysis. In particular, the elements $\lambda_b^{f_\beta}$ of the broken conservation laws associated with the two CRNs are the same. Therefore, the expression of $\dot{W}_{nc}$ is the same for the CRNs with or without the catalysis. However, the external currents I_{f_α} of the two networks are, in general, different, due to the different dynamics underlying the systems. On the other hand, the EPR of $\mathcal{G}_C$ contains additional terms, relating to the added reactions representing the catalyses. However, the difference in dissipation between the two CRNs is also hard to predict, as it depends itself on the dynamics. For this purpose, in the next section we introduce a simple model, that allows us to easily calculate how catalysis affects the efficiency of the energy storage process.

6.3 Toy model

We consider a RAF CRN $\mathcal{G}_C = (\mathcal{S} \cup \{e\}, \mathcal{N}, \mathcal{R})$, with a set of reversible monomolecular spontaneous reactions $r : s \rightleftharpoons s'$, and associated catalyses (s'', r) represented by the Michaelis–Menten equation (Michaelis and Menten, 1913):

$$s + s'' \underset{\kappa_{-1}}{\overset{\kappa_1}{\rightleftharpoons}} \mathrm{e} \underset{\kappa_{-2}}{\overset{\kappa_2}{\rightleftharpoons}} s' + s'', \tag{6.14}$$

where $\{e\}$ is the set of the intermediate complexes associated with spontaneous reactions, such that, for each pair of reaction r, r', it is $(e_r \cdot e_{r'}) \neq 0 \Leftrightarrow r = r'$. We chose rate constants such that $\kappa_1 = \kappa_{-2}$ and $\kappa_2 = \kappa_{-1}$, with $\kappa_2 >> \kappa_1$. We denote with $\mathcal{R}' \subset \mathcal{R}$ the set of spontaneous reactions. The food set $F \subset \mathcal{S}$ is constituted by two chemostatted species, $F = (f_\alpha, f_\beta)$, that are connected by the spontaneous reactions: when not considering the catalyses, the "spontaneous" CRN (denoted with $\mathcal{G}'$) contains a single linkage class, represented by a chain that starts from f_α and ends on f_β. We assume that the chemostatted species do not act as catalysts, neither that a species can catalyse its own production. The stoichiometric matrix ∇' of $\mathcal{G}'$ is represented by a $|S| \times |\mathcal{R}'|$ matrix of elements:

$$\nabla'_{i,j} = \begin{cases} -1, \text{ if } i = j, \\ 1, \text{ if } i = j + 1, \\ 0 \text{ otherwise.} \end{cases}$$

It follows that there is only one conservation law $\lambda_b = \begin{pmatrix} 1, & \cdots, & 1 \end{pmatrix}^T$ that represents the conservation of the total mass. We assume that each spontaneous reaction has the same rate constant κ_s, regardless of its direction, with $\kappa_s << \kappa_1$. Therefore, the local detailed balance condition, Eq. 5.26, reads:

$$\mu_\circ(s) = \mu_\circ(s'), \forall s, s' \in \mathcal{S}. \tag{6.15}$$

The chemostatting of species in the food set breaks the conservation law λ_b, whose elements $\lambda_b^{f_\beta}, \lambda_b^{f_\alpha}$ are equal to 1. Therefore, the fueling power acting on the CRN $\mathcal{G}'$ is (Rao and Esposito, 2018; Falasco et al., 2018):

$$\dot{W}'_{nc} = I'_{f_\alpha}[\mu(f_\alpha) - \mu(f_\beta)] = J_\alpha[\mu(f_\alpha) - \mu(f_\beta)], \tag{6.16}$$

where J_α denotes the flux associated with the reaction $f_\alpha \rightleftharpoons s1$. It follows that the open CRN $\mathcal{G}'$ is detailed balanced if $c(f_\alpha) = c(f_\beta)$; otherwise, the chemostats drive the system out of equilibrium. For the RAF CRN $\mathcal{G}_C$ it results:

$$\dot{W}_{nc} = (J_\alpha + \Delta I_\alpha)[\mu(f_\alpha) - \mu(f_\beta)], \tag{6.17}$$

where ΔI_α takes into account the fluxes deriving from the catalysis associated with reaction $f_\alpha \rightleftharpoons s1$. Note, moreover, that the EPR of $\mathcal{G}_C$ can be expressed as:

$$\begin{aligned} T\Sigma = RT \sum_r J_r \ln \frac{J_{+r}}{J_{-r}} &= RT \sum_{r:s\rightleftharpoons s'} \kappa_s[c(s) - c(s')] \ln \frac{s}{s'} \\ &+ RT \sum_{(s'',r)\in C} \{[\kappa_1 c(s)c(s'') - \kappa_2 c(e_r)] \ln \frac{\kappa_1 c(s)c(s'')}{\kappa_2 c(e_r)} \\ &+ [\kappa_2 c(e_r) - \kappa_1 c(s')c(s'')] \ln \frac{\kappa_2 c(e_r)}{\kappa_1 c(s')c(s'')}\}, \end{aligned} \tag{6.18}$$

where C is the set of catalyses. We are currently investigating the possibility of using the coarse graining method introduced in Wachtel et al. (2018) to find an analytical expression that allows us to estimate the efficiency of the introduced model, as a function of the possible catalysis.

6.3.1 Numerical results

In this section we numerically solve the equations describing the dynamics of a RAF CRN, Eq. 6.2, in order to study how catalyses affect its the thermodynamic efficiency, Eq. 6.8. In particular, the investigated CRNs $\mathcal{G}$ are examples of the model introduced in Section 6.3, with species $\mathcal{S} = (f_\alpha, f_\beta, s1, s2, s3)$ and spontaneous reactions $\mathcal{R}' = (r_1 : f_\alpha \rightleftharpoons s1, r_2 : s1 \rightleftharpoons s2, r_3 : s2 \rightleftharpoons s3, r_4 : s3 \rightleftharpoons f_\beta)$. We choose a set of possible catalyses, $C = \{(s2, r_1), (s3, r_2), (s1, r_3), (s2, r_4)\}$, and we perform various simulations, spanning all the possible combinations of active catalyses in C. Note that $\mathcal{G}$ is a RAF set only if the following combinations of catalyses are present: $C_1 = \{(s2, r_1), (s3, r_2), (s1, r_3)\}$, $C_2 = \{(s3, r_2), (s1, r_3), (s2, r_4)\}$ and $C_3 = \{(s2, r_1), (s3, r_2), (s1, r_3), (s2, r_4)\}$.

The results obtained for all the simulated CRNs are shown in the scatter plot of Figure 6.2, where each CRN i is associated with the maximum value reached by η_i (y-axis), and the time necessary to reach it (x-axis). We observe that the catalysis actually modifies

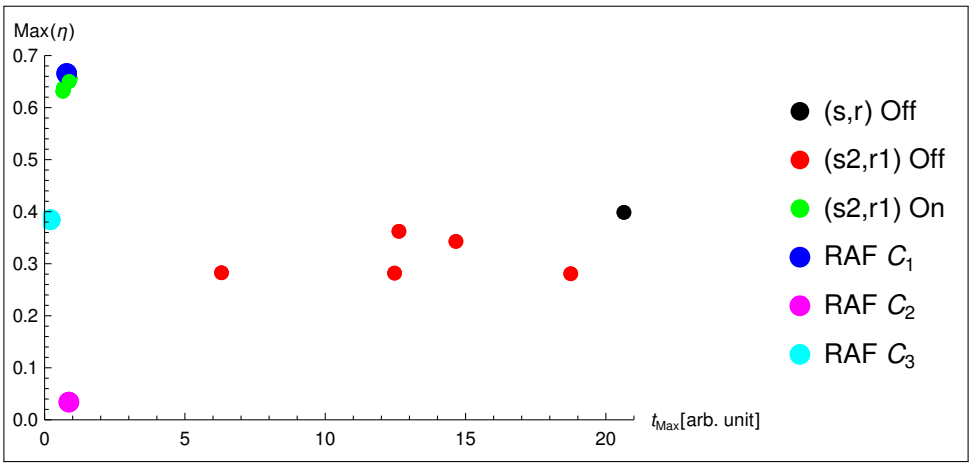

Figure 6.2. Scatter plot of the thermodynamic efficiency. On the x-axis: time t_{Max} (arbitrary units) necessary to reach the maximum value of η. On the y-axis: maximum value reached by η. Black circle: spontaneous CRN. Red circle: catalysis of the inflowing reaction not active. Green circle: catalysis of the inflowing reaction active. Blue, magenta and cyan circles: RAF sets. In all the simulations, we set $\kappa_2 = 10^3\kappa_1 = 10^5\kappa_s$, $\kappa_s = 1[arb.unit]$. At time $t = 0$ the system is at equilibrium.

the energy storage efficiency of the CRNs. In particular, the catalysis of the inflowing reaction $f_\alpha \rightleftharpoons s1$ plays a major role both in increasing the maximum value of the efficiency, and in decreasing the time needed to reach it. Note that the catalysis of the inflowing reaction is the only one that directly modifies the fueling power, Eq. 6.17. Similarly, the catalysis of the outflowing reaction $s3 \rightleftharpoons f_\beta$ determines, in general, the decrease of the maximum efficiency. Moreover, our results show that the reflexively autocatalytic property does not constrain the efficiency of the network: in fact, we note that the three RAF sets present among the simulated CRNs show different efficiencies. In particular, for $C = C_2$ the food set coincides with the waste chemostatted species, and the corresponding RAF set exhibits the lowest value of the maximum efficiency within the simulated sets of CRNs. In fact, the F-generated property does not consider the thermodynamic forces of the system. On the other hand, the RAF set corresponding to the set $C = C_1$ is associated with the maximum value reached by η, while for $C = C_3$ the maximum of the efficiency assumes an average value. We are investigating the biological implications of this result.

6.4 Discussion and conclusions

In this chapter, we established a general set-up for the study of thermodynamic properties of the RAF sets, following the framework introduced in (Polettini and Esposito, 2014; Rao and Esposito, 2016). We performed a preliminary study aimed at connecting the properties of RAF sets with their energy storage efficiency. We introduced a simple model of RAF CRN in order to follow the efficiency as a function of the active catalyses. The model lends

itself to an analytical study of its thermodynamic properties, which we are currently carrying out. By using numerical simulations, we observe that catalysis plays a major role in changing the thermodynamic efficiency of the network. On the other hand, the reflexively autocatalytic property is not sufficient to constrain the resulting efficiency. This preliminary result supports the previous observation (Chapter 4), according to which the CRNs satisfying the RAF properties can actually exhibit very different behaviours. Regarding this point, in the future we will investigate the impact of the F-generated constrain.

Another interesting aspect concerns the possibility of extending this study to stochastic models. In fact, it has been observed that the deterministic EPR is equal to that one of the stochastic dynamics only for a particular class of CRNs, i.e., the zero deficiency CRNs (Polettini et al., 2015). The study of thermodynamic properties of RAF sets taken with stochastic chemical dynamics will be examined in a forthcoming work.

Part IV

Conclusions

Understanding how life could have arisen from inanimate matter is a hard problem. From an experimental point of view, "building" a living system in the laboratory seems yet out of reach, despite the enormous advances in molecular biology. Indeed, a complete knowledge of the conditions and mechanisms that made it possible for first life forms to emerge from chemical molecules has not yet been achieved. Progress can come from the realisation of theoretical models that are able both to capture the peculiar properties of living systems, and to reproduce their emergence within the context in which life is believed to have developed. In this scenario, ASs, and in particular their formalization represented by the RAF sets, are of great interest. The idea behind a RAF set, indeed, is that of a set of chemical reactions that facilitate each other's occurrence, so that the entire system is able to self-organise and collectively emerge, by exploiting the resources available from the environment. These systems are therefore potentially able to self-reproduce and increase their complexity, starting from simple building blocks. Several works have investigated RAF sets in the context of graph theory, and important results have been obtained regarding the probability of observing these networks in generic chemical reaction systems, as well as their presence in real metabolic networks. Furthermore, numerical simulations were carried out to study the dynamical emergence of such sets.

However, the dynamical behaviour of RAF sets has not yet been fully clarified, nor have their thermodynamic properties been investigated. Such arguments represent the main research topics of my Ph.D work. In particular, the question we try to answer are the following:

Are the necessary conditions a set of chemical reactions must satisfy to be a RAF set, sufficient to constrain its dynamical behaviour?

By representing the RAF sets in terms of CRNs, we use the CRN theory to show that the topology associated to a RAF set is not sufficiently constrained to determine the dynamics of the CRN. In particular, we identify further conditions compared to the RAF definition, that are connected with different dynamical behaviours and that allow to define minimal RAF sets (or motifs) with predictable dynamics. The different observed long-term behaviours exhibit peculiar characteristics that can be linked to biological properties, thus being possible targets for natural selection.

Does the RAF set definition imply dynamical self-reproduction?

A RAF set is, in general, a complex network constituted by several subsets, which can in turn meet the RAF definition. We observe that a RAF set in which different motifs are present may not achieve self-reproduction, i.e., there are subsets of chemical species, among those in the RAF set, that disappear during the dynamics, as they are not reproduced

at sufficiently high rates. Importantly, the motifs we introduce satisfy the additional condition of closure imposed by the RAF theory, i.e., they are closed RAF sets. As a result, even if we observe that the reaction rates of a closed RAF set are actually increased by the presence of catalyst species, we show that a closed RAF set may fail to self-reproducing in the long-term dynamics. Note that we achieve this result both in the deterministic model and in the stochastic simulations. However, the topological constraints we introduce allow to detect motifs able to efficiently produce all their components, thus capable of emerging and self-maintaining. Moreover, the ability of self-reproduction can be acquired or lost by a motif consequently to "mutations", i.e., the occurrence of spontaneous reactions. This latter result supports the evolvability of RAF sets.

Do the interactions among RAF sets play a role in the potential biological evolution of such systems?

We investigate interactions among both RAF subsets within the same newtork (intra-network interactions), and RAF sets constituting separate networks (inter-networks interactions). In particular, intra-network interactions are constituted by reactions that connect RAF subsets, and can be responsible of competitive mechanisms that allow the emergence and the self-reproduction of only some of them. We observe such mechanisms both in the stochastic simulations and in the deterministic model. In this latter case, the topological investigation we perform allows us to predict which of the RAF subsets (motifs) dynamically survive the interactions, and which do not. A competition for resources can arise also among RAF subsets belonging to different networks. By introducing composition operations, we model an exchange of chemical species among separated RAF sets, the flow of species being governed by a flowing rate. The stochastic simulations we perform highlight that the flowing rate controls the emergence of RAF subsets belonging to different networks, if the flow affects the basic resources of the subsets themselves. Moreover, the exchange of species can produce other forms of biological interactions, such as facilitation and cheating. Therefore, our study suggests that intra- and inter-network interactions play an important role in the dynamical behaviour of RAF sets, and underlie the variation and evolution of a population of such networks.

Do RAF sets exhibit peculiar thermodynamic properties?

RAF sets are, by definition, systems out of equilibrium , and the thermodynamic observables associated with them can show, in principle, various features. Using recent tools that allow to effectively investigate the thermodynamic properties of nonequilibrium CRNs, we have set up a general framework for the study of the thermodynamics of RAF systems, and we have performed a preliminary numerical study of their thermodynamic efficiency. Our first results suggest that the topology of a RAF set does not strongly constrain the

thermodynamic properties of the system, allowing different networks to exhibit various thermodynamic behaviours. Furthermore, we observe that catalysis plays a major role in the thermodynamic efficiency of CRNs. Regarding this latter point, we are currently investigating the impact of the F-generated property.

Future prospects

The first natural development of this work is a more in-depth study of the thermodynamic properties of RAF sets that takes into account the link between the thermodynamics of CRNs and the dynamics dictated by their topology.

Another possible follow up may be the study of the dynamical evolution in stochastic regime of the motifs we have introduced. A stochastic approach is in fact suitable for the study of chemical networks at low concentrations, and could help to better understand the role of enzymatic complexes on global dynamics, as well as being a proper tool for directly simulating the occurrence of mutations.

Moreover, an important improvement of the previous conclusions will be achieved once we consider larger systems containing various networks, in order to carry out population dynamics study and simulate the biological evolution of a population of RAF sets.

Part V

List of publications

Ravoni, A. *Impact of composition on the dynamics of autocatalytic sets.* Biosystems, Elsevier, 2020, 198, 104250.

Ravoni, A. and Angelani, L. *Lattice model for active flows in microchannels.* Phys. Rev. E, American Physical Society, 2020, 102, 062602.

Ravoni, A. *Long-term behaviours of Autocatalytic sets.* Journal of Theoretical Biology, submitted.

Ravoni, A. *Thermodynamic efficiency of RAF sets.* In prep.

Part VI

Appendix

Appendix A

A

Let $\mathcal{G} = (\mathcal{S}, \mathcal{N}, \mathcal{R})$ be a CRN, $\mathcal{R}^+$ and $\mathcal{R}^-$ be the sets of reversible and irreversible reactions (such that $\mathcal{R} = \mathcal{R}^+ \cup \mathcal{R}^-$), and i, j denote reactions $\nu \to \nu' \in \mathcal{R}$. The function $f(c, \kappa)$ for $\mathcal{G}$ can be written as:

$$f_{\mathcal{G}}(c, \kappa) = \sum_{i \in \mathcal{R}^+} \kappa_i c^{\nu_i} (\nu'_i - \nu_i) + \sum_{j \in \mathcal{R}^-} \kappa_j c^{\nu_j} (\nu'_j - \nu_j). \tag{A.1}$$

Similarly, for $\mathcal{G}_c$ it is:

$$\begin{aligned} f_{\mathcal{G}_C}(c, \kappa) = &\sum_{i \in \mathcal{R}^+} [\kappa_i c^{\nu_i} (\nu'_i - \nu_i) + P_i] + \\ &+ \sum_{j \in \mathcal{R}^-} [\kappa_j c^{\nu_j} (\nu'_j - \nu_j) + I_j], \end{aligned} \tag{A.2}$$

where P_i and I_j denote the additional terms introduced by adding catalysis according to the scheme of Fig. 4.2 for reversible and irreversible reactions, respectively. For each pair (i, i') of reversible reactions such that $i : \nu \to \nu'$ and $i' : \nu' \to \nu$, the term $P_{(i,i')}$ can be written as:

$$\begin{aligned} P_{(i,i')} =& |s2|[\kappa_1 c(s2)c(x) - \kappa_{-1} c(e^*)] \\ &\times (e^* - s2 - x) + \{\kappa_1 c^{(\nu - s2)} [|s2| c(e^*) \\ &+ (1 - |s2|)c(x)] - \kappa_{-1} c(e)\} [e - \nu \\ &+ s2 - |s2| e^* - (1 - |s2|)x] \\ &+ \{\kappa_2 c(e) - \kappa_{-2} c^{(\nu' - p2)} [|p2| c(e^{**}) \\ &+ (1 - |p2|)c(x)]\} [\nu' - p2 + |p2| e^{**} \\ &+ (1 - |p2|)x - e] + |p2| [\kappa_1 c(p2)c(x) \\ &- \kappa_{-1} c(e^{**})] (e^{**} - p2 - x). \end{aligned} \tag{A.3}$$

Here, $s2$ and $p2$ are the vectors having all components equal to zero, except one (corresponding to species $s2$ and $p2$, respectively). Note that due to the above definition, $P_{(i,i')}$ describes the terms to be added for all the catalyses shown in Figure. 4.2, depending on whether the relations $s2 = 0$ and $p2 = 0$ are valid or not, where 0 is the zero complex.

Similarly, for each irreversible reaction $j : \nu \to \nu'$ the term I_j can be written as:

$$\begin{aligned} I_{(j)} =&|s2|[\kappa_1 c(s2)c(x) - \kappa_{-1}c(e^*)] \\ &\times(e^* - s2 - x) + \{\kappa_1 c^{(\nu - s2)}[|s2|c(e^*) \\ &+(1 - |s2|)c(x)] - \kappa_{-1}c(e)\}[e - \nu \\ &+s2 - |s2|e^* - (1 - |s2|)x] \\ &+[\kappa_2 c(e)](\nu' + x - e). \end{aligned} \tag{A.4}$$

Note that I_j can be obtained from $P_{(j,j')}$ assuming $\kappa_{-2} = 0$ and $p2 = 0$. From Eq. A.3 it results:

$$\begin{aligned} \dot{c}(e) =&\{\kappa_1 c^{(\nu - s2)}[|s2|c(e^*) + (1 - |s2|)c(x)] \\ &-\kappa_{-1}c(e) + \kappa_2 c(e) - \kappa_{-2}c^{(\nu' - p2)}[|p2|c(e^{**}) \\ &+(1 - |p2|)c(x)]\}, \end{aligned} \tag{A.5}$$

$$\begin{aligned} \dot{c}(e^*) =&|s2|[\kappa_1 c(s2)c(x) - \kappa_{-1}c(e^*) \\ &-\kappa_1 c^{(\nu - s2)}c(e^*) + \kappa_{-1}c(e)], \end{aligned} \tag{A.6}$$

$$\begin{aligned} \dot{c}(e^{**}) =&|p2|[\kappa_1 c(p2)c(x) - \kappa_{-1}c(e^{**}) \\ &-\kappa_{-2}c^{(\nu' - p2)}c(e^{**}) + \kappa_2 c(e)]. \end{aligned} \tag{A.7}$$

By imposing $\dot{e} = 0$, $\dot{e}^* = 0$ and $\dot{e}^{**} = 0$ (QSS assumption), it follows:

$$\begin{aligned} \kappa_2 c(e) - \kappa_{-2}c^{(\nu' - p2)}c(e^{**}) =&\kappa_1 c^{(\nu - s2)}c(e^*) \\ &-\kappa_{-1}c(e). \end{aligned} \tag{A.8}$$

Again, equivalent expressions for irreversible reactions are obtained assuming $\kappa_{-2} = 0$, $p2 = 0$ and (or) $s2 = 0$. Note that the equivalences of Eq. A.8 imply that, if for $f_{\mathcal{G}}$ it is:

$$f_{\mathcal{G}} = \sum_{\nu \to \nu'} \alpha_{\nu \to \nu'}(\nu' - \nu), \tag{A.9}$$

then $f_{\mathcal{G}_C}$ can be written as:

$$f_{\mathcal{G}_C} = \sum_{\nu \to \nu'} \alpha'_{\nu \to \nu'}(\nu' - \nu), \tag{A.10}$$

where:

$$\alpha'_{\nu \to \nu'} = \alpha_{\nu \to \nu'} + \Delta_{\nu \to \nu'}, \tag{A.11}$$

with $\Delta_{\nu\to\nu'} \geq 0$. For instance, if $\kappa_{-2} \neq 0$, $p2 \neq 0$ and $s2 \neq 0$ it is:

$$\Delta_{\nu\to\nu'} = \kappa_2 c(e) \tag{A.12}$$

for a forward reaction (that is, a reaction with a "spontaneous" rate constant κ_0) and:

$$\Delta_{\nu\to\nu'} = \kappa_{-2} c^{(\nu'-p2)} c(e^{**}) \tag{A.13}$$

for a reverse reaction (that is, a reaction with a "spontaneous" rate constant κ_{-0}). This implies, in particular, that $\mathcal{G}_C$ admits a positive equilibrium only if $\mathcal{G}$ is weakly reversible. An equivalent result holds if $\kappa_{-2} = 0$, $p2 = 0$ and (or) $s2 = 0$.

Bibliography

Christoph Adami and Thomas LaBar. From entropy to information: Biased typewriters andthe origin of life. *arXiv preprint arXiv:1506.06988*, 2015.

Robert Alberty. *Thermodynamics of biochemical reactions*. Wiley-Interscience, Hoboken, N.J, 2003. ISBN 0-471-22851-6.

Jakob L. Andersen, Christoph Flamm, Daniel Merkle, and Peter F. Stadler. Rule composition in graph transformationmodels of chemical reactions. *MATCH Commun. Math. Comput. Chem.*, 80:661–704, 2018. ISSN 0340 - 6253.

Jakob L. Andersen, Christoph Flamm, Daniel Merkle, and Peter F. Stadler. Defining autocatalysis in chemical reaction networks. *J. Syst. Chem*, 8:121–133, 2020.

David F. Anderson and Thomas G. Kurtz. *Continuous Time Markov Chain Models for Chemical Reaction Networks*, pages 3–42. Springer New York, New York, NY, 2011. ISBN 978-1-4419-6766-4. doi: 10.1007/978-1-4419-6766-4_1. URL `https://doi.org/10.1007/978-1-4419-6766-4_1`.

Frank A. L. Anet. The place of metabolism in the origin of life. *Current Opinion in Chemical Biology*, 8(6):654–659, dec 2004. doi: https://doi.org/10.1016/j.cbpa.2004.10.005.

Rutherford Aris. Prolegomena to the rational analysis of systems of chemical reactions. *Archive for Rational Mechanics and Analysis*, 19(2):81–99, jan 1965. doi: https://doi.org/10.1007/BF00282276.

Rutherford Aris. Prolegomena to the rational analysis of systems of chemical reactions II. some addenda. *Archive for Rational Mechanics and Analysis*, 27(5):356–364, jan 1968. doi: https://doi.org/10.1007/BF00251438.

Gonen Ashkenasy, Reshma Jagasia, Maneesh Yadav, and Reza M. Ghadiri. Design of a directed molecular network. *Proceedings of the National Academy of Sciences*, 101(30):10872–10877, jul 2004. doi: https://doi.org/10.1073/pnas.0402674101.

John C. Baez and Blake S. Pollard. A compositional framework for reaction networks. *Reviews in Mathematical Physics*, 29(09):1750028, 2017. doi: 10.1142/S0129055X17500283. URL https://doi.org/10.1142/S0129055X17500283.

Steven A. Benner, Hyo-Joong Kim, and Matthew A. Carrigan. Asphalt, water, and the prebiotic synthesis of ribose, ribonucleosides, and rna. *Accounts of Chemical Research*, 45(12):2025–2034, 2012a. doi: 10.1021/ar200332w. URL https://doi.org/10.1021/ar200332w. PMID: 22455515.

Steven A. Benner, Hyo-Joong Kim, and Zunyi Yang. Setting the stage: the history, chemistry, and geobiology behind rna. *Cold Spring Harbor perspectives in biology*, 4(1): a003541, 2012b.

Claude Berge. *The theory of graphs and its applications. Translated by Alison Doig. Methuen & Co. Ltd., London*. John Wiley & Sons Inc., New York, 1962.

Harold S. Bernhardt. The rna world hypothesis: the worst theory of the early evolution of life (except for all the others) a. *Biology direct*, 7(1):23, 2012.

Alberto M. Bersani, Enrico Bersani, Guido Dell'Acqua, and Morten G. Pedersen. New trends and perspectives in nonlinear intracellular dynamics: one century from michaelis–menten paper. *Continuum Mechanics and Thermodynamics*, 27(4-5):659–684, jun 2015. doi: 10.1007/s00161-014-0367-4.

Michel Bitbol and Pier Luigi Luisi. Autopoiesis with or without cognition: defining life at its edge. *Journal of The Royal Society Interface*, 1(1):99–107, nov 2004. doi: https://doi.org/10.1098/rsif.2004.0012.

Alex Blokhuis, Davis Lacoste, and Philippe Nghe. Universal motifs and the diversity of autocatalytic systems. *Proceedings of the National Academy of Sciences*, 117(41):25230–25236, sep 2020. doi: https://doi.org/10.1073/pnas.2013527117.

José A. M. Borghans, Rob J. De Boer, and Lee A. Segel. Extending the quasi-steady state approximation by changing variables. *Bulletin of Mathematical Biology*, 58(1):43–63, jan 1996. doi: https://doi.org/10.1007/BF02458281.

Balázs Boros. Existence of positive steady states for weakly reversible mass-action systems. *SIAM Journal on Mathematical Analysis*, 51(1):435–449, 2019.

George E. Briggs and John B. S. Haldane. A note on the kinetics of enzyme action. *Biochemical Journal*, 19(2):338–339, 01 1925. ISSN 0006-2936. doi: 10.1042/bj0190338. URL https://doi.org/10.1042/bj0190338.

Xi Chen, Na Li, and Andrew D. Ellington. Ribozyme catalysis of metabolism in the rna world. *Chemistry & Biodiversity*, 4(4):633–655, 2007. doi: https://doi.org/10.1002/cbdv.200790055. URL https://onlinelibrary.wiley.com/doi/abs/10.1002/cbdv.200790055.

Gavin E. Crooks. Entropy production fluctuation theorem and the nonequilibrium work relation for free energy differences. *Physical Review E*, 60(3):2721–2726, sep 1999. doi: https://doi.org/10.1103/PhysRevE.60.2721.

Richard Dawkins. *The selfish gene*. Oxford University Press, New York, 1976. ISBN 0-19-857519-X.

Christian De Duve. A research proposal on the origin of life. closing lecture given at the issol congress in oaxaca, mexico, on july 4, 2002. *Origins of Life and Evolution of the Biosphere*, 33(6):559–574, 2003. doi: https://doi.org/10.1023/A:1025760311436.

Sybren R. De Groot. *Non-equilibrium Thermodynamics*, volume 16. DOVER PUBN INC, 1962. ISBN 0486647412. doi: 10.1063/1.3050930. URL https://www.ebook.de/de/product/3303084/s_r_de_groot_p_mazur_s_r_de_groot_non_equilibrium_thermodynamics.html.

David W. Deamer and Gail R. Fleischaker. *Origins of life: the central concepts*. Jones & Bartlett Pub, 1994.

Alicia Dickenstein and Mercedes Pérez Millán. How far is complex balancing from detailed balancing? *Bulletin of Mathematical Biology*, 73(4):811–828, jan 2011. doi: 10.1007/s11538-010-9611-7.

Peter Dittrich and Pietro Speroni Di Fenizio. Chemical organisation theory. *Bulletin of mathematical biology*, 69(4):1199–1231, 2007.

Freeman Dyson. *Origins of life*. Cambridge University Press, 1985.

Manfred Eigen and Peter Schuster. A principle of natural self-organization. *Naturwissenschaften*, 64(11):541–565, nov 1977. doi: https://doi.org/10.1007/BF00450633.

Manfred Eigen and Peter Schuster. *The Hypercycle : a Principle of Natural Self-Organization*. Springer Berlin Heidelberg, Berlin, Heidelberg, 1979. ISBN 978-3-642-67247-7.

Phillipp R. Ellison. *The advanced deficiency algorithm and its applications to mechanism discrimination*. The University of Rochester, Eastman School of Music, 1998.

Phillipp R. Ellison, Martin Feinberg, Haixia Ji, and Daniel Knight. Chemical reaction network toolbox, version 2.2. *See http://www. crnt. osu. edu/crntwin*, 2012.

Jeremy L. England. Statistical physics of self-replication. *The Journal of Chemical Physics*, 139(12):121923, sep 2013. doi: https://doi.org/10.1063/1.4818538.

Jeremy L. England. Dissipative adaptation in driven self-assembly. *Nature Nanotechnology*, 10(11):919–923, nov 2015. doi: https://doi.org/10.1038/nnano.2015.250.

Gianmaria Falasco, Riccardo Rao, and Massimiliano Esposito. Information thermodynamics of turing patterns. *Physical Review Letters*, 121(10), sep 2018. doi: https://doi.org/10.1103/PhysRevLett.121.108301.

Martin Feinberg. Complex balancing in general kinetic systems. *Archive for Rational Mechanics and Analysis*, 49(3):187–194, jan 1972. doi: https://doi.org/10.1007/BF00255665.

Martin Feinberg. Chemical reaction network structure and the stability of complex isothermal reactors i. the deficiency zero and deficiency one theorems. *Chemical engineering science*, 42(10):2229–2268, 1987.

Martin Feinberg. Necessary and sufficient conditions for detailed balancing in mass action systems of arbitrary complexity. *Chemical Engineering Science*, 44(9):1819–1827, 1989. doi: https://doi.org/10.1016/0009-2509(89)85124-3.

Martin Feinberg. The existence and uniqueness of steady states for a class of chemical reaction networks. *Archive for Rational Mechanics and Analysis*, 132(4):311–370, 1995.

Martin Feinberg. *Foundations of chemical reaction network theory*. Springer, 2019.

Alessandro Filisetti, Alex Graudenzi, Roberto Serra, Marco Villani, Davide De Lucrezia, Rudolf M. Füchslin, Stuart A. Kauffman, Norman Packard, and Irene Poli. A stochastic model of the emergence of autocatalytic cycles. *Journal of Systems Chemistry*, 2(1):2, 2011.

Edward H. Flach and Santiago Schnell. Use and abuse of the quasi-steady-state approximation. *IEE Proceedings - Systems Biology*, 153(4):187, 2006. doi: 10.1049/ip-syb:20050104.

Tibor Gánti. Biogenesis itself. *Journal of Theoretical Biology*, 187(4):583–593, aug 1997. doi: https://doi.org/10.1006/jtbi.1996.0391.

Walter Gilbert. Origin of life: The RNA world. *Nature*, 319(6055):618–618, feb 1986. doi: https://doi.org/10.1038/319618a0.

Daniel T. Gillespie. A general method for numerically simulating the stochastic time evolution of coupled chemical reactions. *Journal of computational physics*, 22(4):403–434, 1976.

Daniel T. Gillespie. Exact stochastic simulation of coupled chemical reactions. *The journal of physical chemistry*, 81(25):2340–2361, 1977.

Daniel T. Gillespie. Stochastic simulation of chemical kinetics. *Annual Review of Physical Chemistry*, 58(1):35–55, 2007. doi: 10.1146/annurev.physchem.58.032806.104637.

Federico S. Gnesotto, Federica Mura, Jannes Gladrow, and Chase P. Broedersz. Broken detailed balance and non-equilibrium dynamics in living systems: a review. *Reports on Progress in Physics*, 81(6):066601, apr 2018. doi: https://doi.org/10.1088/1361-6633/aab3ed.

Geoffrey Grimmett. *Probability and random processes*. Oxford University Press, Oxford, 2020. ISBN 9780198847601.

Peter J. Haas. *Stochastic petri nets: Modelling, stability, simulation*. Springer Science & Business Media, 2006.

John B. S. Haldane. Rationalist annual. *The origin of Life*, 148, 1929.

Eric J. Hayden, Günter Von Kiedrowski, and Niles Lehman. Systems chemistry on ribozyme self-construction: Evidence for anabolic autocatalysis in a recombination network. *Angewandte Chemie*, 120(44):8552–8556, oct 2008. doi: https://doi.org/10.1002/ange.200802177.

Paul G. Higgs and Niles Lehman. The rna world: molecular cooperation at the origins of life. *Nature Reviews Genetics*, 16(1):7–17, 2015.

Wim Hordijk and Mike Steel. Detecting autocatalytic, self-sustaining sets in chemical reaction systems. *Journal of Theoretical Biology*, 227(4):451 – 461, 2004. ISSN 0022-5193. doi: https://doi.org/10.1016/j.jtbi.2003.11.020. URL `http://www.sciencedirect.com/science/article/pii/S0022519303004417`.

Wim Hordijk and Mike Steel. Predicting template-based catalysis rates in a simple catalytic reaction model. *Journal of theoretical biology*, 295:132–138, 2012a.

Wim Hordijk and Mike Steel. Autocatalytic sets extended: Dynamics, inhibition, and a generalization. *Journal of Systems Chemistry*, 3(1):5, 2012b.

Wim Hordijk and Mike Steel. Conditions for evolvability of autocatalytic sets: A formal example and analysis. *Origins of Life and Evolution of Biospheres*, 44(2):111–124, 2014.

Wim Hordijk and Mike Steel. Autocatalytic sets and boundaries. *Journal of Systems Chemistry*, 6(1), feb 2015. doi: 10.1186/s13322-014-0006-2.

Wim Hordijk and Mike Steel. Chasing the tail: The emergence of autocatalytic networks. *Biosystems*, 152:1–10, 2017.

Wim Hordijk and Mike Steel. Autocatalytic networks at the basis of life's origin and organization. *Life*, 8(4):62, 2018.

Wim Hordijk, Jotun Hein, and Mike Steel. Autocatalytic sets and the origin of life. *Entropy*, 12(7):1733–1742, 2010.

Wim Hordijk, Stuart A. Kauffman, and Mike Steel. Required levels of catalysis for emergence of autocatalytic sets in models of chemical reaction systems. *International journal of molecular sciences*, 12(5):3085–3101, 2011.

Wim Hordijk, Mike Steel, and Stuart A. Kauffman. The structure of autocatalytic sets: Evolvability, enablement, and emergence. *Acta biotheoretica*, 60(4):379–392, 2012.

Wim Hordijk, Jonathan Naylor, Natalio Krasnogor, and Harold Fellermann. Population dynamics of autocatalytic sets in a compartmentalized spatial world. *Life*, 8(3):33, 2018a.

Wim Hordijk, Mike Steel, and Peter Dittrich. Autocatalytic sets and chemical organizations: Modeling self-sustaining reaction networks at the origin of life. *New Journal of Physics*, 20(1):015011, 2018b.

Friedrich J. M. Horn. Necessary and sufficient conditions for complex balancing in chemical kinetics. *Archive for Rational Mechanics and Analysis*, 49(3):172–186, jan 1972. doi: https://doi.org/10.1007/BF00255664.

Friedrich J. M. Horn and Roy Jackson. General mass action kinetics. *Archive for Rational Mechanics and Analysis*, 47(2):81–116, jan 1972. doi: https://doi.org/10.1007/BF00251225.

Takeshi Ishida. Simulations of living cell origins using a cellular automata model. *Origins of Life and Evolution of Biospheres*, 44(2):125–141, apr 2014. doi: 10.1007/s11084-014-9372-7.

Sanjay Jain and Sandeep Krishna. Autocatalytic sets and the growth of complexity in an evolutionary model. *Physical Review Letters*, 81(25):5684, 1998.

Atsushi Kamimura and Kunihiko Kaneko. Reproduction of a protocell by replication of a minority molecule in a catalytic reaction network. *Physical Review Letters*, 105(26), dec 2010. doi: https://doi.org/10.1103/PhysRevLett.105.268103.

Kunihiko Kaneko and Tetsuya Yomo. On a kinetic origin of heredity: Minority control in a replicating system with mutually catalytic molecules. *Journal of Theoretical Biology*, 214(4):563–576, feb 2002. doi: 10.1006/jtbi.2001.2481.

Stuart A. Kauffman. Cellular homeostasis, epigenesis and replication in randomly aggregated macromolecular systems. *Journal of Cybernetics*, 1(1):71–96, 1971. doi: 10.1080/01969727108545830. URL https://doi.org/10.1080/01969727108545830.

Stuart A. Kauffman. Autocatalytic sets of proteins. *Journal of theoretical biology*, 119(1): 1–24, 1986.

Stuart A. Kauffman. *The origins of order: Self-organization and selection in evolution*. Oxford University Press, USA, 1993.

Stuart A. Kauffman. *Investigations*. Oxford University Press, 2000.

Stuart A. Kauffman. Approaches to the origin of life on earth. *Life*, 1(1):34–48, 2011.

Stuart A. Kauffman. Answering schrödinger's "what is life?". *Entropy*, 22(8):815, jul 2020. doi: 10.3390/e22080815.

Norio Kitadai and Shigenori Maruyama. Origins of building blocks of life: A review. *Geoscience Frontiers*, 9(4):1117 – 1153, 2018. ISSN 1674-9871. doi: https://doi.org/10.1016/j.gsf.2017.07.007. URL http://www.sciencedirect.com/science/article/pii/S1674987117301305.

Dilip Kondepudi and Ilya Prigogine. *Modern Thermodynamics: From Heat Engines to Dissipative Structures*. Wiley & Sons, 2014. doi: 10.1002/9781118698723.

Doron Lancet, Ella Sadovsky, and Eyal Seidemann. Probability model for molecular recognition in biological receptor repertoires: significance to the olfactory system. *Proceedings of the National Academy of Sciences*, 90(8):3715–3719, apr 1993. doi: https://doi.org/10.1073/pnas.90.8.3715.

Bruno Latour. *The pasteurization of France*. Harvard University Press, 1993. ISBN 9780674657618. URL https://www.ebook.de/de/product/6501851/bruno_latour_the_pasteurization_of_france.html.

Antonio Lazcano and Stanley L. Miller. The origin and early evolution of life: Prebiotic chemistry, the pre-RNA world, and time. *Cell*, 85(6):793–798, jun 1996. doi: 10.1016/S0092-8674(00)81263-5.

Juan C. Letelier, Jorge Soto-Andrade, Flavio Guíñez Abarzúa, Athel Cornish-Bowden, and María L. Cárdenas. Organizational invariance and metabolic closure: Analysis in terms of systems. *Journal of Theoretical Biology*, 238(4):949–961, feb 2006. doi: https://doi.org/10.1016/j.jtbi.2005.07.007.

Gilbert N. Lewis. A new principle of equilibrium. *Proceedings of the National Academy of Sciences*, 11(3):179–183, mar 1925. doi: 10.1073/pnas.11.3.179.

Yunsheng Li, Yufen Zhao, Scott Hatfield, Rong Wan, Qin Zhu, Xionghong Li, Mark McMills, Yuan Ma, Jing Li, Kenneth L. Brown, et al. Dipeptide seryl-histidine and related oligopeptides cleave dna, protein, and a carboxyl ester. *Bioorganic & medicinal chemistry*, 8(12):2675–2680, 2000.

Shneior Lifson. On the crucial stages in the origin of animate matter. *Journal of molecular evolution*, 44(1):1–8, 1997.

Jason D. Lohn, Silvano P. Colombano, Jeffrey Scargle, Dimitris Stassinopoulos, and Gary L. Haith. Evolving catalytic reaction sets using genetic algorithms. In *1998 IEEE International Conference on Evolutionary Computation Proceedings. IEEE World Congress on Computational Intelligence (Cat. No. 98TH8360)*, pages 487–492. IEEE, 1998.

Pier Luigi Luisi. About various definitions of life. *Origins of Life and Evolution of the Biosphere*, 28(4-6):613–622, 1998.

Pier Luigi. Luisi. Autopoiesis: a review and a reappraisal. 90:49–59, 2003. ISSN 0028-1042. doi: 10.1007/s00114-002-0389-9.

Pier Luigi Luisi. *The emergence of life: from chemical origins to synthetic biology*. Cambridge University Press, 2006.

Robert Marsland and Jeremy L. England. Limits of predictions in thermodynamic systems: a review. *Reports on Progress in Physics*, 81(1):016601, nov 2017. doi: https://doi.org/10.1088/1361-6633/aa9101.

Humberto R. Maturana and Francisco J. Varela. *Autopoiesis and Cognition*. Springer Netherlands, 1980. ISBN 9027710155. URL `https://www.ebook.de/de/product/2554357/h_r_maturana_f_j_varela_autopoiesis_and_cognition.html`.

Leonor Michaelis and Maud L. Menten. Die kinetik der invertinwirkung biochem z 49: 333–369. *Find this article online*, 1913.

Stanley L. Miller. A production of amino acids under possible primitive earth conditions. *Science*, 117(3046):528–529, 1953.

Stephen J. Mojzsis, Ramanarayanan Krishnamurthy, and Gustaf Arrhenius. Before rna and after: Geophysical and geochemical constraints on molecular evolution. *COLD SPRING HARBOR MONOGRAPH SERIES*, 37, 1999.

Michael K. Molloy. Performance analysis using stochastic petri nets. *IEEE Transactions on computers*, (9):913–917, 1982.

Elchanan Mossel and Mike Steel. Random biochemical networks: The probability of self-sustaining autocatalysis. *Journal of theoretical biology*, 233(3):327–336, 2005.

ArmenY. Mulkidjanian and MichaelY. Galperin. Physico-chemical and evolutionary constraints for the formation and selection of first biopolymers: Towards the consensus paradigm of the abiogenic origin of life. *Chemistry & Biodiversity*, 4(9):2003–2015, 2007. doi: https://doi.org/10.1002/cbdv.200790167. URL `https://onlinelibrary.wiley.com/doi/abs/10.1002/cbdv.200790167`.

Stefan Müller and Badal Joshi. Detailed balance = complex balance + cycle balance: A graph-theoretic proof for reaction networks and markov chains. *Bulletin of Mathematical Biology*, 82(9), sep 2020. doi: 10.1007/s11538-020-00792-1.

Philippe Nghe, Wim Hordijk, Stuart A. Kauffman, Sara I. Walker, Francis J. Schmidt, Harry Kemble, Jessica A. M. Yeates, and Niles Lehman. Prebiotic network evolution: six key parameters. *Molecular BioSystems*, 11(12):3206–3217, 2015.

Charles Ofria, Christoph Adami, and Travis C. Collier. Selective pressures on genomes in molecular evolution. *Journal of Theoretical Biology*, 222(4):477 – 483, 2003. ISSN 0022-5193. doi: https://doi.org/10.1016/S0022-5193(03)00062-6. URL `http://www.sciencedirect.com/science/article/pii/S0022519303000626`.

Lars Onsager. Reciprocal relations in irreversible processes. i. *Physical Review*, 37(4): 405–426, feb 1931. doi: https://doi.org/10.1103/PhysRev.37.405.

Alexander I. Oparin. Proiskhozhdenie zhizny [the origin oflife]. *Izd. Moskovski Rabochii, Moscow*, 1924.

Leslie E. Orgel. Prebiotic adenine revisited: Eutectics and photochemistry. *Origins of Life and Evolution of the Biosphere*, 34(4):361–369, aug 2004. doi: https://doi.org/10.1023/B:ORIG.0000029882.52156.c2.

Joan Oro, Antonio Lazcano, and Pascale Ehrenfreund. Comets and the origin and evolution of life. In *Comets and the Origin and Evolution of Life*, pages 1–28. Springer, 2006.

Morten G. Pedersen, Alberto M. Bersani, and Enrico Bersani. Quasi steady-state approximations in complex intracellular signal transduction networks – a word of caution. *Journal of Mathematical Chemistry*, 43(4):1318–1344, jun 2007. doi: 10.1007/s10910-007-9248-4.

Emanuele Penocchio, Riccardo Rao, and Massimiliano Esposito. Thermodynamic efficiency in dissipative chemistry. *Nature Communications*, 10(1), aug 2019. doi: https://doi.org/10.1038/s41467-019-11676-x.

Lionel S. Penrose and Roger Penrose. A self-reproducing analogue. *nature*, 179:1183–1183, 1957. ISSN 0028-0836. doi: 10.1038/1791183a0.

M. Perret. Biochemistry and bacteria. *New Biology*, 12(68), 1952.

Nikolay Perunov, Robert A. Marsland, and Jeremy L. England. Statistical physics of adaptation. *Physical Review X*, 6(2), jun 2016. doi: https://doi.org/10.1103/PhysRevX.6.021036.

Stephan Peter and Peter Dittrich. On the relation between organizations and limit sets in chemical reaction systems. *Advances in Complex Systems*, 14(01):77–96, 2011. doi: 10.1142/S0219525911002895. URL `https://doi.org/10.1142/S0219525911002895`.

Carl A. Petri and Wolfgang Reisig. Petri net. *Scholarpedia*, 3(4):6477, 2008.

Kristof Plankensteiner, Alessandro Righi, and Bernd M. Rode. Glycine and diglycine as possible catalytic factors in the prebiotic evolution of peptides. *Origins of Life and Evolution of the Biosphere*, 32(3):225–236, 2002.

Matteo Polettini and Massimiliano Esposito. Irreversible thermodynamics of open chemical networks. i. emergent cycles and broken conservation laws. *The Journal of Chemical Physics*, 141(2):024117, jul 2014. doi: https://doi.org/10.1063/1.4886396.

Matteo Polettini, Artur Wachtel, and Massimiliano Esposito. Dissipation in noisy chemical networks: The role of deficiency. *The Journal of chemical physics*, 143(18):11B606_1, 2015.

Matthew W. Powner, Béatrice Gerland, and John D. Sutherland. Synthesis of activated pyrimidine ribonucleotides in prebiotically plausible conditions. *Nature*, 459(7244):239–242, may 2009. doi: https://doi.org/10.1038/nature08013.

Matthew W. Powner, John D. Sutherland, and Jack W. Szostak. Chemoselective multicomponent one-pot assembly of purine precursors in water. *Journal of the American Chemical Society*, 132(46):16677–16688, 2010. doi: 10.1021/ja108197s. URL `https://doi.org/10.1021/ja108197s`. PMID: 21043502.

Ilya Prigogine. Etude thermodynamics des phenomenes irreversibles (study of the thermodynamics of irreversible phenomenon)., 1947. Presented to the science faculty at the Free University Of Brussels 1945. Dunod, Paris; 1947.

Ilya Prigogine and Gregoire Nicolis. *Biological order, structure and instabilities*, volume 4. 1971. doi: 10.1017/s0033583500000615.

Addy Pross. Causation and the origin of life. metabolism or replication first? 34(3): 307–321, jun 2004. ISSN 1573-0875. doi: 10.1023/b:orig.0000016446.51012.bc. URL https://doi.org/10.1023/B:ORIG.0000016446.51012.bc.

Riccardo Rao and Massimiliano Esposito. Nonequilibrium thermodynamics of chemical reaction networks: Wisdom from stochastic thermodynamics. *Physical Review X*, 6(4), dec 2016. doi: 10.1103/PhysRevX.6.041064.

Riccardo Rao and Massimiliano Esposito. Conservation laws and work fluctuation relations in chemical reaction networks. *The Journal of Chemical Physics*, 149(24):245101, dec 2018. doi: https://doi.org/10.1063/1.5042253.

Steen Rasmussen, Liaohai Chen, David Deamer, David C. Krakauer, Norman H. Packard, Peter F. Stadler, and Mark A. Bedau. Transitions from nonliving to living matter. *Science*, 303(5660):963–965, 2004.

Alessandro Ravoni. Impact of composition on the dynamics of autocatalytic sets. *Biosystems*, 198:104250, 2020a. ISSN 0303-2647. doi: 10.1016/j.biosystems.2020.104250.

Alessandro Ravoni. Long-term behaviours of autocatalytic sets. *arXiv:2010.08523*, 2020b.

Jacques Ricard and Athel Cornish-Bowden. Co-operative and allosteric enzymes: 20 years on. *European Journal of Biochemistry*, 166(2):255–272, jul 1987. doi: 10.1111/j.1432-1033.1987.tb13510.x.

Michael P. Robertson and Gerald F. Joyce. The origins of the RNA world. *Cold Spring Harbor Perspectives in Biology*, 4(5):a003608–a003608, apr 2010. doi: 10.1101/cshperspect.a003608.

Robert Rosen. *Life itself: a comprehensive inquiry into the nature, origin, and fabrication of life*. Columbia University Press, 1991.

Shai Rosenwald, Ran Kafri, and Doron Lancet. Test of a statistical model for molecular recognition in biological repertoires. *Journal of Theoretical Biology*, 216(3):327–336, jun 2002. doi: https://doi.org/10.1006/jtbi.2002.2538.

Michael J. Russell and Allan J. Hall. The emergence of life from iron monosulphide bubbles at a submarine hydrothermal redox and ph front. *Journal of the Geological Society*, 154(3):377–402, 1997. ISSN 0016-7649. doi: 10.1144/gsjgs.154.3.0377. URL https://jgs.lyellcollection.org/content/154/3/377.

Sumantra Sarkar and Jeremy L. England. Design of conditions for self-replication. *Physical Review E*, 100(2), aug 2019. doi: https://doi.org/10.1103/PhysRevE.100.022414.

Martin Schaller and Karl Svozil. Scale-invariant cellular automata and self-similar petri nets. *The European Physical Journal B*, 69(2):297–311, apr 2009. doi: 10.1140/epjb/e2009-00147-x.

Tim Schmiedl and Udo Seifert. Stochastic thermodynamics of chemical reaction networks. *The Journal of Chemical Physics*, 126(4):044101, jan 2007. doi: https://doi.org/10.1063/1.2428297.

Erwin Schrödinger. *What is life? : the physical aspect of the living cell*. Cambridge University Press, Cambridge New York, 1944. ISBN 0-521-42708-8.

Daniel Segrè, Doron Lancet, Ora Kedem, and Yitzhak Pilpel. Graded autocatalysis replication domain (gard): kinetic analysis of self-replication in mutually catalytic sets. *Origins of Life and Evolution of the Biosphere*, 29(4-6):501–514, 1998.

Daniel Segrè, Dafna Ben-Eli, and Doron Lancet. Compositional genomes: Prebiotic information transfer in mutually catalytic noncovalent assemblies. *Proceedings of the National Academy of Sciences*, 97(8):4112–4117, apr 2000. doi: https://doi.org/10.1073/pnas.97.8.4112.

Daniel Segrè, Dafna Ben-Eli, David W. Deamer, and Doron Lancet. The lipid world. *Origins of Life and Evolution of the Biosphere*, 31(1/2):119–145, 2001a. doi: https://doi.org/10.1023/A:1006746807104.

Daniel Segrè, Barak Shenhav, Ran Kafri, and Doron Lancet. The molecular roots of compositional inheritance. *Journal of Theoretical Biology*, 213(3):481–491, dec 2001b. doi: https://doi.org/10.1006/jtbi.2001.2440.

Udo Seifert. Stochastic thermodynamics, fluctuation theorems and molecular machines. *Reports on Progress in Physics*, 75(12):126001, nov 2012. doi: https://doi.org/10.1088/0034-4885/75/12/126001.

Roberto Serra and Marco Villani. Sustainable growth and synchronization in protocell models. *Life*, 9(3):68, 2019.

Edith M. Sevick, Ranganathan Prabhakar, Stephen R. Williams, and Debra J. Searles. Fluctuation theorems. *Annual Review of Physical Chemistry*, 59(1):603–633, may 2008. doi: https://doi.org/10.1146/annurev.physchem.58.032806.104555.

Robert Shapiro. Prebiotic ribose synthesis: A critical analysis. *Origins of Life and Evolution of the Biosphere*, 18(1-2):71–85, mar 1988. doi: https://doi.org/10.1007/BF01808782.

Robert Shapiro. A replicator was not involved in the origin of life. *IUBMB Life*, 49(3): 173–176, mar 2000. doi: https://doi.org/10.1080/713803621.

Alexei A. Sharov. Coenzyme autocatalytic network on the surface of oil microspheres as a model for the origin of life. *International Journal of Molecular Sciences*, 10(4):1838–1852, 2009. ISSN 1422-0067. doi: 10.3390/ijms10041838. URL https://www.mdpi.com/1422-0067/10/4/1838.

Alexei A. Sharov. Coenzyme world model of the origin of life. *Biosystems*, 144:8 – 17, 2016. ISSN 0303-2647. doi: https://doi.org/10.1016/j.biosystems.2016.03.003. URL http://www.sciencedirect.com/science/article/pii/S0303264716300107.

Dane Sievers and Günter Von Kiedrowski. Self-replication of complementary nucleotide-based oligomers. *Nature*, 369(6477):221–224, may 1994. doi: https://doi.org/10.1038/369221a0.

Joshua I. Smith, Mike Steel, and Wim Hordijk. Autocatalytic sets in a partitioned biochemical network. *Journal of Systems Chemistry*, 5(1):2, 2014.

Filipa L. Sousa, Wim Hordijk, Mike Steel, and William F. Martin. Autocatalytic sets in e. coli metabolism. *Journal of Systems Chemistry*, 6(1):4, 2015.

Sol Spiegelman, I. Haruna, I. B. Holland, G. Beaudreau, and D. Mills. The synthesis of a self-propagating and infectious nucleic acid with a purified enzyme. *Proceedings of the National Academy of Sciences*, 54(3):919–927, sep 1965. doi: 10.1073/pnas.54.3.919.

Mike Steel, Wim Hordijk, and Joshua Smith. Minimal autocatalytic networks. *Journal of Theoretical Biology*, 332:96 – 107, 2013. ISSN 0022-5193. doi: https://doi.org/10.1016/j.jtbi.2013.04.032. URL http://www.sciencedirect.com/science/article/pii/S0022519313002002.

Mike Steel, Wim Hordijk, and Joana C. Xavier. Autocatalytic networks in biology: structural theory and algorithms. *Journal of The Royal Society Interface*, 16(151):20180808, 2019. doi: 10.1098/rsif.2018.0808. URL https://royalsocietypublishing.org/doi/abs/10.1098/rsif.2018.0808.

Mike Steel, Joana C. Xavier, and Daniel H. Huson. The structure of autocatalytic networks, with application to early biochemistry. *Journal of The Royal Society Interface*, 17(171):20200488, 2020. doi: 10.1098/rsif.2020.0488. URL https://royalsocietypublishing.org/doi/abs/10.1098/rsif.2020.0488.

Eörs Szathmáry. The evolution of replicators. *Philosophical Transactions of the Royal Society of London. Series B: Biological Sciences*, 355(1403):1669–1676, 2000.

Eörs Szathmáry and John M. Smith. The major evolutionary transitions. *Nature*, 374: 227–232, 1995. ISSN 0028-0836. doi: 10.1038/374227a0.

Jack W. Szostak. The narrow road to the deep past: in search of the chemistry of the origin of life. *Angewandte Chemie International Edition*, 56(37):11037–11043, 2017.

Olga Taran, Oliver Thoennessen, Karin Achilles, and Günter Von Kiedrowski. Synthesis of information-carrying polymers of mixed sequences from double stranded short deoxynucleotides. *Journal of Systems Chemistry*, 1(1), aug 2010. doi: https://doi.org/10.1186/1759-2208-1-9.

Edward N. Trifonov. Vocabulary of definitions of life suggests a definition. *Journal of Biomolecular Structure and Dynamics*, 29(2):259–266, oct 2011. doi: https://doi.org/10.1080/073911011010524992.

Abraham R. Tzafriri. Michaelis-menten kinetics at high enzyme concentrations. *Bulletin of mathematical biology*, 65(6):1111–1129, 2003.

Abraham R. Tzafriri and Elazer R. Edelman. The total quasi-steady-state approximation is valid for reversible enzyme kinetics. *Journal of theoretical biology*, 226(3):303–313, 2004.

Renè Vallery-Radot. *The Life of Pasteur (Devonshire RL, transl.)*. New York: GardenCity Publishing Co., Inc., 1926.

Christian Van den Broeck. Stochastic thermodynamics: A brief introduction. *Proceedings of the International School of Physics "Enrico Fermi"*, 184:155–193, 2013. ISSN 0074-784X. doi: 10.3254/978-1-61499-278-3-155.

Arjan Van der Schaft, Shodhan Rao, and Bayu Jayawardhana. Complex and detailed balancing of chemical reaction networks revisited. *Journal of Mathematical Chemistry*, 53 (6):1445–1458, apr 2015. doi: https://doi.org/10.1007/s10910-015-0498-2.

Francisco J. Varela. *Principles of biological autonomy.* North Holland/Elsevier, New York, 1979.

Francisco J. Varela. *El fenómeno de la vida*. Dolmen Ediciones Santiago de Chile, 2000.

Francisco J. Varela, Humberto R. Maturana, and Ricardo Uribe. Autopoiesis: The organization of living systems, its characterization and a model. *Biosystems*, 5(4):187–196, may 1974. doi: https://doi.org/10.1016/0303-2647(74)90031-8.

Vera Vasas, Eörs Szathmáry, and Mauro Santos. Lack of evolvability in self-sustaining autocatalytic networks constraints metabolism-first scenarios for the origin of life. *Proceedings of the National Academy of Sciences*, 107(4):1470–1475, 2010.

Vera Vasas, Chrisantha Fernando, Mauro Santos, Stuart A. Kauffman, and Eörs Szathmáry. Evolution before genes. *Biology direct*, 7(1):1, 2012.

Carlos R. Vazquez and Manuel Silva. Stochastic continuous petri nets: An approximation of markovian net models. *IEEE Transactions on Systems, Man, and Cybernetics-Part A: Systems and Humans*, 42(3):641–653, 2011.

Marco Villani, Alessandro Filisetti, Alex Graudenzi, Chiara Damiani, Timoteo Carletti, and Roberto Serra. Growth and division in a dynamic protocell model. *Life*, 4(4):837–864, 2014. ISSN 2075-1729. doi: 10.3390/life4040837. URL `https://www.mdpi.com/2075-1729/4/4/837`.

John Von Neumann. *Theory of Self-Reproducing Automata*. University of Illinois Press, Urbana, 1966.

Artur Wachtel, Riccardo Rao, and Massimiliano Esposito. Thermodynamically consistent coarse graining of biocatalysts beyond michaelis–menten. *New Journal of Physics*, 20 (4):042002, apr 2018. doi: https://doi.org/10.1088/1367-2630/aab5c9.

Sara I. Walker. Origins of life: a problem for physics, a key issues review. *Reports on Progress in Physics*, 80(9):092601, aug 2017. doi: https://doi.org/10.1088/1361-6633/aa7804.

Talbot H. Waterman, Harold J. Morowitz, and Joseph G. Hoffman. Theoretical and mathematical biology. *PhT*, 18(10):64, 1965.

Richard Wolfenden and Mark J. Snider. The depth of chemical time and the power of enzymes as catalysts. *Accounts of Chemical Research*, 34(12):938–945, dec 2001. doi: https://doi.org/10.1021/ar000058i.

Joana C. Xavier, Wim Hordijk, Stuart A. Kauffman, Mike Steel, and William F. Martin. Autocatalytic chemical networks at the origin of metabolism. *Proceedings of the Royal Society B*, 287(1922):20192377, 2020.